

2018-04-23

Design Analysis of Roller Coasters

Kristen Hunt

Worcester Polytechnic Institute

Follow this and additional works at: <https://digitalcommons.wpi.edu/etd-theses>

Repository Citation

Hunt, Kristen, "Design Analysis of Roller Coasters" (2018). *Masters Theses (All Theses, All Years)*. 250.
<https://digitalcommons.wpi.edu/etd-theses/250>

This thesis is brought to you for free and open access by Digital WPI. It has been accepted for inclusion in Masters Theses (All Theses, All Years) by an authorized administrator of Digital WPI. For more information, please contact wpi-etd@wpi.edu.

Design Analysis of Roller Coasters

by

Kristen Hunt

A Thesis

Submitted to the Faculty

of

WORCESTER POLYTECHNIC INSTITUTE

in partial fulfillment of the requirements for the

Degree of Master of Science

in

Civil Engineering

May 2018

Approved:

A handwritten signature in black ink, appearing to read 'Nima Rahbar', is written over a horizontal line.

Professor Nima Rahbar, CEE

A handwritten signature in black ink, appearing to read 'Leonard D. Albano', is written over a horizontal line.

Professor Leonard Albano, CEE

A handwritten signature in black ink, appearing to read 'Hussam Saleem', is written over a horizontal line.

Professor Hussam Saleem, CEE

Abstract

Each year 300 million people ride roller coasters at amusement parks across the United States. Although they are meant for joy and entertainment, the design is very crucial and regulated. Understanding the interaction between components and humans can help create a more thrilling and safer ride. This study researched the design of the course and the structural supports. A unique roller coaster was designed, investigating the relationship between velocity and G forces. With the profile design complete, the corresponding forces resulting from the track and train weight and train movement were calculated to determine the required dimensions of the structural support columns. This work investigated the relationship between the features of the roller coaster and the material properties of the structural supports, determining which are most impactful for the loading conditions. These results can be used to determine the required properties of a roller coaster's structural system to maximize the material usage to minimize resources and cost.

Acknowledgements

I would like to thank Professor Nima Rahbar for his continued guidance and helpful insight. I appreciate his support of my thesis that reflects my dreams and interests.

I would like to thank Evan Gracey, Mike Morris and others at Spartan Race for their aide in my project. They provided interesting perspectives and support which was much appreciated throughout my thesis.

I would also like to thank Professor Leonard Albano and Professor Hussam Saleem. They both added interesting feedback and thoughtful considerations to the project.

Lastly, I would like to thank my family. They encouraged me to have fun while creating something for others to enjoy.

Table of Contents

Abstract	i
Acknowledgements	ii
Table of Contents	iii
List of Figures	vi
List of Tables.....	viii
1.0 Introduction	1
2.0 Literature Review	3
2.1 History.....	3
2.2 Trends and Records.....	5
2.3 Materials: Wood vs. Steel	7
2.4 Components and Classifications	7
2.4.1 Lifts	8
2.4.2 Launching Mechanisms	9
2.4.3 Carts	10
2.4.4 Classifications	11
2.5 Design Methods	12
2.5.1 Design Considerations	12
2.5.2 Safety Standards & Regulations	14
2.5.3 Software	18
2.6 Construction.....	19
2.6.1 Economics.....	20
2.7 Maintenance and Operation	20
2.8 Progressions and Possibilities	21
3.0 Methodology	23

3.1 Shape and Components.....	23
3.1.1 Lift Hill	23
3.1.2 Initial Drop.....	25
3.1.3 Clothoid Loop	26
3.1.4 Straight Away	27
3.1.5 Banked Curves	27
3.1.6 Hills and Valleys.....	28
3.1.7 Braking.....	28
3.2 Support Structures.....	29
3.2.1 Bending Moment in Column Supports	29
3.2.2 Axial Loading in Column Supports	31
3.3 Materials	33
3.4 Model and Simulate	33
4.0 Results	35
4.1 Course Profile	35
4.2 Structural Supports.....	41
4.3 Model and Simulation.....	47
5.0 Discussion	49
5.1 Profile Design	49
5.1.1 Velocity and G Forces	49
5.2 Structural Supports.....	50
5.2.1 Bending Moment and Axial Compression.....	50
5.2.2 Material Properties.....	51
5.2.3 Additional Structural Considerations.....	53
6.0 Conclusion.....	54

7.0 Bibliography	55
8.0 Appendices	59
Appendix A: Lift Hill Calculations.....	59
Appendix B: Initial Drop Calculations	60
Appendix C: Straight Away #1 Calculations.....	63
Appendix D: Clothoid Loop Calculations	64
Appendix E: Clothoid Loop Model	67
Appendix F: Banked Curve #1 Calculations	68
Appendix G: Hill #2 Calculations.....	70
Appendix H: Hill #2 Model	72
Appendix I: Straight Away #2 Calculations	73
Appendix J: Hill Series Calculations	74
Appendix K: Hill Series Model	83
Appendix L: Banked Curve #2 Calculations	84
Appendix M: Braking Calculations	85
Appendix N: Calculations for Axial Loads and Bending Moments in Supports.....	87
Appendix O: Material Calculations for Support Structure	103

List of Figures

Figure 1: Knudsen's 1878 Patent	4
Figure 2: Roller Coaster History 1870-2010 (adapted from National Roller Coaster Museum, 2014)	5
Figure 3: Leap the Dip - Opened 1902 Pennsylvania.....	6
Figure 4: Scenic Railway - Opened 1912 Australia.....	6
Figure 5: Inverted Coaster (Fantacoaster, 2008) (left).....	12
Figure 6: Suspended Coaster (Wikimedia Commons, 2014) (center)	12
Figure 7: Pipeline Coaster (Wikipedia, 2018) (right)	12
Figure 8: Bobsled Roller Coaster (McC, 2017) (left).....	12
Figure 9: Flying Roller Coaster (Murphy, 2009) (center)	12
Figure 10: 4D Roller Coaster (Wills, 2009) (right)	12
Figure 11: Rider Envelope (ASTM F2291)	15
Figure 12: Vertical G Force Duration Limits (ASTM, 2017c).....	17
Figure 13: NoLimits 2 Editor Screenshot	34
Figure 14: Track Layout Perspective Views.....	35
Figure 15: Velocity of Train in Clothoid Loop.....	37
Figure 16: Vertical G Forces in Clothoid Loop	37
Figure 17: Velocity of Train in Hill Series	39
Figure 18: Vertical G Forces in Hill Series	39
Figure 19: Color-Coded Flattened Profile	40
Figure 20: Bending Moment Along Course.....	42
Figure 21: Bending Moment Capacity Ratio Along Course (20in Diameter)	42
Figure 22: Bending Moment Capacity Ratio Along Course (Modified Diameters).....	43
Figure 23: Axial Loading Along Course	44
Figure 24: Compression Capacity Ratio Along Course (20in Diameter)	44
Figure 25: Compression Capacity Ratio Along Course (Modified Diameters).....	45
Figure 26: Change in Bending Capacity Due to Change in Yield Strength	46
Figure 27: Change in Compressive Capacity Due to Change in Yield Strength of Modulus of Elasticity	46
Figure 28: Completed Roller Coaster Model.....	47

Figure 29: View Ascending Lift Hill.....	47
Figure 30: View from Start of Initial Drop.....	47
Figure 31: View from Drop after Hill #1.....	48
Figure 32: View from Final Drop of Hill Series.....	48
Figure 33: View from Braking System, Returning to Station	48

List of Tables

Table 1: Summary of Profile Results.....	40
--	----

1.0 Introduction

Over the hundreds of years of roller coaster history, rides have changed from wooden cars traveling down slow inclines around 20 mph to fiberglass trains being launched into inversions and spirals at over 100 mph. And the prospects for more improvement and innovation are promising. Roller coasters are a source of intrigue and enjoyment and the progression in technology has continued to change the industry. Labeled the first successful commercial roller coaster, the Switchback Railroad had people amazed in 1884 with its 6 mph journey along Coney Island's shore. Advances such as the steam driven lift chain and anti-rollback safety systems allowed the rides to evolve into faster and safer creations. The continued learning of the human limits also encouraged more rides to be made that were both thrilling and safe. The inventions and research of the late 1800's combined with the greatest technology and materials of today give engineers the tools to create attractions that launch people over 400 feet into the air before dropping them into a spiral at over 100 mph.

The main goal of this thesis was to investigate the correlation between roller coaster components and governing forces acting on structural systems by designing features and analyzing material properties of supports. To do this four main objectives were defined. The first objective was to design the shape and components of the roller coaster. This would result in a unique roller coaster profile and the ability to see the relationship between features of the ride and the effects on its passengers. The second objective was to design the structural supports and the materials of the supports. Once the profile was complete the corresponding loading conditions along the track were calculated to understand the connection between the train's movement and the types of loading placed on the structural system. The third objective was to investigate the material properties of the structural supports. Through this investigation an analysis of the correlation between the predominant forces on the components and the materials of the supports was performed. Lastly, the fourth objective was to model and simulate the roller coaster. All features of the roller coaster were modeled and the ride could be run virtually to assess the success of the course based on completion, safety and enjoyment.

Continuing to understand the background of the forces, materials and people, engineers can continue to create the next best roller coaster. If the important factors considered in the

design, such as safety and cost, can be maintained while improving the overall experience then the roller coaster industry will thrive in the future.

2.0 Literature Review

2.1 History

Roller coasters were first inspired by ice sleds in Russia that had wooden structures to bring people to the top. When the owners wanted to make a profit year-round, wheels were added to the sleds and wooden hills were built to allow the attraction to keep running throughout the warmer months. These new Russian Mountains led way to the first wheeled roller coaster built in 1804 in Paris, France (Roller Coaster, 2018).

Across the globe, the ideas of the roller coaster in the United States started at the Mauch Chunk Gravity Railway in Pennsylvania. Locals of the area rode the coal trains for the railway down the inclines on an exciting 9 mile ride (American Coaster Enthusiasts, 2018). Realizing the opportunity for profit, fairs started to be charged for rides as the railway became more popular. One of the inspired guests to ride the Mauch Chunk Gravity Railway was LaMarcus Adna Thompson. Thompson is credited for creating the first successful commercial roller coaster (Cypress, 1997). His ride, named Switchback Railway, was opened in 1884 on Coney Island. Switchback Railway was a wooden roller coaster comprised of two tracks. The carts would be brought to the top of 50ft towers where guests would be released to marvel at the 6 mph, one minute journey. The unique benches of the carts sat passengers sideways, allowing them to see the scenes of the shoreline passing by.

Although, Thompson is commonly recognized as the father of roller coasters whom started the frenzy in the early 1800s, he is far from the first. Numerous patents and roller coasters were created prior to 1884 in the United States. Another notable figure in roller coaster history is Richard Knudsen whose patent is shown below in Figure 1 (Sandy, 2018). Knudsen design is notably comparable to Thompson's successful attraction at Coney Island.

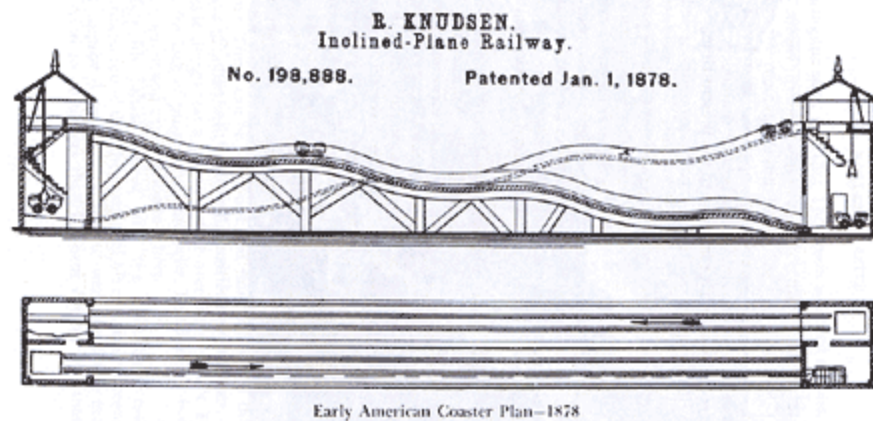


Figure 1: Knudsen's 1878 Patent

Various other patents and concepts were devised in the 1870's and 1880's, including both switchback and circular styled tracks. An innovative addition to the primitive roller coasters was the steam driven hoist invented by Phillip Hinkle in 1885 (Stanton, 2013). This was the first patent for a power lift system designed to be used in roller coaster attractions. The "Golden Age of Roller Coasters" began in the early 1900's and took off around the 1920's. Some of the most innovative concepts that give us the great roller coasters we have today were conceived during this time. With this growing interest in the gravity rides, the International Association of Amusement Parks and Attractions (IAAPA) was formed in 1918 to set standards and safety protocols (National Roller Coaster Museum, 2014). Completing the end of the roller coaster craze was one of the most famous roller coasters built. The Cyclone at Coney Island was built in 1927 (National Roller Coaster Museum, 2014).

Roller coaster production drastically decreased during World War II (CMU, 2015). Both the laborers and the materials changed course to contribute to the war instead of the rides. A few decades passed before the roller coaster industry recovered, "by 1965 only 200 of the 2000 coasters built through the 1920's were still in operation" (Crockett, 2014). However, a very notable ride triggered excitement and interest in roller coasters again. Disneyland opened its doors to the public in 1955 and in 1959 the Matterhorn Bobsleds was introduced (National Roller Coaster Museum, 2014). This ride was the first to use tubular steel for the track and incorporated braking so it was safe to have two trains on the track at once (National Roller Coaster Museum, 2014). With the advancement of wooden tracks to tubular steel, the roller coasters could continue

to become bigger and faster. During the late 1900's and the early 2000's new technology and layouts were invented to create new thrilling experiences. Launching mechanisms such as linear induction motors and compressed air launchers, along with innovative setups such as flying coasters and 4D coasters led to the large array of roller coasters in existence. Notable events of roller coaster history between 1878 and 2001 can be seen on the timeline below in Figure 2.

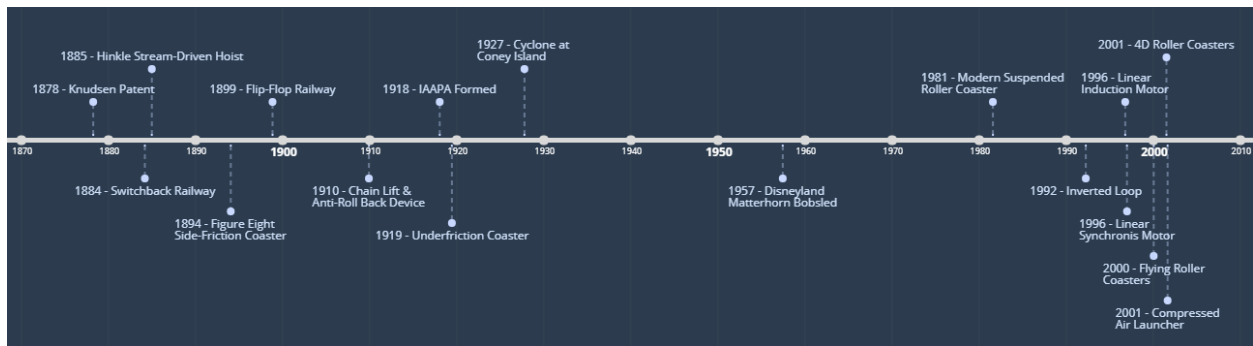


Figure 2: Roller Coaster History 1870-2010 (adapted from National Roller Coaster Museum, 2014)

2.2 Trends and Records

Throughout the years, roller coasters have changed and advanced greatly. New components have been invented and improved, new materials have been incorporated and innovative layouts have been used. Through the progression of roller coasters around the world, some notable records have been set.

The oldest roller coaster still in operation is located in Lakemont Park in Pennsylvania and it is named Leap the Dips. This roller coaster is a wooden structure built in 1902. The coaster is a side friction figure eight layout. It has a total overall height of 41 feet and the highest drop is 9 feet. The vintage ride can reach around 10-18 mph and takes about 1 minute for a complete travel through the track. Leap the Dips accommodates a single car carrying 4 people at a time. During its original construction the wooden roller coaster cost a total of \$15,000 to build (Marden, 2018a). After it's opening in 1902, it continuously was open to the public until 1935 before closing temporarily. It then was closed a second time in the late 1990's but was saved from demolition when it was named a National Historic Landmark in 1996 (Marden, 2018a). Restoration efforts followed from 1997 to 1999, when it most recently reopened. Although missing a few years of operation Leap the Dips is the oldest operating roller coaster at 116 years. The longest continually operated roller coaster is in Melbourne, Australia. Named the Scenic

Railway, this roller coaster was built in 1912 in Luna Park and has been continually operating to the public since (Los Angeles Times, 2014).



Figure 3: Leap the Dip - Opened 1902 Pennsylvania



Figure 4: Scenic Railway - Opened 1912 Australia

Leaps and bounds have been taken in the industry since the early roller coasters were constructed. Advances in understanding of physics and the body's limits, along with new technology in terms of mechanisms and materials have led to impressive record-breaking roller coasters. The record for the fastest roller coaster in the world is held by Formula Rossa in Ferrari World in Abu Dhabi (Borel, 2011). This ride can launch passengers from rest to a staggering 150 mph in 4.9 seconds. The ride is able to do this by using a hydraulic launch system, similar to those used to launch airplanes off of aircraft carriers. The launch creates 1.7g's on the rider and the max G force throughout the ride is a powerful 4.8g's. Intamin Amusement Rides designed the coaster to mimic the course and sensation of driving a Ferrari Formula One car around the Autodromo Nazionale Monza, an Italian racetrack, and they did not disappoint. To ride the fastest roller coaster in the world you must wear safety goggles to protect yourself as you're strapped into the cart before taking off for the 92 second thrill ride around the 1.3 mile course (Borel, 2011).

Although the Formula Rossa is currently the fastest in the world, the previous ride to hold the title was Kingda Ka, which still remains the tallest in the world and the fastest in North America. Kingda Ka is located in Six Flags New Jersey and was completed in 2005 by the same company, Intamin, which manufactured Formula Rossa. This roller coaster stands at a giant height of 456 feet and it includes the world's highest drop at 418 feet (Six Flags, 2017). To accommodate this large rise, the cars are shot up the lift hill at 128 mph in only 3.8 seconds by a

hydraulic launch system. After reaching the top of the 90° incline, the riders plummet down the other side of the 270° downward spiral. Kingda Ka is one of only two strata coasters, which is a “complete-circuit roller coaster with a height between 400 and 499 feet” (Coasterpedia, N.D.). Riders experience a thrilling 50 second ride along the 3,118 feet of track (Six Flags, 2017).

More than twice as long as the tallest roller coaster, the longest roller coaster in the world is the Steel Dragon 2000. Opening in 2000 in Japan, the Steel Dragon 2000 is 8,133.2 feet long. The cars carry a total of 28 passengers along this expansive track, taking around four minutes to complete. Briefly after its opening it held all three titles of longest, tallest and fastest roller coaster in the world. Its initial hill contains a lift chain that bring riders to a 306.8 foot drop reaching speeds of 95 mph (Coasterpedia, 2018). The coaster contains an immense amount of material not only because of its length but also because it contains more steel than a typical coaster for earthquake provisions. Steel Dragon 2000 cost a total of \$50 million to construct (Coasterpedia, 2018).

2.3 Materials: Wood vs. Steel

Various components are made of a variety of materials based on application. As a whole, roller coasters are typically specified as two types: steel or wooden. The designation is typically given based on what material the track itself is made of. Currently, according to the Roller Coaster Database, there are 4,241 steel and 185 wooden roller coasters worldwide. In the United States alone there are 762 steel roller coasters and 123 wooden roller coasters across the country (Harris, 2018). The differences between the two categories are very apparent and each have their own loyal fan-bases based on these differences. Each provides a unique experience for the rider. Wooden rides usually sway more and have a rough rickety course which is iconic to the classic roller coasters of the past. Steel roller coasters are able to be fabricated more precisely allowing for a smoother ride. The stronger nature of the steel and the production accuracy also permit high speeds and more complex shapes.

2.4 Components and Classifications

There are numerous variations of roller coasters across the globe and each one is unique based on its classification, components and location. Roller coasters typically all have basic features such as a track, carts and supports but they can vary greatly in design. Also, additional

components such as a lift or launching mechanism and the differing layouts of the tracks create a wide variety of thrill rides.

2.4.1 Lifts

If the roller coaster is a traditional gravity ride, which is only given energy at the beginning, then a lift is required. The initial lift will bring the carts to their highest point giving them potential energy to complete the course. To reach the highest point, there are a variety of lifts. In the early rides, rope was used as the lifting mechanism to pull the carts to the top of the incline. However, failures were common and newer technology has replaced the vintage design. A frequently used mechanism is a chain lift with an anti-rollback dog system. The chain is chosen specifically for the ride; the engineers must consider strength, durability and application. “The clack-clack-clack sound heard as a roller coaster train ascends the lift hill is due to a safety feature known as the anti-rollback (ARB) dog” (Weisenberger, 2013a). Most roller coasters now have this safety mechanism to keep the cars from rolling back down the hill if there were ever any failure in the lift. The clacking is the result of the dogs attached to the train moving up and over each tooth located on the track. If there were a failure, the train would only be able to roll back a small amount before the teeth on the track catch the dogs. And for extra precaution most rides have multiple anti-rollback systems in place (Weisenberger, 2013a).

Another type of lift used in some roller coasters is a cable lift or elevator lift. As the name indicates the train is brought to the peak by a cable. The cable replaces the chain and engages with the train at the bottom of the hill. It brings the train to the top and then continuously rotates from the bottom of the incline to the top and back. The cable is lighter than a chain allowing for a faster ascent. However, since there is typically only one connection point on the cable for the train to be hooked with, the interval between trains has to be at least one full rotation of the cable, causing increases in wait time if the hill is large (Weisenberger, 2013a).

Other, less traditional, lift systems have also been invented changing the track or the train to engage in the rise. In a vertical lift, a section of the track is lifted vertically with the cart on it (Weisenberger, 2013a). Once it reaches the desired height, it connects with the rest of the track and the cart is sent onto the course. Similar to an elevator, the cart with its riders gets on at one elevation and gets off at a different elevation.

Another technique used in lifts is to alter the characteristics of the track incline. At times a steeper incline may not be possible but there is not space for a gradual climb, in these cases a spiral lift can be used. Creating a corkscrew pattern vertically decreases both the pitch needed and the space needed. There are two common types of spiral lifts: electric spiral lifts and push spiral lifts. Electric spiral lifts contain motors on the trains themselves. Due to power and size restraints these motors do best in the gradual incline of the spiral lift (Weisenberger, 2013a). The motors propel the cart up along the hill. The push spiral lift is true to its name, the cart is pushed up the spiral ascent. The pushing component can be a rotating arm in the center of the spiral that guides the train up or it can be within the track pushing the cart up from behind (Weisenberger, 2013a). The last lift mechanism, and possibly one of the most interesting, is the Ferris wheel lift. This system contains a ride within a ride. The train is lifted through half of a rotation of the Ferris wheel to the peak of the lift before entering into the track (Weisenberger, 2013a). Although very uncommon, this lift is another example of the progression and innovation in roller coaster design.

2.4.2 Launching Mechanisms

Another defining feature found in some roller coasters is a launching mechanism. Whether the ride has an initial lift or not, the coaster could feature a means of launching the cart forward through the course.

Two popular technologies that are commonly used as launching devices are Linear Induction Motors (LIM) and Linear Synchronous Motors (LSM). Both systems use electrically controlled magnets to launch the train, however, they have their slight differences. LIM consist of electromagnets placed along the track that are directed at a metal fin on the underside of the train. As the fin passes through the magnets, they push the cart forward to the next set of magnets (Weisenberger, 2013b). This long succession of magnets quickly passes the train and its fin along the track to launch it into the next section of the course. For a LSM system there are also electromagnets attached to the track. However, instead of a fin there are naturally charged earth metals on the underside of the train. As the train moves from one set of magnets to the next, the magnets on the track switch from positive to negative. This switch pulls the train to a set of magnets on the track and then pushes the train away from the same set of magnets (Weisenberger, 2013b).

Other means of launching a cart into the course are pneumatic and hydraulic launchers. Both systems use storage tanks to store and compress either air or fluid to then use as means of powering the motor which quickly pulls the cart along the track. In hydraulic systems, nitrogen gas is compressed by pumping hydraulic fluid into the system. Once the gas is highly compressed it is released to power motors attached to a cable drum which rapidly winds the cable attached to the train, propelling it forward (Weisenberger, 2013b). Very similarly, the pneumatic launch system uses air versus other gases or fluids. However, as a result, typically pneumatic launches are not as powerful or smooth as hydraulic launches (Weisenberger, 2013a). Another launch system found in modern roller coasters is a wheel driven system. Wheels are lined along the track on either side of the metal fin on the bottom of the train. The wheels pinch, pass and push the fin forward along the track (Weisenberger, 2013b). This system is very comparable to a pitching machine, which uses two spinning wheels to launch softballs or baseballs.

2.4.3 Carts

The carts and trains of a roller coaster, just like most components, can vary based on the type and theming. Typically the body of the cars of a roller coaster are made of fiberglass materials. This material is easy to mold, lightweight and durable. The profile of the body can differ drastically and greatly contributes to the overall ride design. The profile will contribute to the effects of drag on the cart's movement throughout the course.

Within the fiberglass shell, the car usually contains the seating and restraints. Depending on the type of ride, different seating arrangements could be used and different numbers of people could be allowed to ride at once. A critical part to every ride is the safety restraints keeping riders safely secured in their carts. There are different styles of restraints depending on the forces they have to combat throughout the course. The two most common types of restraints are lap bars and over-the-shoulder restraints. Lap bars can be used to hold a rider securely in their seat in noninverting rides, and to prevent people from standing on less intense rides. Over-the-shoulder restraints hold passengers in on more intense rides. With more extreme forces acting on riders, such as in inversions and intense drops, these restraints assure that riders remain safely within the cars (CoasterForce, 2018a). Other variations of restraints include butterfly restraints and t-bars. Butterfly restraints act similarly to over-the-shoulder restraints; however, they close in on the

rider from either side versus from above. T-bars are a more cushioned and more secure version of a lap bar that also typically provide handles for the rider to hold on to (Zink, 2015).

Another important feature of the train is its wheels. The wheels are the main interaction and connection between the train and the track. When choosing the wheels for a ride various aspects must be considered, such as “low rolling resistance, high load endurance, smooth ride performance, and high durability” (Weisenberger, 2013a). The wheels on roller coasters used to be made of steel, however, the material has shifted to polyurethane to allow for a smoother ride and less wear on the track (Weisenberger, 2011a). Modern roller coasters typically have three types of wheels: road wheels, side friction wheels, and up-stop wheels. Road wheels are the wheels that ride along the top of the track, the wheels usually considered when imagining a moving object. Next, the side friction wheels are perpendicular to the road wheels. They travel along the side of the rails allowing the train to maneuver through turns without sliding off the track. Lastly, trains have up-stop wheels located below the track. These prevent the train from rising off the track and derailing. Through the advancements of roller coasters, the types of wheels were introduced to make the rides safer and capable of more advanced movements such as inversions.

2.4.4 Classifications

In addition to being classified by the materials which a roller coaster is made from, rides are also classified based on their layouts, dimensions, and components. The Roller Coaster Database has various main classifications for roller coasters that include sit-down, standup, inverted, suspended, pipeline, bobsled, flying, and 4th dimension. Some are self-explanatory such as sit-down and standup which refer to the seating position of the riders, but others have more complex features that denote their label. Although the majority of roller coasters fall into the sit-down category, there are numerous more innovative and intricate designs as well.

An inverted roller coaster has the carts rigidly secured below the track as opposed to the top side. Also attached below the track are suspended roller coasters. However, suspended designs are connected by a ball and socket system allowing the riders to swing separately from the track as they travel along the curves and turns of the course (Marden, 2018b). On a pipeline style roller coaster, the train does not ride above nor below the track. This design has “riders positioned between the rails” (Marden, 2018b). Bobsled roller coasters have very unique tracks.

They do not have defined rails for the trains to ride along; the course is a trough shape which allows the carts to move along inside the curving space. Two classifications of more intense roller coasters are flying and 4D. During a flying roller coaster riders are shifted to be parallel to the ground to experience the sensation of flying. Lastly, the 4th dimension roller coaster has additional mechanisms within the trains to create movement in the rider's seat outside of the direction of the course. The riders can be spun horizontal while traveling vertically and in some rides the movement is triggered by locations on the track creating the most dizzying experience (Marden, 2018b). Six examples of the classifications can be seen below in Figures 5-10.



Figure 5: Inverted Coaster (Fantacoaster, 2008) (left)

Figure 6: Suspended Coaster (Wikimedia Commons, 2014) (center)

Figure 7: Pipeline Coaster (Wikipedia, 2018) (right)



Figure 8: Bobsled Roller Coaster (McC, 2017) (left)

Figure 9: Flying Roller Coaster (Murphy, 2009) (center)

Figure 10: 4D Roller Coaster (Wills, 2009) (right)

2.5 Design Methods

2.5.1 Design Considerations

When a roller coaster is to be designed, various factors are considered and come into play for all aspects of the design. People of multiple backgrounds and priorities collaborate to design and create a ride that best fits the needs of the park and its guests. Designing a roller coaster

starts with an idea for the ride, which may or may not be for a specific amusement park or location.

During the concept phase, considerations such as the possible classification, components, theming and intended demographic may be taken into account. All considerations are related; a ride intended for a younger audience may not contain as many intense features such as inversion and large drops. An important aspect to decide early in the design phase is who will be riding the ride and what type of experience do you want them to have. At this point, although it is not necessary, a possible theme or particular park may be decided.

Once there is a relatively concrete idea on the design concept, the more particular details must be considered. The location of the roller coaster will greatly impact its overall design. Attention is due to important items such as the environment, the ground conditions, the area resources and the local weather. Typically the new ride will mesh with the existing structures in the park, so the park's current environment has to be considered. Also, the environment of the area as a whole may play a role. For example, if the park is located near an airport perhaps it may not be as tall above ground as intended so tunnels may be incorporated to achieve the same desired effect of height. Another factor from the park's surroundings could be local codes and standards for structures. Both the national and local codes of the area must be followed when designing a roller coaster. The weather the roller coaster will be subjected to is also an important consideration. Roller coasters can be built inside, outside or partially both. But whatever the case, the elements which the material and riders are exposed to come into play. Materials that can withstand both the load conditions and the weather such as galvanized steel may be chosen. Different roller coasters located in different weather conditions around the world will have changing priorities based on the situation. The riders' exposure is also factored into the design. The train configuration or style may be altered to create the best riding experience depending on the common weather of the location.

During design, forethought of the manufacturing and construction must also be included. The ground conditions and area resources should be considered. The roller coaster will have to be safely supported by the ground on which it is located. And also the workers building the roller coaster must have a safe environment to work in when constructing the roller coaster. A large factor that influences a lot of decisions in all aspects of the roller coaster life cycle is cost.

Something that will impact cost is the availability of resources close to the roller coaster site. Manufacturing large steel tracks and shipping them across oceans and countries may not be the best economic decision if a different location is available for the site. Throughout the design of a roller coaster the main considerations are cost, safety and experience.

2.5.2 Safety Standards & Regulations

When designing a roller coaster the most important consideration is the safety of the riders and those surrounding the ride. Although roller coasters can vary greatly in all aspects, there have been rules and guidelines set to assure the safety of all no matter what the ride entails.

2.5.2.1 ASTM Standards

As with most engineering processes, there are set standards and regulations for roller coasters. In 1978 the ASTM International Technical Committee F24 on Amusement Rides and Devices was created (ASTM, N.D.). Three influential standards drafted by the committee are listed below:

- ASTM F770: Standard Practice for Ownership, Operation, Maintenance, and Inspection of Amusement Rides and Devices
- ASTM F1193: Standard Practice for Quality, Manufacture, and Construction of Amusement Rides and Devices
- ASTM F2291: Standard Practice for Design of Amusement Rides and Devices

These standards outline the regulations for various aspects of roller coasters such as design requirements, inspection protocols and owner responsibilities. The scope of ASTM F770 is to “provide guidelines for operations, maintenance, and inspection procedures for amusement rides and devices to be performed by the owner/operator” (ASTM, 2017a). These standards state the requirements the owner is responsible for during the operation, maintenance and inspection. Specific items addressed are evacuation routes on the ride and signage. The regulations also state guidelines such as having a preventative maintenance plan and daily pre-opening inspections. Techniques of maintenance and inspections will be detailed in later sections.

The scope of ASTM F1193 is to “establish the minimum requirements for a quality assurance program and the manufacturing of amusement rides and devices (including major modifications)” (ASTM, 2017b). These guidelines outline more procedures pertaining to the quality assurance and manufacturing of roller coasters through maintenance and inspection plans.

However, this section is directed more towards the engineers' and manufacturers' responsibilities. There must be detailed drawings and plans specifying the materials of different components. Details such as manufacturing, constructing and maintenance of the particular parts must be included.

Although all of the regulations must be taken into account during the design of a roller coaster, the regulation that specifically lays out the guidelines for design is the ASTM F2291. This regulation is commonly referenced in the previously two mentioned sections. The purpose of ASTM F2291 is “to provide designers, engineers, manufacturers, owners, and operators with criteria and references for use in designing amusement rides and devices or a major modification for amusement rides or devices” (ASTM, 2017c). The section begins by focusing on the interaction of the ride with the rider. The safety of the rider is the highest priority in the design of the ride. For example, the rider's envelope is specified in the schematic below (Figure 11). This envelope is the area which must be clear for the rider through the course. It is measured by the average human reaching in all directions with an extra 3 inches added around the perimeter. If objects must enter the envelope, such as at loading and unloading, they must have safety fails to allow for minimum injury (ASTM, 2017c).

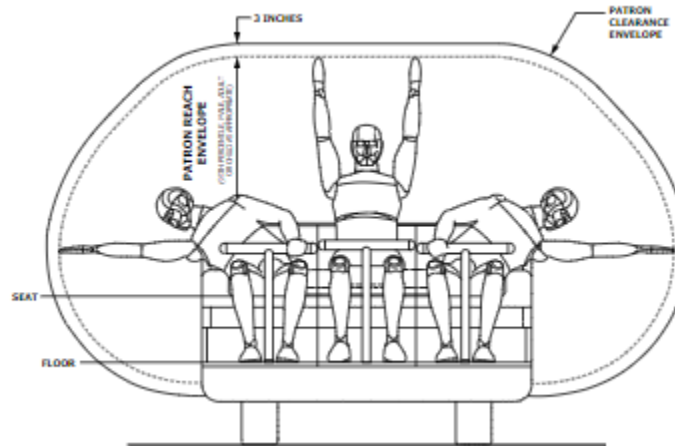


Figure 11: Rider Envelope (ASTM F2291)

The standards also state that the engineer or designer must determine the average height and weight of riders that can safely ride. This determination will specify the upper and lower bounds for rider sizes for the particular ride. Another regulation found in this section pertains to

restraints. Although it is required that each rider be provided with his or her own individual restraint, it is not required to create a redundant system for fail purposes (ASTM, 2017c).

After regulations directly relevant to riders, the subsections for supports, rails and foundations are found. It is stated that all components of the roller coaster must be designed for 35,000 operational hours (ASTM, 2017c). An operational hour is anytime the ride is in use. Due to the high risk of fatigue, this criteria is crucial and there are few exceptions stated. Next, the practice defines the different loads and that each component of the system must undergo a structural analysis. Factors of safety are also stated, including provisions when using both LRFD and ASD approaches. An important factor of safety is for the anti-rollback devices. When undergoing an impact load the factor of safety is 2 (ASTM, 2017c). This is because this device will catch the train if there was ever a failure in the lift mechanism, keeping the train from wildly traveling in the opposite direction on the course. The standards also reference other codes that must be checked depending on the materials used such as IBC and AISC (ASTM, 2017c). These regulations conclude by outlining electrical, mechanical and partitioning systems, such as the placement of fencing.

2.5.2.2 G Forces

The experience which a rider has while on a roller coaster is the product of specifically designed components and features. Two impactful variables that are designed for the rider's experience are G forces and velocity. G forces are the force resulting from a person's change in acceleration or directions; a g is a value that is multiplied by the acceleration of gravity to achieve the equivalent force felt by the person. G forces can be in three orientations. Vertical G forces act perpendicular to the track, pushing the rider into their seat or lifting the rider out of their seat. Linear G forces are felt parallel to the track. They are the product of acceleration or deceleration and can push against a rider's front, pressing them into the back of the seat or push the rider forward, in cases such as braking. Lastly, there are lateral G forces. Lateral G forces also typically act perpendicular to the track, but occur on turns and curves. Lateral g 's are the forces that squish one rider against the other on fast turns.

The limits of the human body under G forces depend on the direction, type and duration. During vertical G forces, positive g 's act on humans from head to toe and negative g 's act on human from toe to head. The typical cutoff for vertical G forces in roller coaster is from 4 or 5 g 's

to -2 or -3g's (Tyson, 2007). These limits are to sustain a comfortable ride for the average human. If too high of G forces are experienced then the blood will rush out of the head causing the person to pass out. If the negative G forces reach too large of values then too much blood will go towards the brain also having detrimental effects on the person. However, in situation such as launches, fighter pilots and astronauts may experience up to 10g's. But these professionals have special suits and specified training for sustaining these forces. The highest recorded vertical G forces during a roller coaster was on the Tower of Terror in South Africa at 6.3g's. Passengers were able to survive this ride because of the short duration of the force, lasting only seconds. The ASTM F2291 regulations provide a graph to determine the acceptable vertical G forces depending on the duration time, as seen in Figure 12 below.

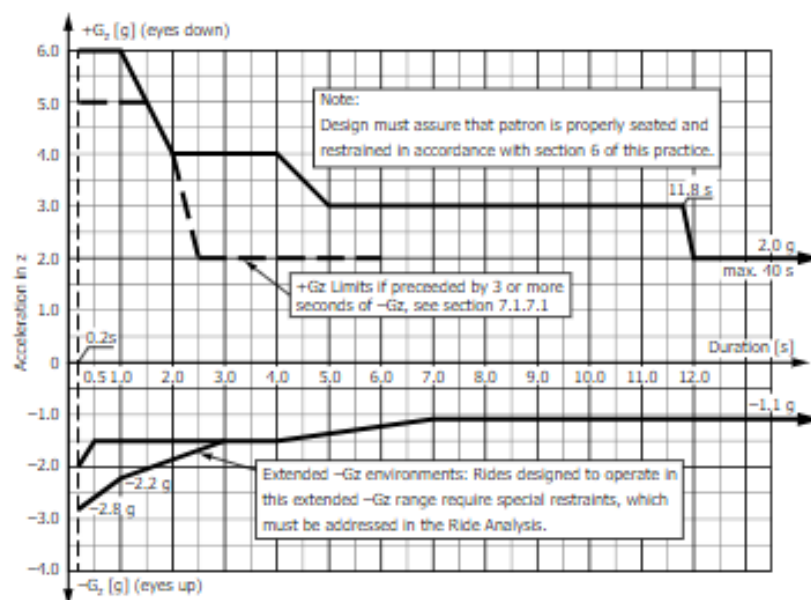


Figure 12: Vertical G Force Duration Limits (ASTM, 2017c)

Humans can tolerate much higher linear and lateral G forces compared to vertical G forces. The average human can comfortably survive 17g's coming towards their front and 12g's coming towards their back. The highest recorded linear G forces survived was by John Stapp in 1954. The Air Force physician famously experienced 46.2g's when he strapped himself to a rocket-powered sled (Tyson, 2007). He lived to the age of 89 but suffered vision problems due to his tests (GForces, 2010). Lateral G forces are typically not specified because the level of risk depends on the riders' restraints. If the rider is properly secured to the seat to prevent lateral movement then large lateral G forces can be withstood without injury (CoasterForce, 2018b).

2.5.3 Software

Various commercial and in-house software is employed by roller coaster designers to make the newest thrills. Common products used are AutoCAD, EnginSoft, Inventor, NoLimits, and SolidWorks. The software is used for an array of purposes, from layout to structural analysis to simulation.

A standard software for most engineers to use is AutoCAD. This software can be used to model and dimension the roller coaster's profile. The shape of the overall ride can be constructed and various measurements can be found. AutoCAD is very useful during the design phase, laying out the track configuration in one plane. Construction documents and reports can also be generated from the software for the later phases of the roller coaster's design and construction.

Another software used in the design of roller coasters is EnginSoft. EnginSoft has the capabilities of performing a finite element analysis on the roller coaster's structural components. The software will run analyses on codes and standards set for the roller coaster. The engineer is also able to create a computational model of the ride which is able to be modified throughout the design and construction process. Additional beneficial features are seismic analysis and fatigue checks (EnginSoft, N.D.).

A second Autodesk product that is helpful in amusement ride design is Inventor. Inventor gives the engineer the capabilities of designing parts of the ride such as the mechanical systems. Material properties, geometry and interactions can be investigated in this software before it is created by the manufacturers.

The software most commonly used by roller coaster designers to simulate their creations is NoLimits. Although labeled as a game, its advanced rendering and physics integration are of great use to professionals. Designers can designate the shape of the track by drawing the vertices comprising the curves and spans. Numerous premade objects such as banked curves and loops can be added and adjusted by specifying the desired dimensions. Once the shape of the course is designed, the user can move on to add in different types of support columns or generating a wooden truss system through the program. The terrain and surrounding rides can also be added and edited. After the design is complete, switching into "Play" mode will allow people to ride the rendered simulation of the roller coaster. Various perspectives can be chosen such as point of view or flying alongside the train.

Lastly, another software that can be used for both modeling and analysis is SolidWorks. This software provides the user the capabilities of modeling basic to complex shapes. Loading conditions both statically and dynamically can be applied. Animations and analysis reports that are produced are helpful to engineers in designing the capacities of the components comprising the roller coaster.

2.6 Construction

The phases of construction of a roller coaster depend on the type, materials and location of the roller coaster. To begin construction, the plot of land is prepped through surveying, testing and leveling of the ground. Just as in a building, the first feature added to a roller coaster is the foundation system. Typically tall piles are dug into the ground, the depth depending on the ground conditions. Once the foundations are set, the supports structures are built. Steel supports are factory made and shipped to the job site to install. Wooden supports can be cut and installed all on site.

A similar process occurs with the tracks depending on the materials. Wooden tracks are typically made from 5 to 8 boards stacked together (Roller Coaster, 2018). The stack is altered to create the curves and inclines of the track. Along the top of the wooden tracks, steel plates are attached to prevent excessive damage from the train. Along areas of the course where the cart raises and the up-stop wheels are engaged, steel plates are placed on the bottom of the track as well. Through the design, the placement is known for the upward force to limit the use of extra plating on the bottom side of the track. Wooden coasters are purposely designed and constructed to sway to allow for an exciting effect and to disperse the stress on the components. Because wooden roller coasters are typically all built on site, environmental factors and human error can become more prominent. The time of construction can be greatly influenced by the weather since the workers must assemble almost all pieces from scratch onsite, and the lack of manufacturing standards can allow for a higher variance in precision.

In comparison, steel tracks are usually created in factories and shipped to the site. This allows for a more precise shape to be formed. The machine standards can create designs to support higher speeds and more extreme features such as loops. Once delivered to site, the segments of the track are bolted together by crews. Once construction is complete, testing and

adjusting of parameters occurs; all components are assured for quality and completeness. Before the ride opens to the public, the theming and landscaping is placed to finalize the ride.

2.6.1 Economics

Roller coasters are a large investment for an amusement park to build. It takes both time and money to manufacture and assemble all the components on site. The cost is another defining difference between wooden and steel roller coasters. The average cost for building a wooden roller coaster is \$10 million, but steel roller coasters are twice as much at \$20 million (Weisenberger, 2013a). Although the initial cost for the steel roller coaster surpasses the wooden roller coaster, the financial benefits may be seen over time. Steel coasters are typically more durable and need less expensive maintenance, such as replacing track segments. This can result in the overall cost of the steel coaster being less than the wooden ride if the entire lifecycle of the roller coaster is analyzed.

Although the averages are around \$10-20 million, as always, there are some outliers. A wooden roller coaster, Giant Dipper, was built in California in 1924. It took construction crews only 47 days to build and set the owners back \$50,000 (Santa Cruz Beach Boardwalk, N.D.). Compared to today, the ride would have cost only just above half a million dollars. And it clearly paid for itself considering that it is still in operation today. On the other end of the spectrum is one of the most expensive roller coasters ever made. The title belongs to Expedition Everest at Disney World's Animal Kingdom. The ride cost upwards of \$100 million to make (CoasterForce, 2018c). However, this roller coaster is not solely a track, it is constructed within a steel reinforced mountain which raises the price.

2.7 Maintenance and Operation

The maintenance and operation of a roller coaster is just as crucial of a part of its life cycle as the design and construction. Both preventative and reactive maintenance have to occur frequently. Once the roller coaster is running and open to the public, the goal is to maintain its quality to provide exhilarating rides for all who attend the park.

As mentioned above, daily pre-opening inspections are required through the ASTM F770 regulations. The inspections may vary in content and length depending on the type and size of the ride, but there are some common tasks most technicians perform before the ride opens each day. During visual inspections of the track and any weldments of the stairs or rails, they look for

cracking or wear. The high stress areas of the ride such as the bottom of drops and the areas where the up-stop wheels are engaged get special notice (Weisenberger, 2011b). Each braking system is also checked and the electrical wiring is assured to still be in good working condition. The components of the lift hill such as the safety catches and lift mechanism must be inspected. The items on the trains like the safety restraints and lubricants must also be looked at. Once the initial inspection is complete, the ride will be sent on an empty run so inspectors can listen and watch for anything unexpected. It is required that the ride be cycled through so many times before it can be opened. The number of cycles is dependent upon the type of ride and size. Lastly, the technicians may take a ride to see if they can feel anything out of the ordinary along the course. This process can take multiple hours but is it for the safety of all involved and must be performed correctly. In addition to the daily inspections, there are also less frequent inspections. For example, yearly all the trains are disassembled and checked before being rebuilt.

Other yearly inspection tasks use more sophisticated equipment to check the quality of the tracks. Equipment for nondestructive testing such as magnetic particle testing, radiography, and ultrasound thickness testing are used (Applied Technical Services, 2017). These techniques allow for a more in-depth inspection compared to the daily visual inspections. Nondestructive testing can convey if there is a defect within the material or perhaps if there is a crack too small for the human eye to see.

Throughout the United States more than 300 million people ride the roller coasters of amusement parks in a year (Yang, 2017). Although this high attendance rate increases revenue of the parks, the wear on the coaster is an issue. Typically an average roller coaster can have an estimated life span of 25 years (Roller Coaster, 2018). However, replacements and repairs have to occur to accommodate the frequent use. The wooden track supports of a wooden coaster may have to be replaced every 4-7 years throughout its life (Roller Coaster, 2018). Rehabilitating wooden roller coasters with steel components has become a technique for limiting the maintenance cost while keeping the traditional wooden personality.

2.8 Progressions and Possibilities

New and improving technology and understanding of concepts has promoted continual progress in roller coasters. Over the hundreds of years of roller coaster history, rides have changed from wooden cars traveling down slow inclines around 20 mph to fiberglass trains being

launched into inversions and spirals at over 100 mph. And the prospects for more improvement and innovation is promising.

Advancement could come in materials, track systems and ride concepts. The majority of roller coasters are built from steel or wood, but there are many more materials to test. These materials could be used for not only the track and supports but also other components such as the lift chains and braking systems. It has been suggested to create wheels that can travel silently along the tracks, allowing for the rider to focus more on the sensations or theming (Bessette, 2015). New materials that are strong in all loading conditions could be used for the structural supports. Or creating hybrid systems where the material is chosen based on the design criteria of the section could optimize resource usage and minimize costs.

Popular concepts already being employed in rides today are virtual reality rides and interactive rides. In virtual reality rides, riders would still experience the sensations while traveling along the course but there would be no limits for the theming. The person's surrounding would be digital and react to the person's movement along the course. Another innovative concept is interactive rides. During these rides multiple courses could be available and onboard surveys could determine which route the train will follow based on what the people want (Sim, 2014).

Modifying the track and the interaction between the track and train have been discussed for future roller coasters. An interaction where the train and track never touch because of magnets would drastically minimize the wear and tear of the course because there would be no friction (Ohio University, N.D.). Another idea is to create tracks from air tunnels. The trains will float on the air in the tubes and be propelled along smoothly without ever touching the course (Ohio University, N.D.).

3.0 Methodology

To complete the goal of designing a roller coaster four distinct steps were taken. These steps were determining the shape and components, designing the structure, testing the materials, and modeling and simulating the results. The preliminary components included were based on the objective of the project, which is to see the differing loading correlating to the type of component. Various lifts, hills, loops, curves, valleys and brakes were incorporated. With the components, an energy analysis was calculated to assure a successful and safe completion of the course. Once the geometry and dimensions of the track was established, the structural support system needed to be designed and various material properties tested for the supports. The entire course and supports were modeled and viewed in a simulator once completed.

3.1 Shape and Components

As mentioned above, the components chosen to be included in the course were incorporated with the objective of the thesis in mind. Each component was given preliminary dimensions and an energy analysis was calculated to assure the cars would complete each component successfully. Also, the velocity, accelerations, and G forces associated with each part were calculated to compare to standard safe limits. Depending on the initial results, the dimensions and geometry were adjusted accordingly. The velocities of the previous feature were carried to the next to create a complete profile of the course.

3.1.1 Lift Hill

Designing the lift hill consisted of determining the type of lift and then finding the variables related. For this thesis a traditional chain lift hill was chosen. Therefore, the incline, distance, initial and final velocities, and train parameters are required. Balancing the energy entering and leaving the system, the overall work necessary for the lift to bring the train to the top was found. The initial kinetic energy, initial potential energy and work is set to equal the final kinetic energy and final potential energy, as seen below.

$$KE_1 + PE_1 + W = KE_2 + PE_2 \quad (\text{Eq. 1})$$

$$\frac{1}{2}mv_1^2 + mgh_1 + F_L d - F_{RF}d - F_{BF}d - F_D d = \frac{1}{2}mv_2^2 + mgh_2 \quad (\text{Eq. 2})$$

Throughout the calculations of the course both friction and drag are considered to determine their effects on the progression of the cart. Friction is divided into rolling friction and bearing friction. Rolling friction is the result of the wheel on the track. The force caused by rolling friction is a result of the normal force of the weight of the train on the track, the coefficient of rolling friction, and the radius of the wheel. To determine the normal force of the weight of the cart on the track at any given point various factors must be known. If the part of track being analyzed is linear then the incline (\emptyset) and the weight (w) of the cart are needed to calculate the normal force in the equation below.

$$N = w \cos(\emptyset) \quad (\text{Eq. 3})$$

However, if the track has a radius then additional parameters such as the radius of the track (r) and the velocity are included.

$$N = w \cos(\emptyset) + \frac{mv^2}{r} \quad (\text{Eq. 4})$$

Referring to a past roller coaster MQP, a common wheel radius (R) and coefficient of rolling friction (b) were determined. Using similar values for a wheel on a steel rail, the radius of the wheel was set at 5 inches and the coefficient of rolling friction at 0.01 (Gallerie, 2002). These variables were incorporated into the equation to find the force of rolling friction. To then find the work due to rolling friction, the force was multiplied by the length of track which it was applied over.

$$F_{RF} = \frac{Nb}{R} \quad (\text{Eq. 5})$$

$$W_{RF} = F_{RF}d \quad (\text{Eq. 6})$$

Using the same normal force due to the weight of the cart (N) above, the bearing friction was determined. The bearing friction is the energy lost due to the interaction between the wheels and the bearings attaching it to the cart. The force due to bearing friction is a product of the normal force of the weight of the car and the coefficient of bearing friction. The coefficient of bearing friction (μ) can differ depending on the bearing materials, setup and lubrication. For this study it was set to 0.0018 (Gallerie, 2002). As with the force of the rolling friction, the force of the bearing friction is multiplied by the distance over which it acts to find the work.

$$F_{BF} = N\mu \quad (\text{Eq. 7})$$

$$W_{BF} = F_{BF}d \quad (\text{Eq. 8})$$

The last outside force that was incorporated into the calculations was drag. Drag is the resistance felt caused by the density of the material which something is traveling through, the profile of the object and the velocity. The car will be travelling through air with a density (ρ) of 0.0765lb/ft³. Based on research of basic roller coaster cart shapes, it was determined that the front profile of the train is 4 feet wide and 3 feet tall. Based on this profile the drag coefficient (C_D) is 1.8, from the coefficients and profiles of railroad trains (Gallerie, 2002). The force and work due to drag were found through the equations below.

$$F_D = \frac{1}{2}\rho v^2 AC_D \quad (\text{Eq. 9})$$

$$W_D = F_D d \quad (\text{Eq. 10})$$

Once calculating the power needed to reach the peak of the lift, taking into account rolling friction, bearing friction and drag, the acceleration and time of the lift were found using the equations below (Weisenberger, 2013a).

$$v_f^2 = v_0^2 + 2ad \quad (\text{Eq. 11})$$

$$v_f = v_0 + at \quad (\text{Eq. 12})$$

3.1.2 Initial Drop

Once the train reaches the peak of the lift, it is released and gravity brings it through the first drop. The most important thing that was considered when designing the initial drop was to limit the G forces exerted on the riders. To do this the bottom of the hill has a curved descent to decrease the force on the passengers. Calculating the radius of curvature starts by deciding the amount of g's which you want the rider to experience. The vertical g's felt by the rider is the force applied by the ride and the force applied by gravity, which is 1g (Weisenberger, 2013a). Once calculating the force applied by the ride, the centripetal acceleration (a) can be found by multiplying G by gravity.

$$G_{felt} = G_{ride} + 1 \quad (\text{Eq. 13})$$

$$G_{ride} = \frac{a}{g} \quad (\text{Eq. 14})$$

Once the desired centripetal acceleration is established the needed radius of curvature can be calculated using the expected velocity at the bottom of the straight hill. The equation to relate the three can be seen below (Weisenberger, 2013a).

$$r = \frac{v^2}{a} \quad (\text{Eq. 15})$$

The start of the curve was found by finding the point on the circle of the designated radius where the initial straight incline was tangent. After creating the profile of the initial straight decline and the curve, the hill's shape was complete. To find the velocity of the cart at the bottom of the hill, the information pertaining to the cart's movement and the track at increments of 10 horizontal feet were found. In AutoCAD the drop's profile was drawn and the coordinates of each increment were recorded. Using Excel, each step's parameters were entered and the pertaining information was calculated. Using the information from the previous increment, the velocity at each point along the drop was found taking into account friction and drag in the energy equation.

3.1.3 Clothoid Loop

Calculating the dimensions and associated effects of the loop started with deciding the desired height of the overall loop. The height must not be higher than the lift hill. Since the ride is only propelled by gravity after the initial lift, then the highest point must be the first hill. This is because as the ride progresses the train will lose energy to friction and drag.

Approximate values for the desired vertical G forces at the entrance and the peak of the loop were first decided. The loop will not be a perfect circle because that would require a constant radius of curvature. A constant radius would create too high of vertical G forces when considering the change in velocity throughout the loop. The clothoid loop is teardrop shaped; there is a radius of curvature at the entrance, a different radius towards the peak, and then the same radius as the entrance at the exit.

Using the same equations detailed above, the tracks' angle was taken into account to calculate the velocity of the train due to the change in height, friction and drag along the track. Once the velocity was calculated at each 10 foot horizontal increment, the corresponding vertical

G force values could be found. Finding the centripetal acceleration, comparing velocity squared over radius of curvature, and dividing by the acceleration of gravity gave the g's at each point. Both the resulting vertical G forces and velocity had to be checked. The dimensions, such as the height and radius of curvature, could be altered to assure the train is able to complete the loop and to limit the vertical G forces felt by the riders.

3.1.4 Straight Away

To calculate the velocity at the end of a straight away, the initial velocity and the effects of friction and drag must be considered. Each area of the track considered a straight away is at 10 feet above grade and consists of a flat straight strip between other components. The equation used before in the energy balance can calculate the velocity the train has at the end of a certain length of track.

$$\frac{1}{2}mv_1^2 + mgh_1 - F_{RF}d - F_{BF}d - F_Dd = \frac{1}{2}mv_2^2 + mgh_2 \quad (\text{Eq. 16})$$

$$\frac{1}{2}mv_1^2 - F_{RF}d - F_{BF}d - F_Dd = \frac{1}{2}mv_2^2 \quad (\text{Eq. 17})$$

3.1.5 Banked Curves

To change direction so the train can travel in a circle back towards the station, two banked curves were added. The velocity from the preceding component was used as the starting velocity for the curve. A radius of the turn must be decided to start the calculations. Next, using the equation for a circumference of a semicircle the length of the curve can be found.

$$\text{length of turn} = \pi r \quad (\text{Eq. 18})$$

The speeds of the train can be found along the length of the turn at 10 foot increments through the above energy equations. An important feature to design for the banked curves is the lateral G forces a rider experiences. The banking angle of the curve is to prevent too high of lateral forces, injuring the riders. The equation to determine the bank angle of the curve to result in 1g is below (Weisenberger, 2013a). In this equation theta is the angle of the embankment, v is the velocity at that point along the curve, r is the radius of the curve and g is the acceleration of gravity.

$$\tan(\theta) = \frac{v^2}{rg} \quad (\text{Eq. 19})$$

3.1.6 Hills and Valleys

The hills later in the course were designed in a similar way to the first drop after the lift hill. The track was divided into segments of 10 foot horizontal pieces. However, this length was adjusted to find the parameters of certain points on the hills such as the start, curvature changes, peaks, base of the valleys, and the end. Arbitrary heights were chosen for the hills and curves to best fit the design of the path, which was drawn in AutoCAD. Once the basic profile was drawn, the pertaining information of each point along the hills were found and inputted into the Excel sheets.

Using the already established energy balance equation and the velocity from the previous feature on the course, the velocities of each point were calculated. From the velocity and radius of curvature, the centripetal acceleration was found, similarly to the initial drop. Once the centripetal acceleration was calculated the applicable G forces at each point could also be calculated. Depending on the velocities and G forces produced, the shape and dimensions of the hills and valleys were adjusted to reach acceptable values. For example, if the vertical G forces were too great at the bottom of a valley then the radius of curvature could be increased, decreasing the centripetal acceleration and G forces resulting from the incoming velocity. If the velocity reached zero, perhaps at the top of a peak, then the Excel would produce an error for the remaining segments. This is because the kinetic energy had decreased too drastically so the energy balance was no longer true and the ride would have theoretically stopped. To change the velocity of a component in the hills and valleys, the heights of the starting hills were increased while the end hills were decreased. This promoted more energy being converted to kinetic energy for the later hills, increasing the velocity to a positive values so the ride continued.

3.1.7 Braking

Once the course is completed, the braking system has to be considered. Unless all the energy is dissipated through friction and drag throughout the ride, then a braking system must be added to slow the velocity of the train as it returns to the station. Various types of braking may be employed but the key of the design is to slow the riders at a deceleration that will not cause injury. Using the entrance velocity and the desired length of the braking system, the power contributed by the system can be calculated. Adjusting the energy equation to account for braking will result in the formula below.

$$\frac{1}{2}mv_1^2 + mgh_1 - F_{RF}d - F_{BF}d - F_Dd - F_Bd = \frac{1}{2}mv_2^2 + mgh_2 \quad (\text{Eq. 20})$$

The added variable of F_B represents the force the braking system exerts. When this force is multiplied over the distance it acts, the work of the braking is found. For the design, a constant braking force was applied over the system. This value was adjusted to result in a reasonable speed for the train's entrance back into the station; this speed was determined to be around 12 mph. The time required for the braking system was determined by dividing the track distance by the average velocity over that span. This gave the time it took to travel each segment. The sum of the segment times results in the time during the entire braking system.

3.2 Support Structures

The structural supports throughout the course were all initially designed using typical steel material properties. This was done using basic principles of steel column design. The column supports were designed for both axial loading and bending moments. The supports have to hold the weight of the track and the forces caused by the train. Each support was designed to have a capacity that was sufficient for both a moving and stationary train to mimic the forces experienced during the ride's use and in case of a stall in the ride.

The columns were placed at critical locations along the course such as peaks, valleys and curve changes. Then the supports were evenly distributed between the designated critical points. The maximum spacing along the track for the supports was decided to be no more than 40 feet. This value comes from the design of the track itself in Gallerie's MQP, determining that the maximum span the track could accommodate was around 40 feet (Gallerie, 2002).

3.2.1 Bending Moment in Column Supports

Starting from the initial lift hill, supports were placed at the critical points. These included the bottom of the lift hill, the top of the lift hill, the curve change in the initial drop, the bottom of the initial drop, and so on accordingly. The bending moments in the supports were calculated by finding any horizontal forces caused by the angle of the track and the movement of the train. This force was then multiplied by the height of the column to determine the bending moment generated by the track and the train.

The horizontal forces were calculated by finding the horizontal component of the load at each support. The load consisted of the effect from the normal force and the G forces. The

horizontal component of the normal force multiplied by the vertical G forces and divided by gravity gave part of the horizontal force on the column from the train's movement. The second part of the horizontal force came from the train's linear G forces. The linear G forces were determined by finding the acceleration of the train between each support. Having only the velocities and the track distance the accelerations were calculated using the following equation. The change in velocity is divided by the distance divided by the average velocity.

$$a = \frac{(v_2 - v_1)}{d/\bar{v}} \quad (\text{Eq. 21})$$

$$\bar{v} = \frac{v_2 + v_1}{2} \quad (\text{Eq. 22})$$

This acceleration was then divided by the acceleration of gravity to produce the G forces. Even though these are the linear G forces they are still relative to the value of the acceleration of gravity. Next, the weight of the train was multiplied by the linear G force to determine the force the train exerts on the column depending on its linear acceleration. The horizontal component of this forces that runs parallel to the track will be the second part contributing to the bending moment on the columns. Once both horizontal forces, from the train and its movement, were calculated it was multiplied by the column height to establish the bending moment. The train was determined to be a live load so the loading was also multiplied by 1.6 in accordance to LRFD provisions.

Next, the required plastic section modulus for each column was determined based on the bending moments. Using the yield strength of the steel (F_y) and the bending moment (M_u) calculated above, the limiting plastic section modulus (Z_x) was found. Equation F2-1 from Chapter F in the AISC Steel Manual for Design of Members for Flexure was used (AISC, 2011).

$$M_u \leq \phi M_n = \phi F_y Z_x \quad (\text{Eq. 23})$$

To begin, a standard 20 inch diameter solid steel column was used for each location. The capacity of the columns were calculated by multiplying the plastic section modulus of the column by the yield strength of the steel and phi ($\phi=0.9$). The plastic section modulus was found by cubing the diameter and dividing the results by 6. The capacity of each column was then compared to the bending moment to determine if the size was sufficient for the loading. In cases

where the bending moment exceeded the capacity the column size was increased. For ease of calculation and repetition in the design, column sizes were chosen from 5, 10, 15, 20, 25, and 30 inch diameters. The diameter greater than and closest to the required diameter for bending, found from the required section modulus, was selected and tested for compressive strength.

3.2.2 Axial Loading in Column Supports

To begin the compression design of the structural supports, the axial forces within each support along the track had to be determined. The calculations of the shape, the normal force, velocity, radius of curvature, centripetal acceleration and G forces were compiled to determine the necessary forces on each column.

First, the force of a stalled ride was found. This was done by calculating the vertical component of the normal force caused by the weight of the car and the force caused by the weight of the track. The track's weight was determined by finding the tributary area that each column needed to hold. This was half the distance to either support on both sides of the current column.

Next, the axial force of the ride in motion was determined. The weight of the track was calculated in the same way as the stalled ride; the tributary area and weight of the track per foot were multiplied. The axial force was determined by multiplying the vertical component of the normal force by the vertical G forces and then dividing by gravity to get the value into units of kips. The vertical component of the linear force on the train from the linear G forces, as calculated above, was also found. The total axial force applied to each column was the sum of the track's weight and the train's weight accounting for the effects of the G forces during motion. The loads due to the track were designated as dead loads and those due to the train were live loads. The load combination $1.2DL+1.6LL$ was used to factor the loads in accordance with LRFD procedures.

Once the axial forces were determined for each column, the required areas were calculated. To begin the standard 20 inch diameter solid steel column was used for each location. The slenderness ratio was found for each column using the equation below, taking into account the K value pertaining to the end conditions (K), the column length (L) and the radius of gyration (r).

$$slenderness = \frac{KL}{r} \quad (\text{Eq. 23})$$

Using Equations E3-1 and E3-2 of Chapter E in the AISC Steel Manual for Design of Members for Compression, the capacity of each standard 20 inch column was calculated (AISC, 2011). The slenderness ratio for each column was compared to the equation below.

$$\frac{KL}{r} \leq \text{or} > 4.71 \sqrt{\frac{E}{F_y}} \quad (\text{Eq. 24})$$

Depending on the outcome of the inequality, different equations were used to calculate the critical stress of the column.

$$\frac{KL}{r} \leq 4.71 \sqrt{\frac{E}{F_y}} \quad F_{cr} = [0.658^{\frac{F_e}{F_y}}] F_y \quad (\text{Eq. 25})$$

$$\frac{KL}{r} > 4.71 \sqrt{\frac{E}{F_y}} \quad F_{cr} = 0.877 F_e \quad (\text{Eq. 26})$$

The elastic buckling stress (F_e) for both critical stress equations was calculated using the following equation.

$$F_e = \frac{\pi^2 E}{\left(\frac{KL}{r}\right)^2} \quad (\text{Eq. 27})$$

Once the critical stress was established, it was multiplied by the area of the column and phi ($\phi=0.9$) to calculate the nominal compressive strength. This compressive strength was then compared to the axial loading of each column to determine if the column size was sufficient for each location, as seen below.

$$P_u \leq \phi P_n = \phi F_{cr} A_g \quad (\text{Eq. 28})$$

Next, the capacities and loading were compared using the new diameters found from the bending moment calculations. The same equations as above were used, however different capacities were determined because the area and radius of gyration changed with the column diameter. When calculating the capacities of the new column diameters, attention had to be paid

to the slenderness ratio. For serviceability purposes, the slenderness ratio should not exceed 200. However, because of the low loads and high heights of some of the columns the slenderness ratio was very large. The diameters had to be adjusted to bring their value below 200. Then the diameters were checked to reassure they were still sufficient for both bending and compression.

3.3 Materials

Once the locations and forces were determined for each structural support, the material properties could be adjusted. This was done to see the effects the material properties of the steel had on the capacities of the columns. Two important material properties were tested, yield strength and modulus of elasticity.

Using the already established Excel sheet which calculated the capacities for both bending and compression of the columns, the material properties were tested. The analysis was done on the new diameters of the columns determined to be the best options for the control scenario. The control yield strength was set to be equal to 50ksi and the modulus of elasticity was set at 29,000ksi. To adjust the yield strength, values of 60ksi and 35ksi were used to represent an increase in yield strength and a decrease in yield strength respectively. These increases were 20% and 30% of the original property. The same percentage increase and decrease were used to alter the modulus of elasticity. The new values were 34,800ksi and 20,300ksi. The required section modulus for bending was found for the two new yield strength conditions and compared to the section modulus of the column cross sections. These ratios of bending capacity were plotted on the same graph to see the change due to yield strength change in the bending capacity. Similarly, the new compressive capacities were found for the four new conditions and compared to the compressive load of the system. These ratios of compressive capacity were also plotted on the same graph for analysis.

3.4 Model and Simulate

Once the profile of the course was established and the supports designed, the roller coaster was modeled in the simulation software, NoLimits 2. This roller coaster simulation software is very easy to learn and is a very powerful tool for modeling and simulating amusement park rides.

The process begins by adding vertices that comprise the curve of the track being created. Each vertex could be hand placed and then the coordinates could be adjusted manually to better

match the calculated numbers for each component. Various premade features such as the loop and banked curves were used. The specific parameters of each were adjusted to match the calculations of the design. Once the track was laid out different sections were assigned different types such as lift, station and braking. This was to let the program know what to render there and to adjust how the train reacted with the course. After the modeling was complete, the roller coaster could be rendered by the software and the simulation could be run. Below is a screenshot taken during the process of constructing the vertices and sections of the track (Figure 13).

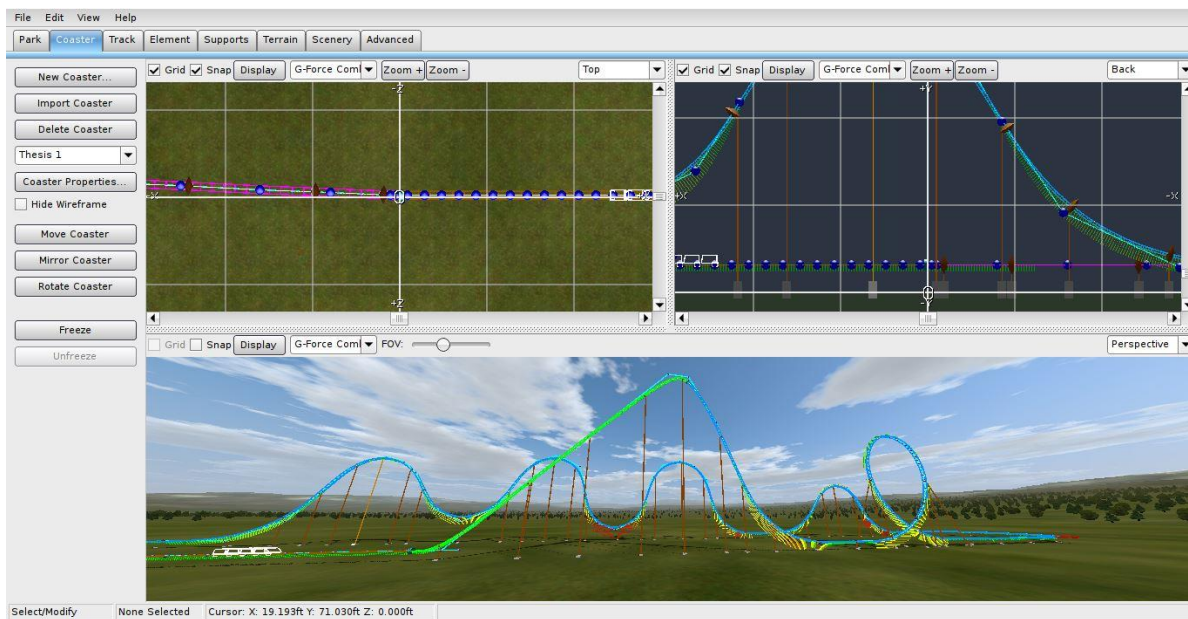


Figure 13: NoLimits 2 Editor Screenshot

4.0 Results

This section outlines the results obtained by following the previously stated methods, processes, and equations. The calculations were carried out by hand and in a Microsoft Excel sheet. The dimensions and increments of track were visualized in Autodesk AutoCAD. And then the roller coaster course and supports were modeled and simulated in NoLimits 2. The detailed results of the calculations and visual representations can be seen in the tables and documents found in the Appendices.

4.1 Course Profile

The below images display the layout of the track (Figure 14). The top image is the track viewed from the lift hill side. The bottom two images display the perspective view of the track as if you were standing near either end at the curves.

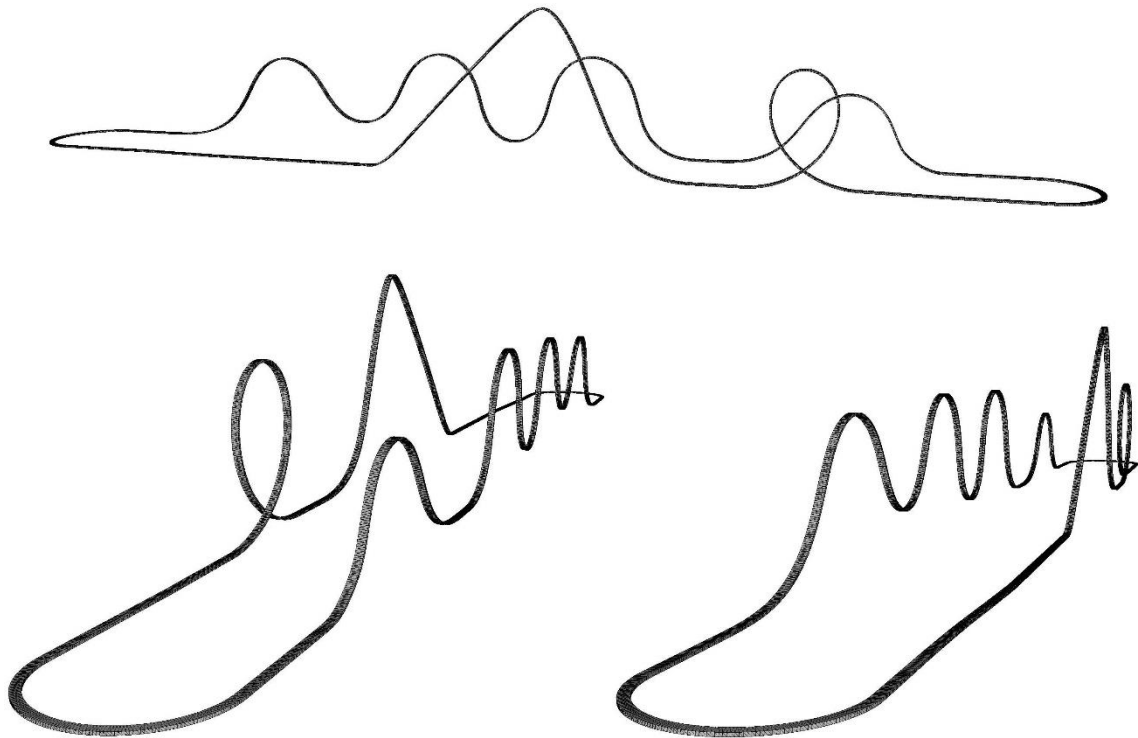


Figure 14: Track Layout Perspective Views

The course starts at the station located 10 feet above grade. Once two passengers are safely seated in each of the 4 cars comprising the train, the ride begins. The train leaves the station at 8 mph starting up the 45° lift hill. The lift brings the train up the 240 feet of track in

16.4 seconds. At the peak of the first hill the cart is 180 feet above grade travelling at 12 mph before it is released into the first drop.

The first drop has an initial incline of 65° for the first 137 feet of track. Then to reduce the G forces experienced by the riders to between 2.21g's and 3.24g's the track begins a radius of curvature of 102.634 feet. As a result of the lift hill and drop of the hill, the cart reaches its maximum velocity for the course at the bottom of the 170 foot hill at 70.58 mph. The train then enters a 100 foot straight away slowing from 70.58 mph to 69.54 mph due to outside forces of friction and drag.

Next, the riders enter the clothoid loop. The loop starts at a radius of curvature of 80.764 feet with an entrance velocity of 69.54 mph. This curve and speed cause the rider to experience 4g's at the start of the loop. As the train climbs the right side of the loop the velocity drops to 45 mph when riders are heading up perpendicular to the ground. Once the train reaches the top of the loop the track has changed to a radius of curvature of 38.158 feet. At the top, the train is moving at only 19.95 mph and there are 0.67g's on the passengers. This amount of G forces while upside down will cause people to feel a suspended feeling where gravity at 1g wants to pull the rider towards the earth and 0.67g's is pushing the rider into their seat. After passing the peak of the loop both the G forces and velocity begin to increase again. At the far left side of the loop the train has increased to 43.9 mph and the radius of curvature has changed to 80.764 feet again. Once reaching the end of the loop the passengers are traveling at 66.29 mph and experience 3.63g's. The progression of the velocity and the vertical G forces relative to the distance through the loop can be seen in the graphs below (Figures 15 & 16). The vertical G forces displayed do not include the additional effects of gravity. The sudden change in the G forces on either side of the peak of the loop is due to the change in radius of curvature. Because of the nature of the equation for centripetal acceleration, even as the velocity smoothly progresses, since the radius of curvature changes at one point, the G forces are effected accordingly around that point.

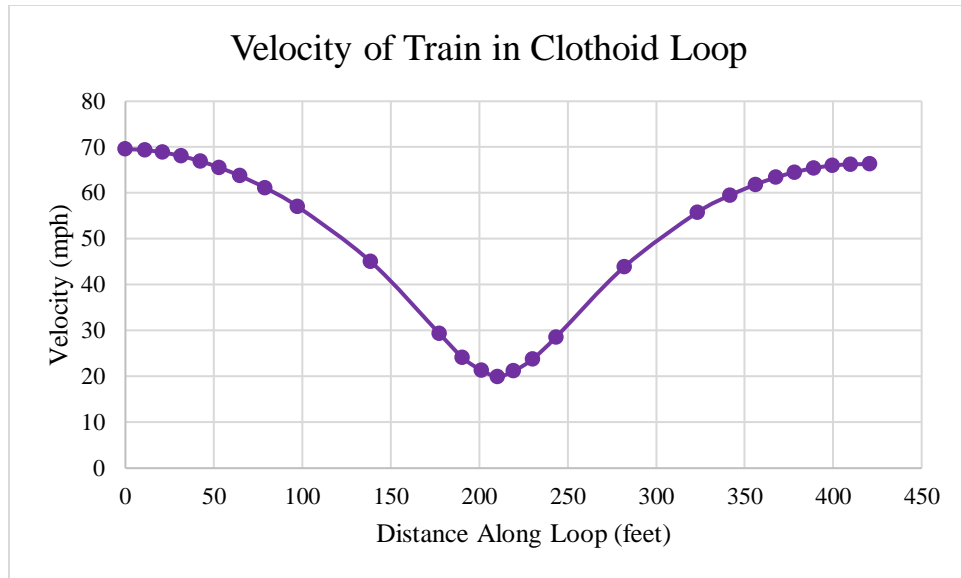


Figure 15: Velocity of Train in Clothoid Loop

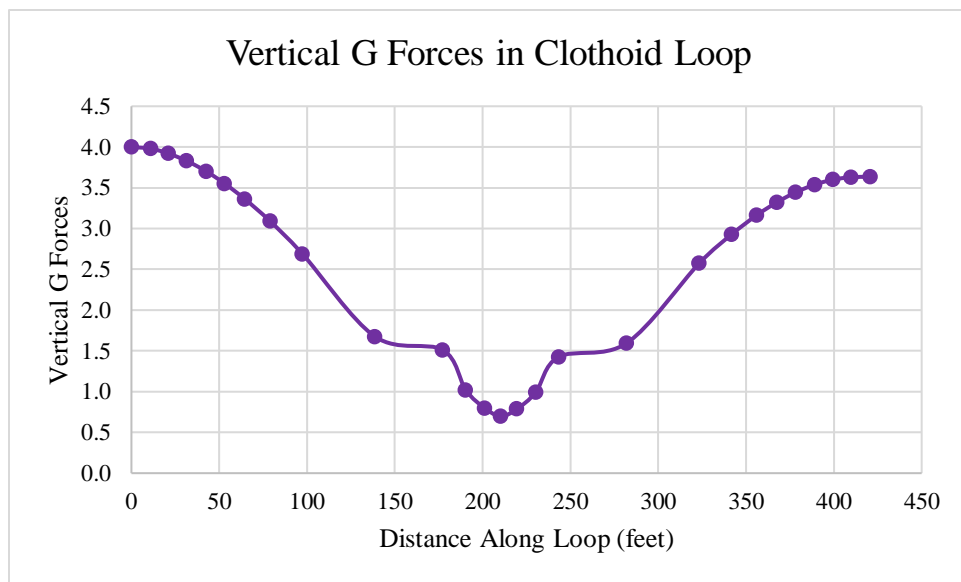


Figure 16: Vertical G Forces in Clothoid Loop

After exiting the loop the train enters a 100 foot straight away. Due to drag and friction the train's velocity decreases from 66.29 mph to 65.29 mph. Next the riders enter into the banked curve. The radius of the turn is 50 feet and 180° after the start of the banked curve is the end. At the middle of the turn the velocity of the cart is 64.53 mph and at the exit it is going 63.78 mph. To reduce the lateral G forces on the riders to 1g, the curve must be banked at 80.04° at the start, 79.81° in the middle, and 79.57° at the end. To gradually introduce the embankment to the riders the track starts to angle inwards about 20 feet before the curve and ends about 20 feet after the

curve. The train enters into an 80 foot straight away before ascending a hill 90 feet above grade. The entrance velocity is 63.01 mph and riders experience 4.39g's because of the 60 foot radius of curvature. At the peak of the hill the velocity decreases to 38.22 mph. This velocity and a radius of curvature of 40 feet result in a vertical G force of about 2.44g's. The descent on the back side of the hill is symmetrical to the entrance; the radius of curvature is 60 feet. Although it is symmetric, the velocity only increases back to 61.2 mph which causes 4.17g's on the rider. After exiting the first hill the train travels through a 40 foot straight away decreasing its velocity to 60.83 mph from the entrance into the final hill series.

The final hill series is comprised of three hills with two valleys. The first hill starts with a radius of curvature of 60 feet. The peak of the first hill has a radius of curvature of 50 feet and it is located 120 feet above grade. The train decreases to 17.38 mph causing the passengers to feel only 0.4g's. The descent of the first hill transitions into the first valley. The bottom of the first valley is located 20 feet above grade. Because of the 50 foot radius of curvature and 56.63 mph, the resulting vertical G forces is 4.28g's. Then the train climbs the second hill through the 55 foot radius of curvature reaching the 120 foot high second peak. Because of the nature of the relationship between the first and second hill the riders are only traveling at 9.25 mph, which results in 0.1g's. This slow speed and low vertical G force creates a sensation of floating and the riders question if the train will make it up and over the hill. The force of gravity is pushing the rider down while their acceleration from the curve lifts them up. Once passing the peak, the train descends again gaining speed into the second valley. The base of the second valley has a radius of curvature of 70 feet and a height of 30 feet. After traveling through the second valley at 52.4 mph and 2.62g's, riders begin to climb the final hill. The peak of the fourth hill is at 110 feet. At the peak the radius of curvature is 50 feet and the train slows to 16.57 mph. The riders once again experience weightlessness with 0.37g's pulling them from their seats. The final descent has a radius of curvature of 80 feet to minimize the vertical G forces to 2.64g's and the velocity to 56.28 mph. The progression of both the velocity and vertical G forces along the distance of the hill series can be seen in the graphs below (Figure 17 & 18). The vertical G forces displayed do not include the direction of the force or the additional effects of gravity.

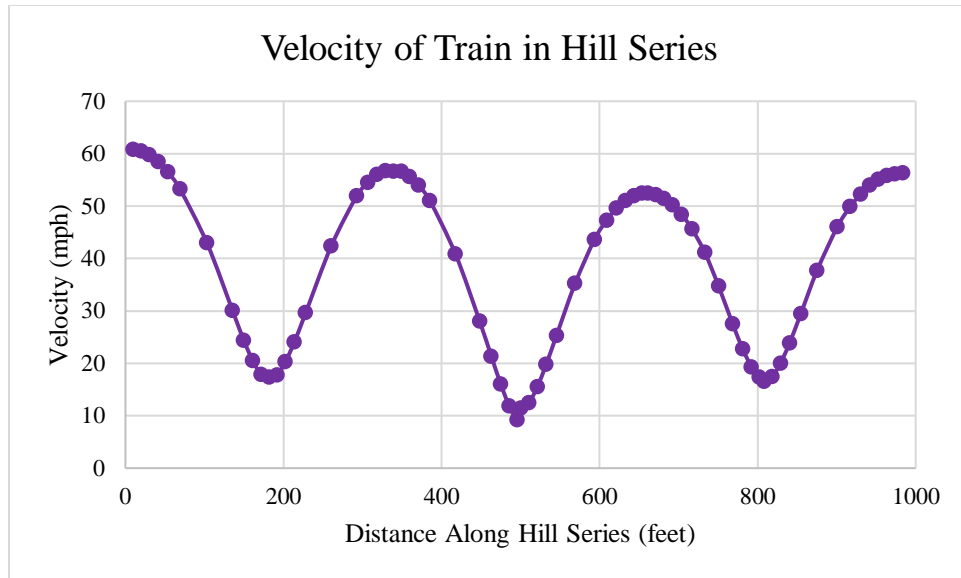


Figure 17: Velocity of Train in Hill Series

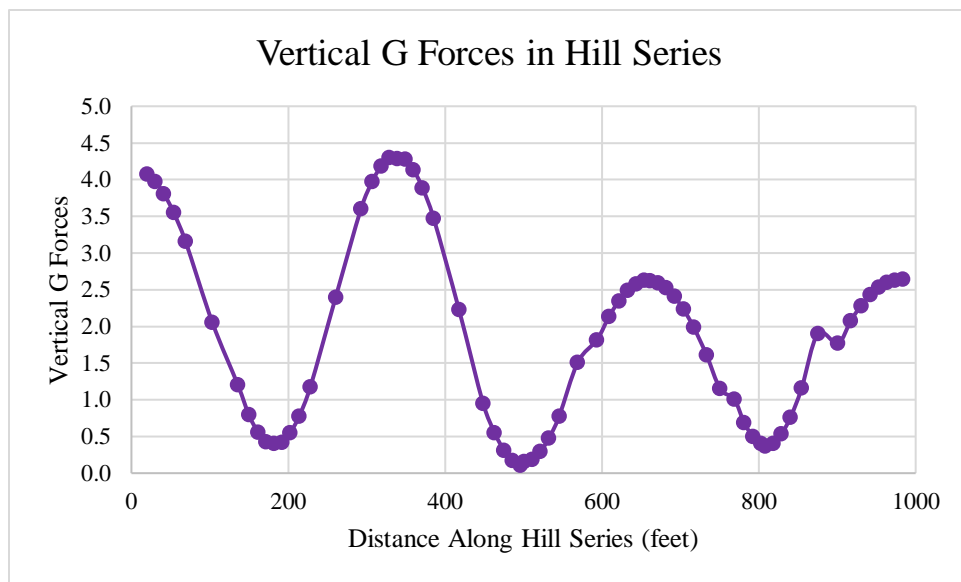


Figure 18: Vertical G Forces in Hill Series

After finishing the final hill series the train goes through a short 40 foot straight away and then the second banked curve. Entering into the banked curve the train is going 55.93 mph. Once again the banking of the curve starts 20 feet before the curve and ends 20 feet after the curve. To reduce the lateral G forces to 1 g the curve starts at 76.55° before decreasing to 76.23° in the middle and ending at 75.90° . Exiting the banked curve the train is travelling at 54.59 mph before going through the last straight away. 162 feet before the train returns to the station, the braking

system is engaged. Starting at 54.59 mph the riders slow to 12.41 mph creating just under 1 g of linear G forces due to the onset of the deceleration. This braking will occur over 2.85 seconds.

Below in Figure 19 is the color-coded flattened profile of the roller coaster course. The far left is the station where riders board the trains. The passengers travel through the lift hill, initial drop, straight away #1, clothoid loop, and straight away #2 before entering the banked curve. The banked curve, represented in orange would be where the course curves 180° to travel in the opposite direction. After the turn the riders will go through the third straight away, the first hill, the fourth straight away, the hill series, and a fifth straight away before turning again entering into the final straight away and braking to return to the station.

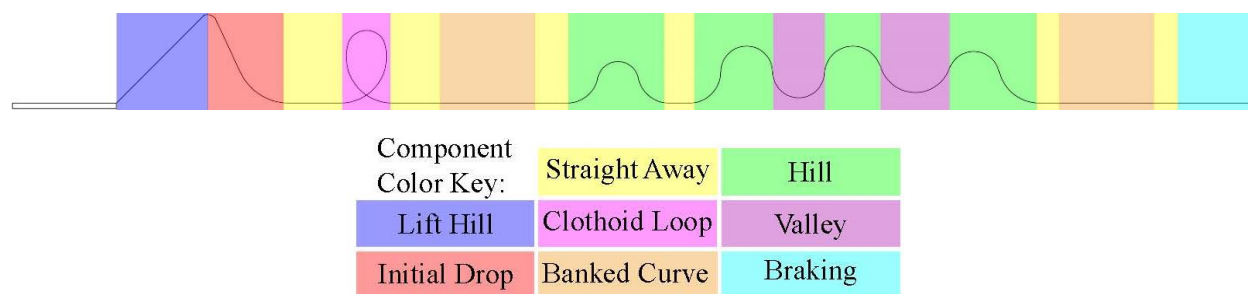


Figure 19: Color-Coded Flattened Profile

The velocities, radius of curvature, vertical G forces and linear G forces for each critical point is summarized in Table 1 below. The vertical G force directions are relative to the position of the rider, and the value includes the additional forces of gravity. Negative vertical G forces are pushing from toe to head, and the positive vertical G forces are pushing head to toe.

Table 1: Summary of Profile Results

Location	Velocity (mph)	Radius of Curvature (feet)	Vertical G Forces	Linear G Forces
Lift Hill Start	8.00	0.000	1.00	0.000
Lift Hill Peak	12.00	0.000	1.00	0.012
Curve in Initial Drop	58.33	102.634	2.64	1.184
Bottom of Initial Drop/ Straight Away #1 Starts	70.58	102.634	4.24	0.094
End of Straight Away #1/Start of Loop	69.54	0.000	5.00	-0.049
Right Side of Loop	45.01	80.764	1.92	-0.568
Peak of Loop	19.95	38.158	-0.30	0.104

Left Side of Loop	64.38	80.764	1.84	-0.023
End of Loop/Start of Straight Away #2	66.29	0.000	4.63	0.685
End of Straight Away #2/Banked Curve #1 Starts	65.29	50.000	1.00	-0.043
Middle of Banked Curve #1	64.53	50.000	1.00	-0.042
Banked Curve #1 Ends/Start of Straight Away #3	63.78	50.000	1.00	-0.041
End of Straight Away #3/Start of Hill #1	63.01	60.000	5.39	-0.040
Peak of Hill #1	38.22	40.000	-1.44	-0.557
End of Hill #1/Start of Straight Away #4	61.20	60.000	5.17	0.608
End of Straight Away #4/Start of Hill Series	60.83	60.000	5.08	-0.038
Peak of Hill #2	17.38	50.000	0.60	-0.516
Valley #1	56.63	50.000	5.28	0.466
Peak of Hill #3	9.25	55.000	0.90	-0.011
Valley #2	52.40	70.000	3.62	0.615
Peak of Hill #4	16.57	50.000	0.63	-0.443
End of Hill #4/Start of Straight Away #5	56.28	80.000	3.64	0.609
End of Straight Away #5/Banked Curve #2 Starts	55.93	50.000	1.00	-0.033
Middle of Banked Curve #2	55.26	50.000	1.00	-0.064
End of Banked Curve #2/Start of Straight Away #6	54.59	50.000	1.00	-0.024
End of Straight Away #6/Start of Braking	54.08	0.000	1.00	-0.015
End of Braking/Returns to Station	12.41	0.000	1.00	-0.307

4.2 Structural Supports

Spacing the support columns at each critical point and with no more than 40 foot spacing between them, resulted in the placement and design of 88 columns along the 3,118 foot course. The column capacity of the standard 20 inch diameter solid steel was calculated and compared to the bending moment of each column. This comparison was done by finding the required section modulus (Z_x) for the loading condition and dividing it by the section modulus of the 20 inch diameter column. The value of the capacity was greatly influenced by the track angle, G forces and the height of the column. The first graph below in Figure 20 shows the bending moment at each discrete location of the support columns along the course distance. The x-axis displays the value of the bending moment in each column in units of foot kips. Along the course there are 12

columns that experience negative bending. The sign of the bending corresponds to the relationship of the direction of bending to the direction of the train's movement. If the bending is in the opposite direction of the train's progression, as with the 12 columns, then the system results in negative bending. However, due to the symmetry of the solid circular columns the sign of the bending is only important in determining the direction of bending. Also, the ratio of bending moment to capacity is plotted over the distance of the course below (Figure 21).

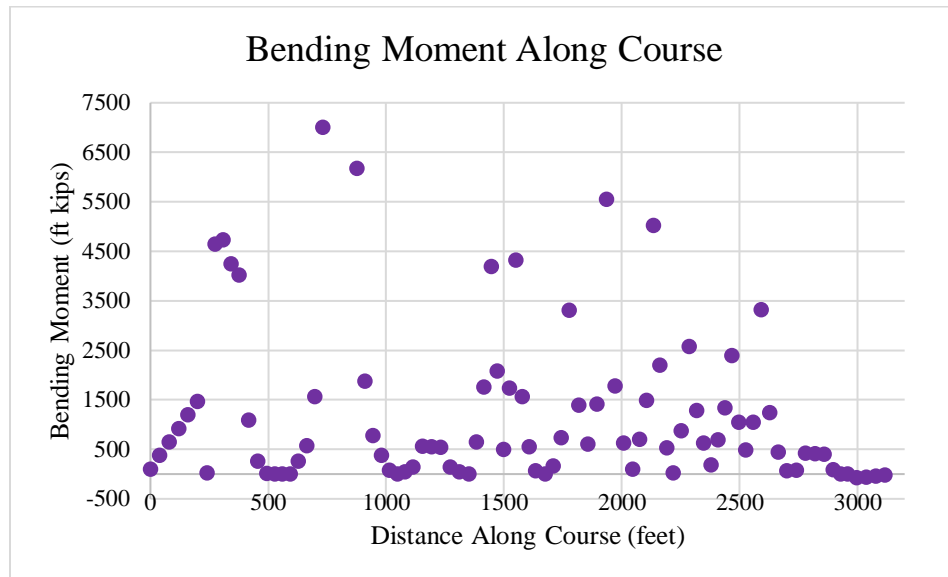


Figure 20: Bending Moment Along Course

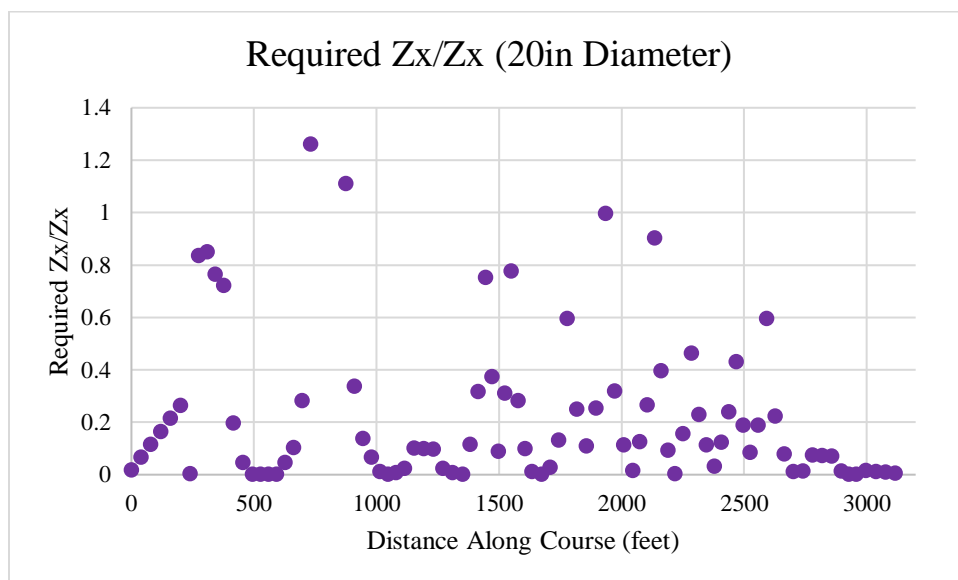


Figure 21: Bending Moment Capacity Ratio Along Course (20in Diameter)

As seen in Figure 21 above, the capacities of some of the columns were surpassed by the loading. This would create a failing condition designated by a ratio greater than or equal to one when comparing the required section modulus to the current section modulus. Next, the columns' sizes were modified to establish the most effective diameter for the given loading. As can be seen in Figure 21 above, there was a wide range of capacity usage in the columns along the course. Once changing the columns' sizes to the closest set size greater than the required section modulus, percentage of capacities used was increased. The column sizes were adjusted from the standard 20 inch diameter to 25 or 30 inch diameters if a larger cross section was needed. And the size was decreased if the 20 inch diameter was an over design, so the size was changed to 5, 10, or 15 inch diameters. The comparison of the loading conditions to the new column sizes can be seen in Figure 22 below.

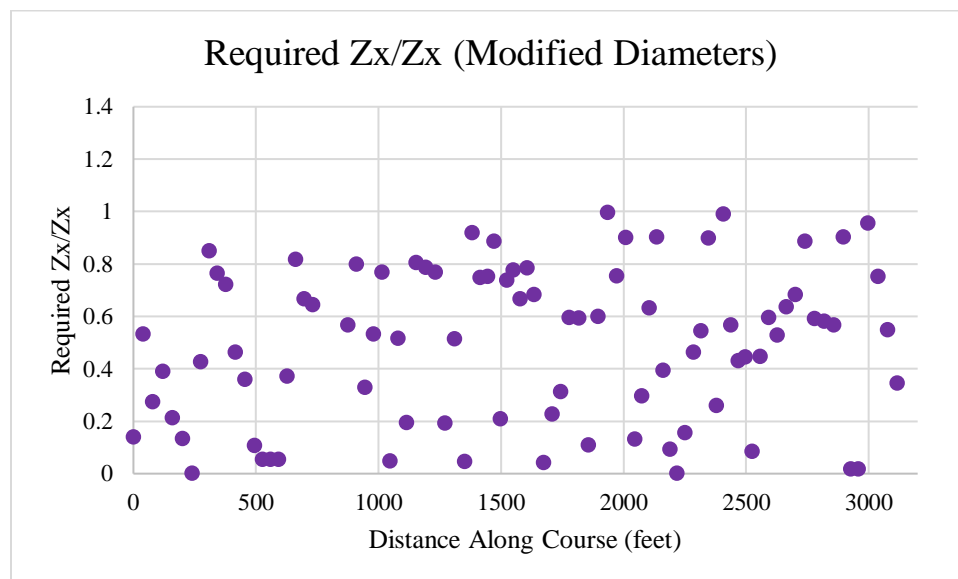


Figure 22: Bending Moment Capacity Ratio Along Course (Modified Diameters)

While adjusting the column sizes, special attention had to be paid to the new slenderness ratios. It was found that two columns exceeded their capacities even though the required cross section was met. This was because the columns had extremely high slenderness ratios. Two of the tallest columns, at the peak of the lift hill and the peak of the fourth hill, had slenderness ratios of over 1000 when the limit is 200. This caused an increase in cross sectional diameters for serviceability purposes. The diameter needed for bending was only 5 inches but because of the tall height, diameters of 30 inches were chosen to account for the slenderness ratio.

Next the results of the compression designs were investigated. The compressive loading for each column is a result of the weight of the track and the weight of the train effected by both vertical G forces and linear G forces. The compressive axial loading of each column is displayed next in Figure 23 along the distance of the course. Once the axial loading was calculated for each column, the outcome was compared to the capacity calculated for each column if it was the standard 20 inch diameter solid steel column. The results of the capacity ratio for the 20 inch diameter columns can be viewed in Figure 24.

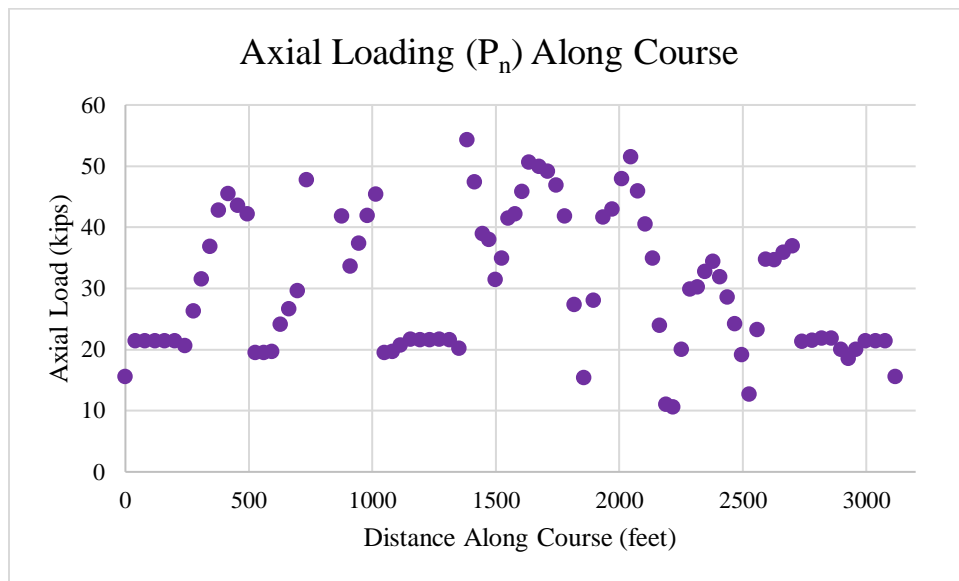


Figure 23: Axial Loading Along Course

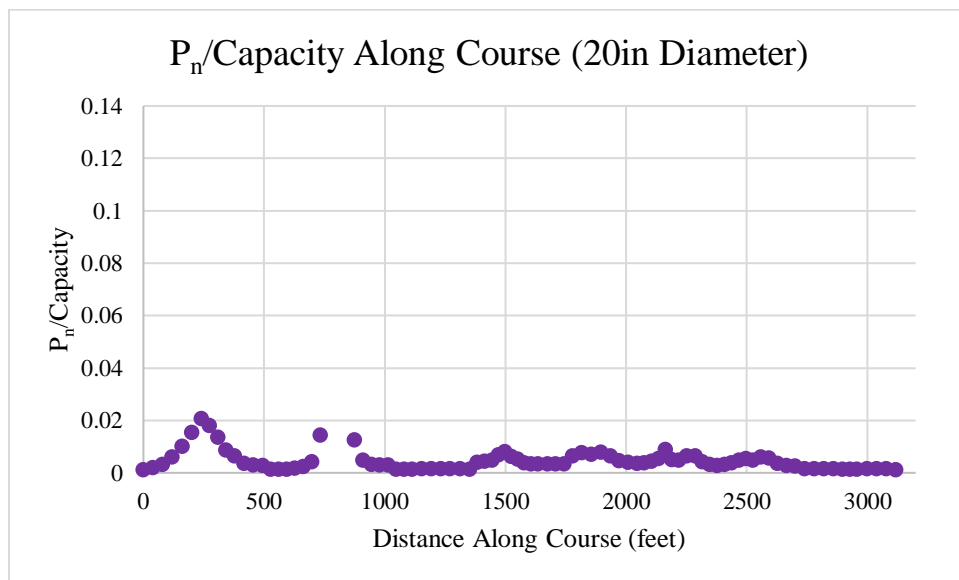


Figure 24: Compression Capacity Ratio Along Course (20in Diameter)

The results from adjusting the cross sectional diameters to maximize the bending capacities were next checked for their compressive capacities. The change in diameter similarly affected the compression capacity ratios as it did the bending capacity ratios, increasing the percent of capacity used (Figure 25). However, while the columns reached nearly their bending capacity in certain locations, such as the 99.7% at the approach to the first valley, the capacity for compressive strength did not even pass 7% in the columns once adjusting the diameters.

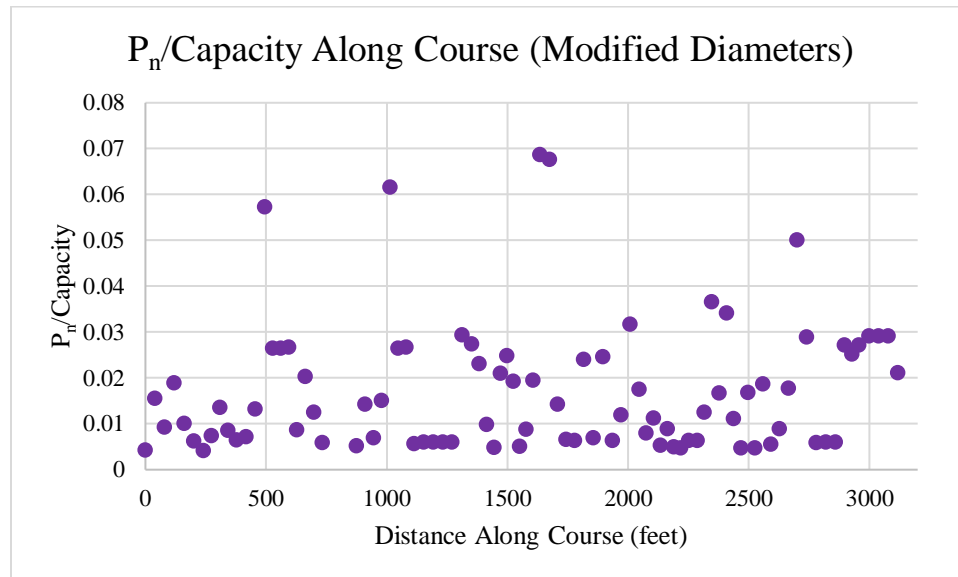


Figure 25: Compression Capacity Ratio Along Course (Modified Diameters)

The ratio of the required section modulus to sustain the bending moment on each column was compared to the give section modulus by the column's diameter. By changing the yield strength of the columns, the ratio of the capacity of the columns used for bending was increased or decreased. For example, a column that used 53% of its capacity at the control state, would decrease its capacity usage to 44% if the yield strength of the material was increased to 60ksi from 50ksi. If the yield strength was decreased to 35ksi, the column would then require 74% of its capacity to sustain the loading conditions given by the bending moment. The results of the yield strength change for all the columns are plotted on the graph below (Figure 26).

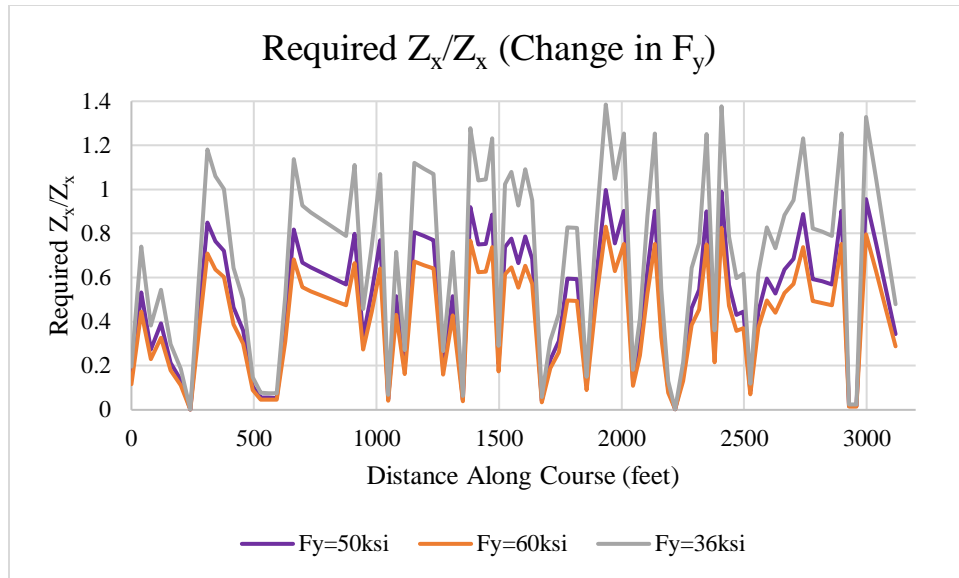


Figure 26: Change in Bending Capacity Due to Change in Yield Strength

Using the same thought process, the new usage of the columns' compressive capacities, resulting from the material property changes of yield strength and modulus of elasticity, are shown below for comparison (Figure 27).

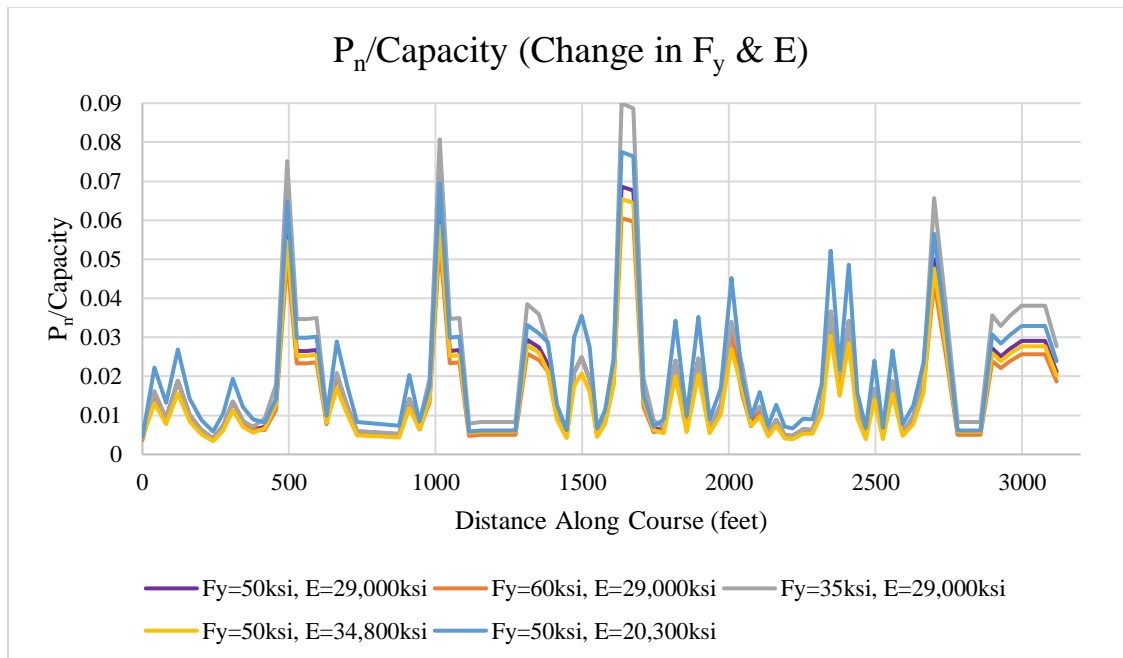


Figure 27: Change in Compressive Capacity Due to Change in Yield Strength of Modulus of Elasticity

4.3 Model and Simulation

The roller coaster was modeled in NoLimits2 and the simulation was run to virtually ride the ride. Below are images resulting from the work done in the software. The first image is the perspective view of the entire course (Figure 28). The program was an extremely useful tool for modeling and simulating the roller coaster. The only drawback was the lack of precision in determining the radii of the track in locations. Another setback of the software was the inability for the user to easily bank the turns. When attempting to bank the curves, the whole track would rotate and sometimes result in the train returning to the station upside down.



Figure 28: Completed Roller Coaster Model

The following images are taken from the simulation of the roller coaster. Figure 29 is the view as the train is traveling up the lift hill. Figure 30 is as the train begins the initial drop. Figure 31 is the drop of the first hill after the banked curve. Figure 32 is the final descent from the hill series, and Figure 33 is in the braking system returning to the station.



Figure 29: View Ascending Lift Hill



Figure 30: View from Start of Initial Drop



Figure 31: View from Drop after Hill #1



Figure 32: View from Final Drop of Hill Series



Figure 33: View from Braking System, Returning to Station

5.0 Discussion

The following section will analyze the results described above. The various results and implications of the results will be discussed. The effects of the components on the profile's design, along with the relationship between the velocities and G forces of the course will be outlined. Also, the discussion of the structural supports will include the comparison of the bending moments and axial compression in the columns, and the outcomes of altering the material properties of the columns.

5.1 Profile Design

Infinite numbers of profiles could have been designed for the roller coaster. With so many differing components, classifications and geometries to use, the combinations and results are endless. The components for this thesis were chosen with the goal in mind to create a variety of sections to analyze the loading. Going through the shape of the profile, the previous components only effected the next by providing the starting velocity. However, within a component's design, the parts greatly affected one another. For example, the height of the peak is dependent on the velocity; the train must have enough energy to reach the tallest point. Another area where many adjustments had to be made was the hill series. The heights and radii of curvature had to be changed multiple times to minimize the vertical G forces on the riders. Due to the high speeds in some locations larger radii of curvature had to be used than intended because the train still maintained so much energy that allowed it to reach high speeds and high vertical G forces.

5.1.1 Velocity and G Forces

The graphs presented in the results for the clothoid loop show the relationship between the velocity and vertical G forces. As the velocity decreases, so do the vertical G forces. This is due to the relationship of the velocity squared over the radius of curvature giving the centripetal acceleration. The dip in the vertical G force graph is due to the instant change of the radius of curvature of the track. Although the loop is symmetrical in geometry, it results in lower vertical G forces and lower velocities at the exit due to the energy lost to friction and drag.

The graphs comparing the vertical G forces and velocity of the hill series also show a similar relationship. Because the velocity is squared in the equation to calculate the vertical G force, it is the defining feature of the components that creates the G forces. With the increase in velocity there is also an increase in vertical G forces. The graphs both have the same path going

up and down matching the inverse of the dimensions of the hills. This is because the lowest velocity is when the potential energy is greatest at the top of the hills and the highest velocities are in the valleys where most of the energy has been converted back to kinetic energy due to the drop in height. The greatest velocity of the roller coaster was reached at the bottom of the initial hill because it had just descended from the highest point of the roller coaster. The maximum speed of the roller coaster is 70.6 mph.

The linear G forces throughout the ride are very low because there is no sudden change in speed. Linear G forces are the result of acceleration or deceleration. The most notable location of the linear G forces are the bottom of the hills and in the braking system. At the bottom of the hills riders experience positive linear G forces due to the increase in speed and at the braking section riders experience negative linear G forces as the ride slows to return to the station.

5.2 Structural Supports

The outcomes of analyzing the bending moments and axial compressive loading in the columns is discussed below. The modes of loading are compared against each other and in term of their value due to the roller coaster components. Also, the effects of differing yield strengths and moduli of elasticities are discussed.

5.2.1 Bending Moment and Axial Compression

In almost all columns the bending moment was the loading condition that governed the column design. In Figure 22 and Figure 25 from the results it can be seen that the bending capacity ratio of the column in some locations was around 99%, while the compressive capacity ratios did not ever exceed 7%. This is due to the nature of the roller coaster. The bending moments play such a large roll because of the height of the columns. None of the columns are under 10 feet tall, and they all experience at least 100 pounds in lateral forces from the train's movement. Along the entire course there were only four columns in which the ratio of the column's capacity was higher for compression than bending. The locations are the peak of the lift hill, the peak of hill #4, and the end of the straight away before braking begins. These columns all have similar forces acting on them. The track sections at these points are all horizontal, meaning that any lateral force is due to the linear movement of the train. Also, these locations experience small speeds and more importantly small changes in speed. Before and after each of these locations there are large accelerations or decelerations due to the hills or braking. However, at the actual column the change in speed is not that great diminishing the effects that

the train's linear motion has on the lateral forces. So although these areas do not have higher compressive forces, they do experience low enough bending moments that the compressive capacity of the column surpass the bending capacity in importance.

Another observation to note, is the relationship between the components' geometry and the resulting loading. Areas with steep inclines experience higher bending moments than those of horizontal tracks. When the train is climbing hills, it is reducing speed which is creating a linear G force against the movement of the train. Also, when the train is climbing hills the angle of the track creates a moment in the same direction of the lateral force due to the linear motion. The same concept applies when the train is descending a hill. The only locations where the linear force from motion acts against the bending moment caused by the tracks incline is during the lift hill when the train is accelerating uphill. The columns which experience the highest bending moment are the ones supporting the clothoid loop on the left and right side. This is due to the extreme angle of the track and because it supports a higher tributary area compared to the others due to the peak of the loop. Although these results are specific to this roller coaster design and may vary depending on designs, the general relationship between track angle, speed, and G forces with the loading conditions will remain similar.

As mentioned, the bending moment governed in almost all cases. However, as predicted, both the compressive capacity ratios and bending moment capacity ratios change when the diameters of the columns were changed. This is due to the increase or decrease of column size to better fit the ratios of the bending capacity results. Despite the change in size, some ratios remain nearly at zero. This is because the loading on these columns were not as great compared to other column loads. Since there were standard column sizes, even if a column did not need such a big cross section, it was design for repetition in construction. Also, some of the low ratios are due to the fact that columns had to be increase to accommodate the 200 limit set for the slenderness ratio. So although the cross section was not needed for compressive or buckling capacity, it was still used for serviceability. In all cases the columns would have failed due to buckling versus squashing because of the high slenderness values resulting from the height of the columns.

5.2.2 Material Properties

As expected, when the material properties, both yield strength and modulus of elasticity, were changed the required section modulus and capacities changed. With the increase in yield

strength the required section modulus for the same loading condition decreased. This caused a decrease in the bending moment ratio. Since the bending moment remained the same and the yield strength increased or decreased, the section modulus decreased and increased respectfully. In the conditions using the adjusted diameters, when the yield strength was lowered, the capacity was surpassed by the bending moment. This would create a failing column. However, when the yield strength was increased all the columns still had excess capacity which could result in another decrease in diameter, saving material in some columns.

Increasing the yield strength also increased the compressive capacity of the columns. And similarly, decreasing the yield strength decreased the column's compressive capacity. However, no column capacities were decreased to the point of failure through compression. This is because a small percentage of the column's capacity for compression is used because the diameters are the result of the design for bending moments. The same pattern was followed for the change in modulus of elasticity. An increase caused a larger capacity and a decreased resulted in a lower capacity. Looking at the decrease in the compressive capacity ratios due to the increase of yield strength and modulus of elasticity, it was determined that different columns would benefit more than others from each material property change. Some columns did not increase in capacity compared to the control while others more drastically changed. In the case of columns that were considered to be long columns due to their slenderness ratios, the flexural buckling stress did not take into account the yield strength because of the nature of equation E3-3 in the AISC Steel Manual. Therefore, the change caused by changing the yield strength in long columns was nonexistent. However, intermediate columns were affected by the yield strength when finding their compression capacities. In intermediate columns the change in yield strength had the greatest effect when compared to the change in modulus of elasticity. But if a column was long then it was most beneficial to change the modulus of elasticity. However, changing the modulus of elasticity would be the result of changing the chemicals of the material itself so I would be difficult.

Although increasing both material properties would increase the capacity in both loading conditions, it is only necessary to increase the yield strength for beneficial results. Since the change in modulus of elasticity only affected the compressive capacity of the columns, it is not as important because the columns are oversized for compression already. Because the

bending moment is the governing load, then changing the material properties of the column to increase the bending capacity would be the best approach.

5.2.3 Additional Structural Considerations

In addition to the bending and compression considered in this study, other loading situations should be taken into account for further analysis of the structural supports. Two important factors that must be considered for the components of a roller coaster are vibration and fatigue. Due to the movement of the train, vibrations can be created throughout the track and supports. It must be checked that the frequency of the train's movement does not cause resonance in any of the parts of the roller coaster. Reaching resonance would be detrimental to the system. Also, vibrations can lead to the degradation of the column's materials. Additional forces from the wind could also contribute to the vibration of the support system.

Due to the nature of roller coasters, the support columns are quickly loaded and unloaded. This, along with the continuous use throughout the year, can promote fatigue within the materials. The cycles applied by the loading can lead to irreversible damage; this damage can occur before the material yields. Because of this, the ASTM standards specifically state that all components of the ride must be designed for 35,000 hours to account for the various loadings that contribute toward the fatigue of the materials. The columns can be analyzed by using a typical S-N curve for steel. The stresses that are applied based on the forces found in earlier sections must allow the system to reach the required number of cycles for a sufficient design.

6.0 Conclusion

While designing a roller coaster the forces generated by each component can be calculated to decide what governs. It is possible for different forces to govern the structural support designs such as compression, tension or bending. For the design of this roller coaster, the bending moments governed in most columns due to the lateral forces acting on tall heights. The columns were first designed with standard 20 inch diameter solid steel, with the properties of 50ksi yield strength and 29,000ksi modulus of elasticity. These columns did not suffice for all locations so the diameters were adjusted to maximize the column's capacity. The material properties of the steel were also adjusted to determine the effects on the compressive and bending capacities. It was found that due to the nature of the roller coaster, the most beneficial material property change would be to increase the yield strength of the steel columns.

In future works different designs resulting in different governing loads could be analyzed. Also, differing materials could be tested. Perhaps if there was a design where columns were drastically governed by compressive loading over bending moments then concrete could be used. By determining the loads of the course and testing different materials the best choice of materials can be concluded. This conclusion would be based on cost, practicality, and resource availability. In an industry that is getting increasingly more expensive and with the increase of scale in all aspects of the ride, optimizing the materials for the specific use would be very valuable.

7.0 Bibliography

American Coaster Enthusiasts (2018) A Brief History of Roller Coasters. Retrieved from <http://www.aceonline.org/coasterhistory/>.

American Institute of Steel Construction (AISC) (2011) Steel Construction Manual. *Fourteenth Edition*.

Applied Technical Services (2017) NDT Rope Access Inspections. Retrieved from <http://www.atslab.com/rope-access/rope-access-ndt.php>.

ASTM (N.D.) ASTM International Technical Committee F24 on Amusement Rides and Devices. *ASTM International*. Retrieved from https://www.astm.org/COMMIT/F24_Fact_Sheet_2016.pdf.

ASTM (2017a) ASTM F770: Standard Practice for Ownership, Operation, Maintenance, and Inspection of Amusement Rides and Devices. *ASTM Compass*. Retrieved from https://compass-astm-org.ezproxy.wpi.edu/EDIT/html_annot.cgi?F770+17e1.

ASTM (2017b) ASTM F1193: Standard Practice for Quality, Manufacture, and Construction of Amusement Rides and Devices. *ASTM Compass*. Retrieved from https://compass-astm-org.ezproxy.wpi.edu/EDIT/html_annot.cgi?F1193+17.

ASTM (2017c) ASTM F2291: Standard Practice for Design of Amusement Rides and Devices. *ASTM Compass*. Retrieved from https://compass-astm-org.ezproxy.wpi.edu/EDIT/html_annot.cgi?F2291+17.

Bessette, W. (2015) Materials Used in Roller Coasters. *AZO Materials*. Retrieved from <https://www.azom.com/article.aspx?ArticleID=11958>.

Borel, B. (2011) How It Works: The World's Fastest Roller Coaster. *Popular Science*. Retrieved from <https://www.popsci.com/technology/article/2011-03/how-it-works-worlds-fastest-rollercoaster#page-2>.

CMU, A. (2015) First Golden Age, Decline, and Revitalization. *Roller Coasters: Background and Design*. Retrieved from [http://www.andrew.cmu.edu/user/jzink/98-186/pdf/week03Notes\(fga\).pdf](http://www.andrew.cmu.edu/user/jzink/98-186/pdf/week03Notes(fga).pdf).

CoasterForce (2018a) Restraints. Retrieved from <http://coasterforce.com/trains/>.

CoasterForce (2018b) How a Coaster Moves. Retrieved from <http://coasterforce.com/physics/>.

CoasterForce (2018c) World Records. Retrieved from <http://coasterforce.com/records/>.

Coasterpedia (N.D.) Strata Roller Coaster. Retrieved from http://rollercoaster.wikia.com/wiki/Strata_Roller_Coaster.

Coasterpedia (2018) Steel Dragon 2000. Retrieved from https://coasterpedia.net/wiki/Steel_Dragon_2000.

Crockett, Z. (2014) The Business of Building Roller Coasters. *Pricenomics*. Retrieved from <https://priceconomics.com/the-business-of-building-roller-coasters/>.

Cypress, A. (1997) A Brief History of the Roller Coaster. *The Washington Post*. Retrieved from https://www.washingtonpost.com/archive/1997/08/13/a-brief-history-of-the-roller-coaster/4490a0f9-6a82-451d-86b7-f36a7bc0fbbf/?utm_term=.423c94f699ef.

EnginSoft (N.D.) The Structural Design of Roller Coasters. *Structural: Roller Coasters*. Retrieved from <http://www.enginsoft.com/technologies/civil-engineering/structural-roller-coasters.html>.

Fantacoaster (2008) Raptor side winder. *Wikimedia Commons*. Retrieved from <https://commons.wikimedia.org/wiki/File:Raptorsidewinder.JPG>.

Gallerie, K. (2002) Roller Coaster. *Worcester Polytechnic Institute*. Retrieved from <https://web-wpi-edu.ezproxy.wpi.edu/Pubs/E-project/Scanned/02D205M.pdf>.

GForces (2010) Human Tolerance of Horizontal Axis G Force. Retrieved from <http://www.gforces.net/human-tolerance-horizontal.html>.

Harris, T. (2018) How Roller Coasters Work. *How stuff works*. Retrieved from <https://science.howstuffworks.com/engineering/structural/roller-coaster.htm>.

Los Angeles Times (2014) Photos: 21 oldest roller coasters in the world. Retrieved from <http://www.latimes.com/travel/deals/la-trb-oldest-roller-coasters-photos-07201118-pg-photogallery.html>.

Marden, D. (2018a) Leap The Dips. *Roller Coaster Database*. Retrieved from <https://rcdb.com/243.htm>.

Marden, D. (2018b) Glossary. *Roller Coaster Database*. Retrieved from <https://rcdb.com/g.htm>.

McC, W. (2007) BPB bobsled. *Wikimedia Commons*. Retrieved from <https://commons.wikimedia.org/wiki/File:BPBbobsled.jpg>.

Murphy, T. (2009) Seaworld Manta Roller Coaster. *Flickr*. Retrieved from <https://www.flickr.com/photos/tedmurphy/3551503275>.

National Roller Coaster Museum (2014) History of the Roller Coaster.

Ohio University (N.D.) Engineering the Amusement Park. *Amusement Park and Roller Coaster Engineering*. Retrieved from <https://onlinemasters.ohio.edu/amusement-park-and-roller-coaster-engineering/>.

Roller Coaster (2018) *How Products are Made, Volume 6*. Retrieved from <http://www.madehow.com/Volume-6/Roller-Coaster.html>.

Sandy, A. (2018) Knudsen's Inclined Plane Railway Patent. *Ultimate Roller Coaster*. Retrieved from <https://www.ultimaterollercoaster.com/coasters/history/start/america4.shtml>.

Santa Cruz Beach Boardwalk (N.D.) The Boardwalk's Most Popular Ride – The Giant Dipper. Retrieved from <https://news.beachboardwalk.com/press-kit/giant-dipper>.

Sim, N. (2014) The Future of Theme Parks: 5 Innovative Ride Concepts for 2020. *Theme Park Tourist*. Retrieved from <https://www.themeparktourist.com/features/20140105/15599/future-theme-parks-5-innovative-ride-concepts-2020>.

Six Flags (2017). Experience the World's Tallest Coaster! *Kingda Ka*. Retrieved from <https://www.sixflags.com/greatadventure/attractions/kingda-ka>.

Stanton, J. (2013) History of Early Roller Coasters. *Westland*. Retrieved from <https://www.westland.net/coneyisland/articles/EarlyRollerCoasters-1870-1886.htm>.

Tyson, P. (2007) All About G Forces. *NOVA*. Retrieved from <http://www.pbs.org/wgbh/nova/space/gravity-forces.html>.

Weisenberger, N. (2011a) Coasters-101: Wheel Design. *Coaster101*. Retrieved from <https://www.coaster101.com/2011/10/24/coasters-101-wheel-design/>.

Weisenberger, N. (2011b) Coasters-101: Daily Inspections. *Coaster101*. Retrieved from <https://www.coaster101.com/2011/01/31/coasters-101-daily-inspections/>.

Weisenberger, N. (2013a) Coasters 101 An Engineer's Guide to Roller Coaster Design. *Third Edition*.

Weisenberger, N. (2013b) Coasters-101: Launch Systems. *Coaster101*. Retrieved from <https://www.coaster101.com/2013/10/08/coasters-101-launch-systems/>.

Wikimedia Commons (2014) Roller Coaster. Retrieved from https://commons.wikimedia.org/wiki/File:Roller_coaster_-dw.jpg.

Wikipedia (2018) Ultra Twister (Nagashima Spa Land). Retrieved from [https://en.wikipedia.org/wiki/Ultra_Twister_\(Nagashima_Spa_Land\)](https://en.wikipedia.org/wiki/Ultra_Twister_(Nagashima_Spa_Land)).

Wills, T. (2009) Kirnu. *Wikimedia Commons*. Retrieved from <https://commons.wikimedia.org/wiki/File:Kirnu-crop.JPG>.

Yang, J. (2017) New Roller Coasters are Faster and Safer. *abc News*. Retrieved from <http://abcnews.go.com/WNT/story?id=130111&page=1>.

Zink, J. (2015) Basics of Roller Coaster Design. Retrieved from
<https://pdfs.semanticscholar.org/presentation/8d71/2d7def3903d3f1e3868b8855a5886f9f0f0c.pdf>.

8.0 Appendices

Appendix A: Lift Hill Calculations

Location	Cart Mass	Gravity	Cart Weight	Height	Track Distance	Velocity	Velocity
	lb	ft/sec ²	lb ft/sec ²	Feet	Feet	ft/sec	mph
Hill 1 Bottom	6100	32.2	196420	10	0	11.73333	8
Hill 1 Top	6100	32.2	196420	180	240.4163	17.6	12

Incline 45 degrees
 Vertical Distance 170 feet
 Incline Distance 240.4163 feet
 Horizontal Distance 170 feet

Acceleration of Lift 0.357898 ft/sec²
 Lift Time 16.39202 seconds

Potential Energy	Kinetic Energy	Angle of Track	Radius of Wheel	Coefficient of Rolling Friction	Normal Force on Wheel
lb ft ² /sec ²	lb ft ² /sec ²	degrees	in	in	lb ft/sec ²
1964200	419896.8889	45	5	0.01	138889.914
35355600	944768	45	5	0.01	138889.914

Rolling Friction Force	Rolling Friction Work	Coefficient of Bearing Friction	Bearing Load	Bearing Friction Force	Bearing Friction Work
lb ft/sec ²	lb ft ² /sec ²		lb ft/sec ²	lb ft/sec ²	lb ft ² /sec ²
277.7798279	0	0.0018	138889.91	250.0018451	0
277.7798279	66782.8	0.0018	138889.91	250.0018451	60104.52

Denisty of Air	Area of Cross Section	Drag Coefficient	Drag Force	Drag Work	Power of Lift	Power of Lift
lb/ft ³	ft ²		lb ft/sec ²	lb ft ² /sec ²	lb ft/sec ²	Newtons
0.0765	12	1.8	113.743872	0		
0.0765	12	1.8	255.923712	61528.23336	141607.8334	19577.98449

Appendix B: Initial Drop Calculations

Location	Car Mass	Gravity	Car Weight	Track Height	Horizontal Distance	Angle of Track
	lbs	ft/sec ²	lb ft/sec ²	feet	feet	degrees
Hill #1 Top	6100	32.2	196420	180	180	0
10ft over	6100	32.2	196420	174.2264973	190	30
20ft over	6100	32.2	196420	152.7814281	200	65
30ft over	6100	32.2	196420	131.3363589	210	65
40ft over	6100	32.2	196420	109.8912897	220	65
50ft over	6100	32.2	196420	88.44622049	230	65
Curve Starts	6100	32.2	196420	69.26041667	238.9479167	65
10ft after Curve	6100	32.2	196420	52.61762184	248.9479167	59
20ft after Curve	6100	32.2	196420	40.70008592	258.9479167	50
30ft after Curve	6100	32.2	196420	31.69604547	268.9479167	42
40ft after Curve	6100	32.2	196420	24.95096031	278.9479167	34
50ft after Curve	6100	32.2	196420	19.63386599	288.9479167	28
60ft after Curve	6100	32.2	196420	15.59360373	298.9479167	22
70ft after Curve	6100	32.2	196420	12.72614987	308.9479167	16
80ft after Curve	6100	32.2	196420	10.96288007	318.9479167	10
Hill #1 Bottom	6100	32.2	196420	10.0527389	331.9635417	4

Track Distance	Potential Energy	Kinetic Energy	Radius of Wheel	Coefficient of Rolling Friction
feet	lb ft ² /sec ²	lb ft ² /sec ²	in	in
10	3.54E+07	944768	5	0.01
11.54700538	3.42E+07	2068776.202	5	0.01
23.66201583	3.00E+07	6267081.782	5	0.01
23.66201583	2.58E+07	10431688.26	5	0.01
23.66201583	2.16E+07	14569600.89	5	0.01
23.66201583	1.74E+07	18680990.79	5	0.01
21.17257458	1.36E+07	22322263.04	5	0.01
19.41604026	1.03E+07	25427247.96	5	0.01
15.55723827	7.99E+06	27594797.51	5	0.01
13.4563273	6.23E+06	29210324.11	5	0.01
12.06217949	4.90E+06	30393758.21	5	0.01
11.32570051	3.86E+06	31305276.7	5	0.01
10.78534743	3.06E+06	31969867.44	5	0.01
10.40299436	2.50E+06	32407223.92	5	0.01
10.15426612	2.15E+06	32630149.71	5	0.01
13.04740783	1.97E+06	32687334.26	5	0.01

Radius of Curvature of Track	Normal Force on Wheel	Rolling Friction Force	Rolling Friction Work	Coefficient of Bearing Friction	Bearing Load
feet	lb ft/sec ²	lb ft/sec ²	lb ft ² /sec ²		lb ft/sec ²
N/A	196420	392.84	3928.4	0.0018	196420
N/A	170104.71	340.2094196	3928.4	0.0018	170104.71
N/A	83010.67897	166.0213579	3928.4	0.0018	83010.679
N/A	83010.67897	166.0213579	3928.4	0.0018	83010.679
N/A	83010.67897	166.0213579	3928.4	0.0018	83010.679
N/A	83010.67897	166.0213579	3928.4	0.0018	83010.679
102.634	447041.912	894.0838241	18930.06	0.0018	447041.912
102.634	536151.4638	1072.302928	20819.87682	0.0018	536151.464
102.634	621749.9986	1243.499997	19345.42574	0.0018	621749.999
102.634	683700.5937	1367.401187	18400.19792	0.0018	683700.594
102.634	732052.9611	1464.105922	17660.30842	0.0018	732052.961
102.634	765703.216	1531.406432	17344.2506	0.0018	765703.216
102.634	792154.6081	1584.309216	17087.32533	0.0018	792154.608
102.634	811798.8712	1623.597742	16890.27815	0.0018	811798.871
102.634	824946.4308	1649.892862	16753.45118	0.0018	824946.431
102.634	831796.1152	1663.59223	21705.56629	0.0018	831796.115

Bearing Friction Force	Bearing Friction Work	Denisty of Air	Area of Cross Section	Drag Coefficient	Drag Force
lb ft/sec ²	lb ft ² /sec ²	lb/ft ³	ft ²		lb ft/sec ²
353.556	3535.56	0.0765	12	1.8	255.923712
306.1884777	3535.56	0.0765	12	1.8	560.4009501
149.4192221	3535.56	0.0765	12	1.8	1697.65999
149.4192221	3535.56	0.0765	12	1.8	2825.790439
149.4192221	3535.56	0.0765	12	1.8	3946.689921
149.4192221	3535.56	0.0765	12	1.8	5060.404783
804.6754417	17037.0508	0.0765	12	1.8	6046.771711
965.0726348	18737.88913	0.0765	12	1.8	6887.866317
1119.149998	17410.88317	0.0765	12	1.8	7475.02351
1230.661069	16560.17813	0.0765	12	1.8	7912.645828
1317.69533	15894.27758	0.0765	12	1.8	8233.220666
1378.265789	15609.82554	0.0765	12	1.8	8480.137577
1425.878295	15378.59279	0.0765	12	1.8	8660.165403
1461.237968	15201.25034	0.0765	12	1.8	8778.638819
1484.903575	15078.10607	0.0765	12	1.8	8839.026129
1497.233007	19535.00966	0.0765	12	1.8	8854.516578

Drag Work	Velocity	Velocity	G Forces
lb ft ² /sec ²	ft/sec	mph	
2559.23712	17.6	12	
6470.952788	26.04395	17.757238	
40170.05755	45.32969	30.906608	
66863.8981	58.4827	39.874565	
93386.63938	69.11525	47.124037	
119739.3781	78.26184	53.360343	
128025.725	85.54984	58.329435	2.214579
133735.0897	91.30609	62.254154	2.522623
116290.7218	95.11821	64.853328	2.737665
106475.152	97.86294	66.724733	2.89794
99310.58541	99.82568	68.062964	3.015348
96043.49846	101.3115	69.07604	3.105779
93402.89264	102.3813	69.805409	3.171713
91324.13011	103.0792	70.281266	3.215103
89753.82354	103.4331	70.52258	3.237219
115528.4889	103.5237	70.584349	3.242892

Appendix C: Straight Away #1 Calculations

Location	Cart Mass	Gravity	Cart Weight	Height	Track Distance	Velocity	Velocity
	lb	ft/sec ²	lb ft/sec ²	Feet	Feet	ft/sec	mph
Start	6100	32.2	196420	10	0	103.5237	70.58435
End	6100	32.2	196420	10	100	101.992	69.54002

Potential Energy	Kinetic Energy	Angle of Track	Radius of Wheel	Coefficient of Rolling Friction	Normal Force on Wheel
lb ft ² /sec ²	lb ft ² /sec ²	degrees	in	in	lb ft/sec ²
1964200	32687334.26	0	5	0.01	196420
1964200	31727243	0	5	0.01	196420

Rolling Friction Force	Rolling Friction Work	Coefficient of Bearing Friction	Bearing Load	Bearing Friction Force	Bearing Friction Work
lb ft/sec ²	lb ft ² /sec ²		lb ft/sec ²	lb ft/sec ²	lb ft ² /sec ²
392.84	0	0.0018	196420	353.556	0
392.84	39284	0.0018	196420	353.556	35355.6

Denisty of Air	Area of Cross Section	Drag Coefficient	Drag Force	Drag Work
lb/ft ³	ft ²		lb ft/sec ²	lb ft ² /sec ²
0.0765	12	1.8	8854.51658	0
0.0765	12	1.8	8854.51658	885451.6578

Appendix D: Clothoid Loop Calculations

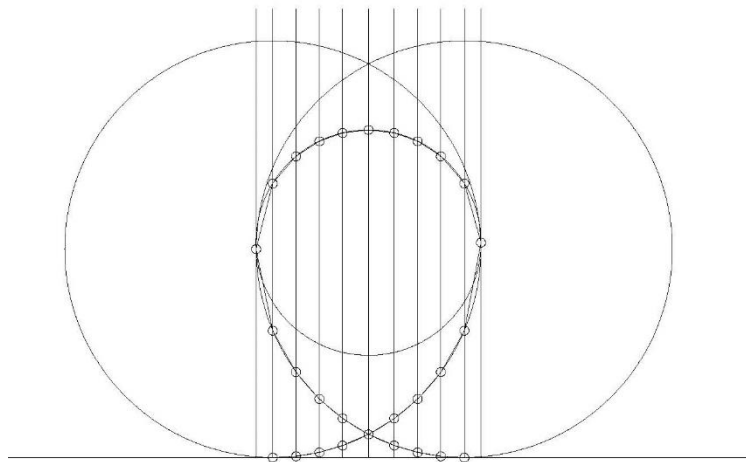
Location	Height	G Force Felt	Centripetal Acceleration	Velocity	Velocity	Cart Mass	Gravity
	feet	g's	ft/sec^2	ft/sec	mph	lb	ft/sec^2
Entrance	10.0000	-1.0000	-32.2000	101.9920	69.5400	6100	32.2
	10.7641	-0.9953	-32.0477	101.7505	69.3754	6100	32.2
	12.5274	-0.9814	-31.6006	101.0383	68.8898	6100	32.2
	15.5847	-0.9597	-30.9030	99.9168	68.1251	6100	32.2
	20.0370	-0.9294	-29.9259	98.3246	67.0395	6100	32.2
Bottom Middle	25.4916	-0.8928	-28.7471	96.3685	65.7058	6100	32.2
	32.5843	-0.8462	-27.2476	93.8215	63.9692	6100	32.2
	42.9396	-0.7793	-25.0941	90.0377	61.3893	6100	32.2
	58.3382	-0.6807	-21.9191	84.1491	57.3744	6100	32.2
Right Side	98.4460	-0.4286	-13.8008	66.7714	45.5260	6100	32.2
	135.7665	1.6095	51.8262	44.4701	30.3205	6100	32.2
	144.1575	1.1174	35.9787	37.0524	25.2630	6100	32.2
	148.1978	0.8950	28.8190	33.1613	22.6100	6100	32.2
Top	150.0000	0.7934	25.5462	31.2216	21.2875	6100	32.2
	148.1978	0.8823	28.4117	32.9262	22.4497	6100	32.2
	144.1575	1.0887	35.0572	36.5748	24.9373	6100	32.2
	135.7665	1.5216	48.9964	43.2389	29.4811	6100	32.2
Left Side	98.4460	-0.4096	-13.1897	65.2764	44.5066	6100	32.2
	58.3382	-0.6562	-21.1289	82.6185	56.3308	6100	32.2
	42.9396	-0.7473	-24.0639	88.1701	60.1160	6100	32.2
	32.5843	-0.8083	-26.0259	91.6941	62.5187	6100	32.2
Middle Bottom	25.4916	-0.8493	-27.3472	93.9928	64.0860	6100	32.2
	20.0370	-0.8806	-28.3539	95.7072	65.2549	6100	32.2
	15.5847	-0.9057	-29.1632	97.0634	66.1796	6100	32.2
	12.5274	-0.9220	-29.6885	97.9338	66.7730	6100	32.2
	10.7641	-0.9303	-29.9571	98.3758	67.0744	6100	32.2
Exit	10.0000	-0.9325	-30.0274	98.4911	67.1530	6100	32.2

Cart Weight	Potential Energy	Kinetic Energy	Radius of Curvature	Horizontal Distance	Track Distance	Angle of Track	Radius of Wheel
lb ft/sec^2	lb ft^2/sec^2	lb ft^2/sec^2	feet	feet	feet	degrees	in
196420	1.96E+06	3.17E+07	-323.055	0.0000	0.0000	0	5
196420	2.11E+06	3.16E+07	-323.055	10.9271	10.9538	4	5
196420	2.46E+06	3.11E+07	-323.055	20.9271	10.1543	10	5
196420	3.06E+06	3.04E+07	-323.055	30.9271	10.4569	17	5
196420	3.94E+06	2.95E+07	-323.055	40.9271	10.9464	24	5
196420	5.01E+06	2.83E+07	-323.055	50.0052	10.5908	31	5
196420	6.40E+06	2.68E+07	-323.055	59.0833	11.5203	38	5
196420	8.43E+06	2.47E+07	-323.055	69.0833	14.3956	46	5
196420	1.15E+07	2.16E+07	-323.055	79.0833	18.3608	57	5
196420	1.93E+07	1.36E+07	-323.055	89.0833	41.3357	76	5
196420	2.67E+07	6.03E+06	38.158	79.0833	38.6370	75	5
196420	2.83E+07	4.19E+06	38.158	69.0833	13.0541	40	5
196420	2.91E+07	3.35E+06	38.158	59.0833	10.7853	22	5
196420	2.95E+07	2.97E+06	38.158	50.0052	9.1463	7	5
196420	2.91E+07	3.31E+06	38.158	40.9271	9.1463	7	5
196420	2.83E+07	4.08E+06	38.158	30.9271	10.7853	22	5
196420	2.67E+07	5.70E+06	38.158	20.9271	13.0541	40	5
196420	1.93E+07	1.30E+07	-323.055	10.9271	38.6370	75	5
196420	1.15E+07	2.08E+07	-323.055	20.9271	41.3357	76	5
196420	8.43E+06	2.37E+07	-323.055	30.9271	18.3608	57	5
196420	6.40E+06	2.56E+07	-323.055	40.9271	14.3956	46	5
196420	5.01E+06	2.69E+07	-323.055	50.0052	11.5203	38	5
196420	3.94E+06	2.79E+07	-323.055	59.0833	10.5908	31	5
196420	3.06E+06	2.87E+07	-323.055	69.0833	10.9464	24	5
196420	2.46E+06	2.93E+07	-323.055	79.0833	10.4569	17	5
196420	2.11E+06	2.95E+07	-323.055	89.0833	10.1543	10	5
196420	1.96E+06	2.96E+07	-323.055	100.0104	10.9538	4	5

Coefficient of Rolling Friction	Normal Force on Wheel	Rolling Friction Force	Rolling Friction Work	Coefficient of Bearing Friction	Bearing Load
in	lb ft/sec^2	lb ft/sec^2	lb ft^2/sec^2		lb ft/sec^2
0.01	0.00E+00	0.0000	0.0000	0.0018	0.00E+00
0.01	4.51E+02	0.9014	9.8734	0.0018	4.51E+02
0.01	6.72E+02	1.3444	13.6512	0.0018	6.72E+02
0.01	-6.71E+02	-1.3415	-14.0280	0.0018	-6.71E+02
0.01	-3.11E+03	-6.2192	-68.0780	0.0018	-3.11E+03
0.01	-6.99E+03	-13.9845	-148.1080	0.0018	-6.99E+03
0.01	-1.14E+04	-22.8586	-263.3382	0.0018	-1.14E+04
0.01	-1.66E+04	-33.2585	-478.7745	0.0018	-1.66E+04
0.01	-2.67E+04	-53.4570	-981.5134	0.0018	-2.67E+04
0.01	-3.67E+04	-73.3334	-3031.2855	0.0018	-3.67E+04
0.01	3.67E+05	733.9545	28357.8258	0.0018	3.67E+05
0.01	3.70E+05	739.8736	9658.3639	0.0018	3.70E+05
0.01	3.58E+05	715.8264	7720.4361	0.0018	3.58E+05
0.01	3.51E+05	701.5753	6416.8180	0.0018	3.51E+05
0.01	3.68E+05	736.5340	6736.5615	0.0018	3.68E+05
0.01	3.96E+05	791.9329	8541.2718	0.0018	3.96E+05
0.01	4.49E+05	898.6892	11731.5538	0.0018	4.49E+05
0.01	-2.96E+04	-59.2401	-2288.8633	0.0018	-2.96E+04
0.01	-8.14E+04	-162.7363	-6726.8128	0.0018	-8.14E+04
0.01	-3.98E+04	-79.6234	-1461.9476	0.0018	-3.98E+04
0.01	-2.23E+04	-44.6265	-642.4239	0.0018	-2.23E+04
0.01	-1.20E+04	-24.0737	-277.3363	0.0018	-1.20E+04
0.01	-4.59E+03	-9.1879	-97.3072	0.0018	-4.59E+03
0.01	1.54E+03	3.0865	33.7861	0.0018	1.54E+03
0.01	6.74E+03	13.4751	140.9083	0.0018	6.74E+03
0.01	1.07E+04	21.3951	217.2511	0.0018	1.07E+04
0.01	1.28E+04	25.5493	279.8613	0.0018	1.28E+04

Bearing Friction Force	Bearing Friction Work	Denisty of Air	Area of Cross Section	Drag Coefficient	Drag Force	Drag Work
lb ft/sec^2	lb ft^2/sec^2	lb/ft^3	ft^2		lb ft/sec^2	lb ft^2/sec^2
0.0000	0.0000	0.0765	12	1.8	8594.4420	0.0000
0.8112	8.8860	0.0765	12	1.8	8594.4420	94141.5082
1.2099	12.2861	0.0765	12	1.8	8553.7865	86857.4249
-1.2073	-12.6252	0.0765	12	1.8	8434.4611	88198.4647
-5.5973	-61.2702	0.0765	12	1.8	8248.2547	90288.3886
-12.5861	-133.2972	0.0765	12	1.8	7987.4762	84594.1130
-20.5727	-237.0043	0.0765	12	1.8	7672.8244	88393.2844
-29.9326	-430.8970	0.0765	12	1.8	7272.6069	104693.2879
-48.1113	-883.3620	0.0765	12	1.8	6697.8205	122977.2387
-66.0001	-2728.1570	0.0765	12	1.8	5850.3867	241829.5680
660.5591	25522.0433	0.0765	12	1.8	3683.5518	142321.5109
665.8862	8692.5275	0.0765	12	1.8	1633.8811	21328.8032
644.2437	6948.3925	0.0765	12	1.8	1134.2710	12233.5065
631.4177	5775.1362	0.0765	12	1.8	908.5510	8309.8798
662.8806	6062.9053	0.0765	12	1.8	805.3725	7366.1790
712.7396	7687.1446	0.0765	12	1.8	895.7099	9660.5422
808.8202	10558.3984	0.0765	12	1.8	1105.2187	14427.6050
-53.3161	-2059.9770	0.0765	12	1.8	1544.6678	59681.3814
-146.4627	-6054.1315	0.0765	12	1.8	3520.4443	145519.8705
-71.6610	-1315.7529	0.0765	12	1.8	5639.4830	103545.3319
-40.1639	-578.1815	0.0765	12	1.8	6422.8462	92460.5027
-21.6663	-249.6027	0.0765	12	1.8	6946.5273	80026.1196
-8.2691	-87.5765	0.0765	12	1.8	7299.1901	77304.5826
2.7779	30.4075	0.0765	12	1.8	7567.8841	82840.8046
12.1276	126.8175	0.0765	12	1.8	7783.8876	81395.4705
19.2555	195.5260	0.0765	12	1.8	7924.1008	80463.4283
22.9944	251.8752	0.0765	12	1.8	7995.7982	87584.1041

Appendix E: Clothoid Loop Model



Appendix F: Banked Curve #1 Calculations

Location	Cart Mass	Gravity	Cart Weight	Height	Track Distance	Velocity	Velocity
	lb	ft/sec ²	lb ft/sec ²	Feet	Feet	ft/sec	mph
End of Loop	6100	32.2	196420	10	0	98.49107	67.153
Start of Curve	6100	32.2	196420	10	100	97.02189	66.15129
	6100	32.2	196420	10	26.17994	96.64411	65.89371
	6100	32.2	196420	10	26.17994	96.26754	65.63696
Middle of Curve	6100	32.2	196420	10	26.17994	95.89218	65.38103
	6100	32.2	196420	10	26.17994	95.51802	65.12592
	6100	32.2	196420	10	26.17994	95.14506	64.87163
End of Curve	6100	32.2	196420	10	26.17994	94.77329	64.61815
End (80 feet after)	6100	32.2	196420	10	80	93.63628	63.84292

Potential Energy	Kinetic Energy	Angle of Track	Radius of Wheel	Coefficient of Rolling Friction	Normal Force on Wheel
lb ft ² /sec ²	lb ft ² /sec ²	degrees	in	in	lb ft/sec ²
1964200	29586497.08	0	5	0.01	196420
1964200	28710402.93	0	5	0.01	196420
1964200	28487255.07	0	5	0.01	196420
1964200	28265689.71	0	5	0.01	196420
1964200	28045695.65	0	5	0.01	196420
1964200	27827261.73	0	5	0.01	196420
1964200	27610376.89	0	5	0.01	196420
1964200	27395030.14	0	5	0.01	196420
1964200	26741645.7	0	5	0.01	196420

Rolling Friction Force	Rolling Friction Work	Coefficient of Bearing Friction	Bearing Load	Bearing Friction Force	Bearing Friction Work
lb ft/sec ²	lb ft ² /sec ²		lb ft/sec ²	lb ft/sec ²	lb ft ² /sec ²
392.84	0	0.0018	196420	353.556	0
392.84	39284	0.0018	196420	353.556	35355.6
392.84	10284.52715	0.0018	196420	353.556	9256.074435
392.84	10284.52715	0.0018	196420	353.556	9256.074435
392.84	10284.52715	0.0018	196420	353.556	9256.074435
392.84	10284.52715	0.0018	196420	353.556	9256.074435
392.84	10284.52715	0.0018	196420	353.556	9256.074435
392.84	10284.52715	0.0018	196420	353.556	9256.074435
392.84	31427.2	0.0018	196420	353.556	28284.48

Denisty of Air	Area of Cross Section	Drag Coefficient	Drag Force	Drag Work	Radius of Curvature	Theta	G Force Before Bank
lb/ft^3	ft^2		lb ft/sec^2	lb ft^2/sec^2	ft	(degrees)	
0.0765	12	1.8	8014.54554	0	0	0	
0.0765	12	1.8	8014.54554	801454.5538	50	80.2943	5.846737182
0.0765	12	1.8	7777.22456	203607.2628	50	80.21973	5.801294179
0.0765	12	1.8	7716.77709	202024.7519	50	80.14457	5.756173447
0.0765	12	1.8	7656.75831	200453.4638	50	80.06879	5.711372701
0.0765	12	1.8	7597.16516	198893.3188	50	79.99241	5.66688967
0.0765	12	1.8	7537.99464	197344.2381	50	79.9154	5.622722103
0.0765	12	1.8	7479.24373	195806.143	50	79.83777	5.578867761
0.0765	12	1.8	7420.90948	593672.7581	0	0	

Appendix G: Hill #2 Calculations

Location	Car Mass	Gravity	Car Weight	Track Height	Horizontal Distance	Angle of Track
	lbs	ft/sec^2	lb ft/sec^2	feet	feet	degrees
Start of Hill #2	6100	32.2	196420	10	0	0
	6100	32.2	196420	10.64354519	9.203125	4
	6100	32.2	196420	13.13682522	19.203125	14
	6100	32.2	196420	17.58911207	29.203125	24
	6100	32.2	196420	24.59118745	39.203125	35
	6100	32.2	196420	35.6973126	49.203125	48
Change in Curve	6100	32.2	196420	60.44818114	59.203125	68
	6100	32.2	196420	76.73801505	67.86458333	62
	6100	32.2	196420	84.83585539	77.86458333	39
	6100	32.2	196420	88.87611764	87.86458333	22
Peak of Hill	6100	32.2	196420	90	97.86458333	7
	6100	32.2	196420	88.87611764	107.8645833	7
	6100	32.2	196420	84.83585539	117.8645833	22
	6100	32.2	196420	76.73801505	127.8645833	39
Change in Curve	6100	32.2	196420	60.44818114	136.5260417	62
	6100	32.2	196420	35.6973126	146.5260417	68
	6100	32.2	196420	24.59118745	156.5260417	48
	6100	32.2	196420	17.58911207	166.5260417	35
	6100	32.2	196420	13.13682522	176.5260417	24
	6100	32.2	196420	10.64354519	186.5260417	14
Bottom of Hill #2	6100	32.2	196420	10	195.7291667	4

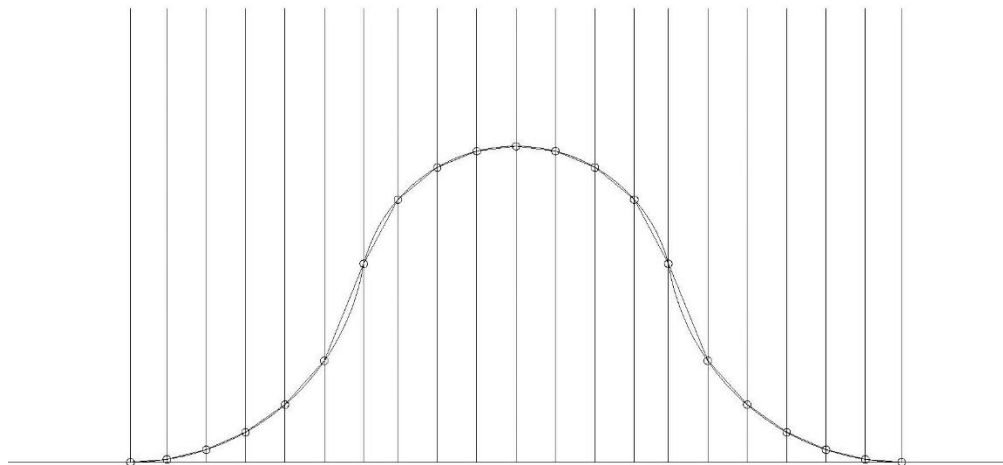
Track Distance	Potential Energy	Kinetic Energy	Radius of Wheel	Coefficient of Rolling Friction
feet	lb ft^2/sec^2	lb ft^2/sec^2	in	in
10	1.96E+06	26741645.7	5	0.01
9.225598093	2.09E+06	26535337.42	5	0.01
10.30613629	2.58E+06	25972424.3	5	0.01
10.94636279	3.45E+06	25017932.85	5	0.01
12.20774589	4.83E+06	23560937.87	5	0.01
14.9447655	7.01E+06	21294095.18	5	0.01
26.69467163	1.19E+07	16338860.39	5	0.01
18.44937802	1.51E+07	13013597.8	5	0.01
12.86759566	1.67E+07	11351517.53	5	0.01
10.78534743	1.75E+07	10510897.93	5	0.01
10.07509825	1.77E+07	10251972.45	5	0.01
10.07509825	1.75E+07	10437281.83	5	0.01
10.78534743	1.67E+07	11194920.8	5	0.01
12.86759566	1.51E+07	12745327.65	5	0.01
18.44937802	1.19E+07	15893087.22	5	0.01
26.69467163	7.01E+06	20668759.63	5	0.01
14.9447655	4.83E+06	22693300.99	5	0.01
12.20774589	3.45E+06	23969315.01	5	0.01
10.94636279	2.58E+06	24757105.15	5	0.01
10.30613629	2.09E+06	25165961.28	5	0.01
9.225598093	1.96E+06	25214644.63	5	0.01

Radius of Curvature of Track	Normal Force on Wheel	Rolling Friction Force	Rolling Friction Work	Coefficient of Bearing Friction	Bearing Load
feet	lb ft/sec ²	lb ft/sec ²	lb ft ² /sec ²		lb ft/sec ²
0	196420	392.84	3928.4	0.0018	196420
60	195941.53	391.8830615	3615.355625	0.0018	195941.531
60	190585.4866	381.1709731	3928.4	0.0018	190585.487
60	179438.60	358.8771976	3928.4	0.0018	179438.599
60	160897.8445	321.7956891	3928.4	0.0018	160897.845
60	131430.63	262.8612674	3928.4	0.0018	131430.634
60	73580.22708	147.1604542	3928.4	0.0018	73580.2271
40	92213.60	184.4272087	3402.567292	0.0018	92213.6044
40	152647.0097	305.2940195	3928.4	0.0018	152647.01
40	182117.4527	364.2349054	3928.4	0.0018	182117.453
40	194955.9151	389.9118302	3928.4	0.0018	194955.915
40	194955.9151	389.9118302	3928.4	0.0018	194955.915
40	182117.4527	364.2349054	3928.4	0.0018	182117.453
40	152647.0097	305.2940195	3928.4	0.0018	152647.01
60	92213.60436	184.4272087	3402.567292	0.0018	92213.6044
60	73580.22708	147.1604542	3928.4	0.0018	73580.2271
60	131430.6337	262.8612674	3928.4	0.0018	131430.634
60	160897.8445	321.7956891	3928.4	0.0018	160897.845
60	179438.5988	358.8771976	3928.4	0.0018	179438.599
60	190585.4866	381.1709731	3928.4	0.0018	190585.487
60	195941.5308	391.8830615	3615.355625	0.0018	195941.531

Bearing Friction Force	Bearing Friction Work	Denisty of Air	Area of Cross Section	Drag Coefficient	Drag Force
lb ft/sec ²	lb ft ² /sec ²	lb/ft ³	ft ²		lb ft/sec ²
353.556	3535.56	0.0765	12	1.8	7243.917272
352.6947554	3253.820063	0.0765	12	1.8	7188.031403
343.0538758	3535.56	0.0765	12	1.8	7035.546542
322.9894778	3535.56	0.0765	12	1.8	6776.988892
289.6161202	3535.56	0.0765	12	1.8	6382.310448
236.5751407	3535.56	0.0765	12	1.8	5768.256209
132.4444087	3535.56	0.0765	12	1.8	4425.956214
165.9844879	3062.310563	0.0765	12	1.8	3525.19164
274.7646175	3535.56	0.0765	12	1.8	3074.958618
327.8114149	3535.56	0.0765	12	1.8	2847.247172
350.9206472	3535.56	0.0765	12	1.8	2777.108079
350.9206472	3535.56	0.0765	12	1.8	2827.305655
327.8114149	3535.56	0.0765	12	1.8	3032.538873
274.7646175	3535.56	0.0765	12	1.8	3452.521215
165.9844879	3062.310563	0.0765	12	1.8	4305.20284
132.4444087	3535.56	0.0765	12	1.8	5598.862034
236.5751407	3535.56	0.0765	12	1.8	6147.280418
289.6161202	3535.56	0.0765	12	1.8	6492.93379
322.9894778	3535.56	0.0765	12	1.8	6706.334515
343.0538758	3535.56	0.0765	12	1.8	6817.087609
352.6947554	3253.820063	0.0765	12	1.8	6830.275211

Drag Work	Velocity	Velocity	Centripetal Acceleration	G Forces
lb ft ² /sec ²	ft/sec	mph	ft/sec ²	G's
72439.17272	93.63628	63.842917		
66313.88881	93.27438	63.596171	145.0018439	4.503163
72509.30156	92.27973	62.917999	141.9258158	4.407634
74183.37901	90.56821	61.751053	136.7100156	4.245653
77913.62412	87.8914	59.925952	128.7482944	3.998394
86205.23638	83.55639	56.970267	116.3611758	3.613701
118149.4477	73.19155	49.903331	89.28339009	2.772776
65037.59318	65.32039	44.53663	106.6688344	3.312697
39567.32416	61.00663	41.59543	93.04522567	2.889603
30708.54996	58.70431	40.025666	86.15490111	2.675618
27979.63676	57.97674	39.529596	84.03256109	2.609707
28485.38227	58.49837	39.885254	85.5514904	2.656879
32706.98534	60.58437	41.307525	91.76164589	2.849741
44425.647	64.64361	44.075187	104.4698988	3.244407
79428.31467	72.18621	49.217867	86.84747116	2.697126
149459.7835	82.32037	56.127522	112.9440417	3.507579
91869.6643	86.25791	58.812209	124.0071092	3.851152
79264.08577	88.64983	60.443064	130.9798634	4.067698
73409.97056	90.09486	61.428313	135.2847276	4.201389
70257.83402	90.83576	61.933471	137.5189141	4.270774
63013.37396	90.92358	61.993347	137.7849433	4.279036

Appendix H: Hill #2 Model



Appendix I: Straight Away #2 Calculations

Location	Cart Mass	Gravity	Cart Weight	Height	Track Distance	Velocity	Velocity
	lb	ft/sec ²	lb ft/sec ²	Feet	Feet	ft/sec	mph
Start	6100	32.2	196420	10	0	90.92358	61.99335
End	6100	32.2	196420	10	40	90.3755	61.61966

Potential Energy	Kinetic Energy	Angle of Track	Radius of Wheel	Coefficient of Rolling Friction	Normal Force on Wheel
lb ft ² /sec ²	lb ft ² /sec ²	degrees	in	in	lb ft/sec ²
1964200	25214644.63	0	5	0.01	196420
1964200	24911577.78	0	5	0.01	196420

Rolling Friction Force	Rolling Friction Work	Coefficient of Bearing Friction	Bearing Load	Bearing Friction Force	Bearing Friction Work
lb ft/sec ²	lb ft ² /sec ²		lb ft/sec ²	lb ft/sec ²	lb ft ² /sec ²
392.84	0	0.0018	196420	353.556	0
392.84	15713.6	0.0018	196420	353.556	14142.24

Denisty of Air	Area of Cross Section	Drag Coefficient	Drag Force	Drag Work
lb/ft ³	ft ²		lb ft/sec ²	lb ft ² /sec ²
0.0765	12	1.8	6830.27521	0
0.0765	12	1.8	6830.27521	273211.0084

Appendix J: Hill Series Calculations

Location	Car Mass	Gravity	Car Weight	Track Height	Horizontal Distance	Angle of Track
	lbs	ft/sec^2	lb ft/sec^2	feet	feet	degrees
Start of Hill #3	6100.00	32.20	196420.00	10.00	0.00	0.00
	6100.00	32.20	196420.00	10.87	10.00	5.00
	6100.00	32.20	196420.00	13.55	20.00	15.00
	6100.00	32.20	196420.00	18.22	30.00	25.00
	6100.00	32.20	196420.00	25.48	40.00	36.00
Curve Change	6100.00	32.20	196420.00	36.99	50.00	49.00
	6100.00	32.20	196420.00	69.70	60.00	73.00
	6100.00	32.20	196420.00	100.47	70.00	72.00
	6100.00	32.20	196420.00	110.47	80.00	45.00
	6100.00	32.20	196420.00	116.25	90.00	30.00
Top of 1st Peak	6100.00	32.20	196420.00	119.49	100.00	18.00
	6100.00	32.20	196420.00	120.00	110.00	6.00
	6100.00	32.20	196420.00	119.49	120.00	6.00
	6100.00	32.20	196420.00	116.25	130.00	18.00
	6100.00	32.20	196420.00	110.47	140.00	30.00
Curve Change	6100.00	32.20	196420.00	100.47	150.00	45.00
	6100.00	32.20	196420.00	69.70	160.00	72.00
	6100.00	32.20	196420.00	38.92	170.00	72.00
	6100.00	32.20	196420.00	28.92	180.00	45.00
	6100.00	32.20	196420.00	23.14	190.00	30.00
Bottom of 1st Valley	6100.00	32.20	196420.00	19.90	200.00	18.00
	6100.00	32.20	196420.00	20.00	210.00	6.00
	6100.00	32.20	196420.00	19.90	220.00	6.00
	6100.00	32.20	196420.00	23.14	230.00	18.00
	6100.00	32.20	196420.00	28.92	240.00	30.00
Curve Change	6100.00	32.20	196420.00	38.92	250.00	45.00
	6100.00	32.20	196420.00	69.70	260.00	72.00
	6100.00	32.20	196420.00	98.74	270.00	71.00
	6100.00	32.20	196420.00	109.46	280.00	47.00
	6100.00	32.20	196420.00	115.95	290.00	33.00
Top of 2nd Peak	6100.00	32.20	196420.00	119.79	300.00	21.00
	6100.00	32.20	196420.00	121.56	310.00	10.00
	6100.00	32.20	196420.00	120.00	314.88	6.00
	6100.00	32.20	196420.00	119.13	324.88	5.00
	6100.00	32.20	196420.00	116.26	334.88	16.00
Curve Change	6100.00	32.20	196420.00	111.16	344.88	27.00
	6100.00	32.20	196420.00	102.77	354.88	40.00
	6100.00	32.20	196420.00	82.57	367.02	59.00
	6100.00	32.20	196420.00	60.11	377.02	66.00
	6100.00	32.20	196420.00	48.60	387.02	49.00
Curve Change	6100.00	32.20	196420.00	40.79	397.02	38.00
	6100.00	32.20	196420.00	35.47	407.02	28.00
	6100.00	32.20	196420.00	32.03	417.02	19.00
	6100.00	32.20	196420.00	30.08	427.02	11.00

Bottom of 2nd Valley	6100.00	32.20	196420.00	30.00	434.80	3.00
	6100.00	32.20	196420.00	30.70	444.80	4.00
	6100.00	32.20	196420.00	32.82	454.80	12.00
	6100.00	32.20	196420.00	36.66	464.80	21.00
	6100.00	32.20	196420.00	42.44	474.80	30.00
	6100.00	32.20	196420.00	50.83	484.80	40.00
Curve Change	6100.00	32.20	196420.00	63.63	494.80	52.00
	6100.00	32.20	196420.00	79.54	501.88	66.00
	6100.00	32.20	196420.00	94.36	511.88	56.00
	6100.00	32.20	196420.00	102.18	521.88	38.00
	6100.00	32.20	196420.00	106.84	531.88	25.00
	6100.00	32.20	196420.00	109.15	541.88	13.00
Top of 3rd Peak	6100.00	32.20	196420.00	110.00	547.71	3.00
	6100.00	32.20	196420.00	108.95	557.71	6.00
	6100.00	32.20	196420.00	105.70	567.71	18.00
	6100.00	32.20	196420.00	99.93	577.71	30.00
	6100.00	32.20	196420.00	89.93	587.71	45.00
	6100.00	32.20	196420.00	71.25	596.42	65.00
Curve Change	6100.00	32.20	196420.00	47.69	606.42	67.00
	6100.00	32.20	196420.00	34.89	616.42	52.00
	6100.00	32.20	196420.00	26.20	626.42	41.00
	6100.00	32.20	196420.00	19.95	636.42	32.00
	6100.00	32.20	196420.00	15.50	646.42	24.00
	6100.00	32.20	196420.00	12.44	656.42	17.00
Bottom of Hill #5	6100.00	32.20	196420.00	10.86	666.42	9.00
	6100.00	32.20	196420.00	10.00	676.42	3.00

Track Distance	Potential Energy	Kinetic Energy	Radius of Wheel	Coefficient of Rolling Friction
feet	lb ft ² /sec ²	lb ft ² /sec ²	in	in
10.00	1964200.00	24911577.78	5.00	0.010
10.04	2136045.23	24664786.80	5.00	0.01
10.35	2662351.04	24063948.55	5.00	0.01
11.03	3578272.54	23073077.90	5.00	0.01
12.36	5005347.37	21569576.26	5.00	0.01
15.24	7264901.00	19230336.71	5.00	0.01
34.20	13689509.71	12718862.42	5.00	0.01
32.36	19734695.71	6548370.95	5.00	0.01
14.14	21698895.71	4519303.77	5.00	0.01
11.55	22832927.11	3360495.43	5.00	0.01
10.51	23471134.38	2704312.87	5.00	0.01
10.06	23570400.00	2589880.71	5.00	0.01
10.06	23471134.38	2674628.12	5.00	0.01
10.51	22832927.11	3298086.35	5.00	0.01
11.55	21698895.71	4415259.99	5.00	0.01
14.14	19734695.71	6358185.48	5.00	0.01
32.36	13689509.71	12371549.98	5.00	0.01
32.36	7644323.71	18300822.64	5.00	0.01
14.14	5680123.71	20097133.10	5.00	0.01
11.55	4546092.31	21146710.52	5.00	0.01
10.51	3907885.04	21711308.75	5.00	0.01
10.06	3928400.00	21621490.46	5.00	0.01
10.06	3907885.04	21575649.42	5.00	0.01
10.51	4546092.31	20871211.00	5.00	0.01
11.55	5680123.71	19670269.09	5.00	0.01
14.14	7644323.71	17637078.23	5.00	0.01
32.36	13689509.71	11516862.46	5.00	0.01
30.72	19393960.72	5703990.32	5.00	0.01
14.66	21500307.34	3542720.35	5.00	0.01
11.92	22775873.73	2245618.54	5.00	0.01
10.71	23529859.47	1476915.64	5.00	0.01
10.15	23876200.92	1118824.84	5.00	0.01
4.91	23570400.00	1414084.32	5.00	0.01
10.04	23398554.77	1580407.31	5.00	0.01
10.40	22835329.48	2131871.19	5.00	0.01
11.22	21834519.59	3119209.47	5.00	0.01
13.05	20186360.10	4750421.93	5.00	0.01
23.57	16217616.79	8694903.05	5.00	0.01
24.59	11805951.35	13041986.47	5.00	0.01
15.24	9546397.73	15207216.94	5.00	0.01
12.69	8011796.50	16671563.96	5.00	0.01
11.33	6967412.84	17651173.78	5.00	0.01
10.58	6291084.54	18265884.93	5.00	0.01
10.19	5909282.73	18587892.14	5.00	0.01

7.79	5892600.00	18545816.64	5.00	0.01
10.02	6029950.24	18363543.59	5.00	0.01
10.22	6447453.84	17888710.43	5.00	0.01
10.71	7201439.58	17077720.28	5.00	0.01
11.55	8335470.98	15886672.66	5.00	0.01
13.05	9983630.47	14181357.06	5.00	0.01
16.24	12497691.83	11609684.26	5.00	0.01
17.42	15622621.51	8426209.11	5.00	0.01
17.88	18534667.76	5469125.44	5.00	0.01
12.69	20069268.99	3900566.61	5.00	0.01
11.03	20985190.49	2963772.63	5.00	0.01
10.26	21438661.79	2493978.98	5.00	0.01
5.84	21606200.00	2312043.29	5.00	0.01
10.06	21399754.26	2510483.78	5.00	0.01
10.51	20761546.99	3134389.10	5.00	0.01
11.55	19627515.60	4252029.00	5.00	0.01
14.14	17663315.60	6195465.06	5.00	0.01
20.61	13995156.17	9832426.35	5.00	0.01
25.59	9367790.95	14398409.33	5.00	0.01
16.24	6853729.59	16805185.74	5.00	0.01
13.25	5146276.58	18431233.56	5.00	0.01
11.79	3918908.20	19584983.40	5.00	0.01
10.95	3044390.02	20389478.87	5.00	0.01
10.46	2443873.81	20922072.07	5.00	0.01
10.12	2132775.10	21166442.45	5.00	0.01
10.01	1964200.00	21269502.11	5.00	0.01

Radius of Curvature of Track	Normal Force on Wheel	Rolling Friction Force	Rolling Friction Work	Coefficient of Bearing Friction	Bearing Load
feet	lb ft/sec^2	lb ft/sec^2	lb ft^2/sec^2		lb ft/sec^2
0.00	196420.00	392.84	3928.40	0.0018	196420.00
60.00	195672.56	391.35	3928.40	0.0018	195672.56
60.00	189727.15	379.45	3928.40	0.0018	189727.15
60.00	178016.98	356.03	3928.40	0.0018	178016.98
60.00	158907.12	317.81	3928.40	0.0018	158907.12
60.00	128863.11	257.73	3928.40	0.0018	128863.11
60.00	57427.65	114.86	3928.40	0.0018	57427.65
50.00	60697.12	121.39	3928.40	0.0018	60697.12
50.00	138889.91	277.78	3928.40	0.0018	138889.91
50.00	170104.71	340.21	3928.40	0.0018	170104.71
50.00	186806.52	373.61	3928.40	0.0018	186806.52
50.00	195343.99	390.69	3928.40	0.0018	195343.99
50.00	195343.99	390.69	3928.40	0.0018	195343.99
50.00	186806.52	373.61	3928.40	0.0018	186806.52
50.00	170104.71	340.21	3928.40	0.0018	170104.71
50.00	138889.91	277.78	3928.40	0.0018	138889.91
50.00	60697.12	121.39	3928.40	0.0018	60697.12
50.00	60697.12	121.39	3928.40	0.0018	60697.12
50.00	138889.91	277.78	3928.40	0.0018	138889.91
50.00	170104.71	340.21	3928.40	0.0018	170104.71
50.00	186806.52	373.61	3928.40	0.0018	186806.52
50.00	195343.99	390.69	3928.40	0.0018	195343.99
50.00	195343.99	390.69	3928.40	0.0018	195343.99
50.00	186806.52	373.61	3928.40	0.0018	186806.52
50.00	170104.71	340.21	3928.40	0.0018	170104.71
50.00	138889.91	277.78	3928.40	0.0018	138889.91
50.00	60697.12	121.39	3928.40	0.0018	60697.12
55.00	63948.10	127.90	3928.40	0.0018	63948.10
55.00	133958.12	267.92	3928.40	0.0018	133958.12
55.00	164731.67	329.46	3928.40	0.0018	164731.67
55.00	183373.87	366.75	3928.40	0.0018	183373.87
55.00	193435.94	386.87	3928.40	0.0018	193435.94
55.00	195343.99	390.69	1917.14	0.0018	195343.99
55.00	195672.56	391.35	3928.40	0.0018	195672.56
55.00	188811.02	377.62	3928.40	0.0018	188811.02
55.00	175011.50	350.02	3928.40	0.0018	175011.50
55.00	150466.45	300.93	3928.40	0.0018	150466.45
55.00	101163.78	202.33	4769.32	0.0018	101163.78
70.00	79891.21	159.78	3928.40	0.0018	79891.21
70.00	128863.11	257.73	3928.40	0.0018	128863.11
70.00	154781.07	309.56	3928.40	0.0018	154781.07
70.00	173428.57	346.86	3928.40	0.0018	173428.57
70.00	185718.76	371.44	3928.40	0.0018	185718.76
70.00	192811.21	385.62	3928.40	0.0018	192811.21

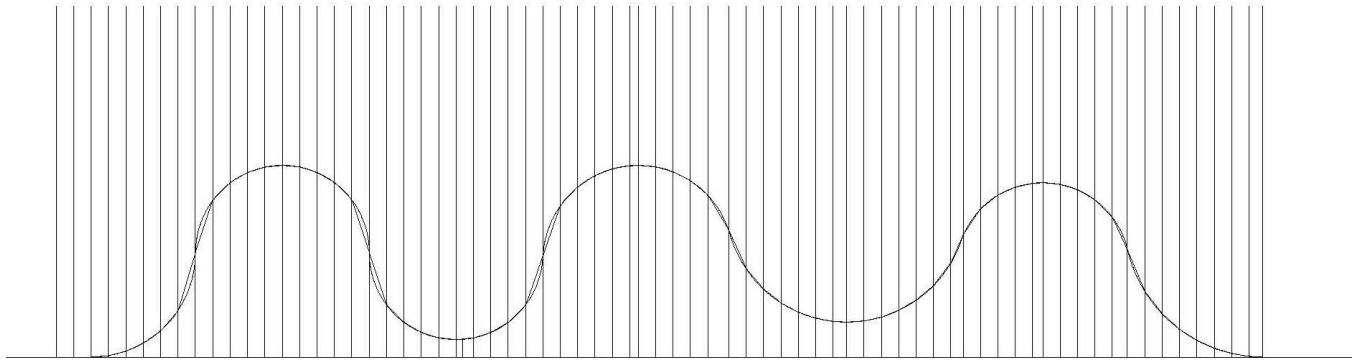
70.00	196150.81	392.30	3054.74	0.0018	196150.81
70.00	195941.53	391.88	3928.40	0.0018	195941.53
70.00	192127.75	384.26	3928.40	0.0018	192127.75
70.00	183373.87	366.75	3928.40	0.0018	183373.87
70.00	170104.71	340.21	3928.40	0.0018	170104.71
70.00	150466.45	300.93	3928.40	0.0018	150466.45
70.00	120928.23	241.86	3928.40	0.0018	120928.23
70.00	79891.21	159.78	2782.62	0.0018	79891.21
50.00	109836.67	219.67	3928.40	0.0018	109836.67
50.00	154781.07	309.56	3928.40	0.0018	154781.07
50.00	178016.98	356.03	3928.40	0.0018	178016.98
50.00	191385.77	382.77	3928.40	0.0018	191385.77
50.00	196150.81	392.30	2289.52	0.0018	196150.81
50.00	195343.99	390.69	3928.40	0.0018	195343.99
50.00	186806.52	373.61	3928.40	0.0018	186806.52
50.00	170104.71	340.21	3928.40	0.0018	170104.71
50.00	138889.91	277.78	3928.40	0.0018	138889.91
50.00	83010.68	166.02	3420.98	0.0018	83010.68
80.00	76747.41	153.49	3928.40	0.0018	76747.41
80.00	120928.23	241.86	3928.40	0.0018	120928.23
80.00	148240.06	296.48	3928.40	0.0018	148240.06
80.00	166573.61	333.15	3928.40	0.0018	166573.61
80.00	179438.60	358.88	3928.40	0.0018	179438.60
80.00	187837.38	375.67	3928.40	0.0018	187837.38
80.00	194001.74	388.00	3928.40	0.0018	194001.74
80.00	196150.81	392.30	3928.40	0.0018	196150.81

Bearing Friction Force	Bearing Friction Work	Denisty of Air	Area of Cross Section	Drag Coefficient	Drag Force
lb ft/sec^2	lb ft^2/sec^2	lb/ft^3	ft^2		lb ft/sec^2
353.56	3535.56	0.0765	12.00	1.80	6748.18
352.21	3535.56	0.0765	12.00	1.80	6681.33
341.51	3535.56	0.0765	12.00	1.80	6518.57
320.43	3535.56	0.0765	12.00	1.80	6250.16
286.03	3535.56	0.0765	12.00	1.80	5842.88
231.95	3535.56	0.0765	12.00	1.80	5209.21
103.37	3535.56	0.0765	12.00	1.80	3445.35
109.25	3535.56	0.0765	12.00	1.80	1773.86
250.00	3535.56	0.0765	12.00	1.80	1224.21
306.19	3535.56	0.0765	12.00	1.80	910.31
336.25	3535.56	0.0765	12.00	1.80	732.56
351.62	3535.56	0.0765	12.00	1.80	701.56
351.62	3535.56	0.0765	12.00	1.80	724.52
336.25	3535.56	0.0765	12.00	1.80	893.40
306.19	3535.56	0.0765	12.00	1.80	1196.03
250.00	3535.56	0.0765	12.00	1.80	1722.34
109.25	3535.56	0.0765	12.00	1.80	3351.27
109.25	3535.56	0.0765	12.00	1.80	4957.42
250.00	3535.56	0.0765	12.00	1.80	5444.02
306.19	3535.56	0.0765	12.00	1.80	5728.33
336.25	3535.56	0.0765	12.00	1.80	5881.27
351.62	3535.56	0.0765	12.00	1.80	5856.94
351.62	3535.56	0.0765	12.00	1.80	5844.53
336.25	3535.56	0.0765	12.00	1.80	5653.70
306.19	3535.56	0.0765	12.00	1.80	5328.39
250.00	3535.56	0.0765	12.00	1.80	4777.62
109.25	3535.56	0.0765	12.00	1.80	3119.75
115.11	3535.56	0.0765	12.00	1.80	1545.13
241.12	3535.56	0.0765	12.00	1.80	959.67
296.52	3535.56	0.0765	12.00	1.80	608.30
330.07	3535.56	0.0765	12.00	1.80	400.07
348.18	3535.56	0.0765	12.00	1.80	303.07
351.62	1725.43	0.0765	12.00	1.80	383.05
352.21	3535.56	0.0765	12.00	1.80	428.11
339.86	3535.56	0.0765	12.00	1.80	577.49
315.02	3535.56	0.0765	12.00	1.80	844.95
270.84	3535.56	0.0765	12.00	1.80	1286.82
182.09	4292.39	0.0765	12.00	1.80	2355.32
143.80	3535.56	0.0765	12.00	1.80	3532.88
231.95	3535.56	0.0765	12.00	1.80	4119.41
278.61	3535.56	0.0765	12.00	1.80	4516.08
312.17	3535.56	0.0765	12.00	1.80	4781.44
334.29	3535.56	0.0765	12.00	1.80	4947.96
347.06	3535.56	0.0765	12.00	1.80	5035.19

353.07	2749.27	0.0765	12.00	1.80	5023.79
352.69	3535.56	0.0765	12.00	1.80	4974.41
345.83	3535.56	0.0765	12.00	1.80	4845.79
330.07	3535.56	0.0765	12.00	1.80	4626.10
306.19	3535.56	0.0765	12.00	1.80	4303.47
270.84	3535.56	0.0765	12.00	1.80	3841.52
217.67	3535.56	0.0765	12.00	1.80	3144.89
143.80	2504.35	0.0765	12.00	1.80	2282.54
197.71	3535.56	0.0765	12.00	1.80	1481.51
278.61	3535.56	0.0765	12.00	1.80	1056.61
320.43	3535.56	0.0765	12.00	1.80	802.84
344.49	3535.56	0.0765	12.00	1.80	675.58
353.07	2060.57	0.0765	12.00	1.80	626.30
351.62	3535.56	0.0765	12.00	1.80	680.05
336.25	3535.56	0.0765	12.00	1.80	849.06
306.19	3535.56	0.0765	12.00	1.80	1151.81
250.00	3535.56	0.0765	12.00	1.80	1678.26
149.42	3078.88	0.0765	12.00	1.80	2663.46
138.15	3535.56	0.0765	12.00	1.80	3900.32
217.67	3535.56	0.0765	12.00	1.80	4552.28
266.83	3535.56	0.0765	12.00	1.80	4992.75
299.83	3535.56	0.0765	12.00	1.80	5305.28
322.99	3535.56	0.0765	12.00	1.80	5523.21
338.11	3535.56	0.0765	12.00	1.80	5667.48
349.20	3535.56	0.0765	12.00	1.80	5733.68
353.07	3535.56	0.0765	12.00	1.80	5761.59

Drag Work	Velocity	Velocity	Centripetal Acceleration	G Forces					
lb ft ² /sec ²	ft/sec	mph	ft/sec ²	G's					
67481.79	90.38	61.62			39118.80	77.98	53.17	86.87	2.70
67068.48	89.93	61.31	134.78	4.19	49865.60	77.59	52.91	86.01	2.67
67485.19	88.82	60.56	131.50	4.08	49540.46	76.58	52.22	83.79	2.60
68962.85	86.98	59.30	126.08	3.92	49552.26	74.83	51.02	79.99	2.48
72221.97	84.10	57.34	117.87	3.66	49692.14	72.17	49.21	74.41	2.31
79401.61	79.40	54.14	105.08	3.26	50147.49	68.19	46.49	66.42	2.06
117841.51	64.58	44.03	69.50	2.16	51081.52	61.70	42.07	54.38	1.69
57403.22	46.34	31.59	42.94	1.33	39750.44	52.56	35.84	39.47	1.23
17312.98	38.49	26.25	29.63	0.92	26493.64	42.35	28.87	35.86	1.11
10511.34	33.19	22.63	22.04	0.68	13408.52	35.76	24.38	25.58	0.79
7702.58	29.78	20.30	17.73	0.55	8858.38	31.17	21.25	19.43	0.60
7054.25	29.14	19.87	16.98	0.53	6933.53	28.60	19.50	16.35	0.51
7285.08	29.61	20.19	17.54	0.54	3655.15	27.53	18.77	15.16	0.47
9393.79	32.88	22.42	21.63	0.67	6837.99	28.69	19.56	16.46	0.51
13810.55	38.05	25.94	28.95	0.90	8927.54	32.06	21.86	20.55	0.64
24357.55	45.66	31.13	41.69	1.29	13299.98	37.34	25.46	27.88	0.87
108449.39	63.69	43.42	81.12	2.52	23734.18	45.07	30.73	40.63	1.26
160425.57	77.46	52.81	120.01	3.73	54882.37	56.78	38.71	64.47	2.00
76990.02	81.17	55.35	131.78	4.09	99820.99	68.71	46.85	59.01	1.83
66145.08	83.27	56.77	138.67	4.31	73941.23	74.23	50.61	68.87	2.14
61839.37	84.37	57.53	142.37	4.42	66154.58	77.74	53.00	75.54	2.35
58892.04	84.20	57.41	141.78	4.40	62558.75	80.13	54.64	80.27	2.49
58767.18	84.11	57.35	141.48	4.39	60459.05	81.76	55.75	83.56	2.60
59446.55	82.72	56.40	136.86	4.25	59264.38	82.82	56.47	85.75	2.66
61526.90	80.31	54.76	128.99	4.01	58051.48	83.31	56.80	86.75	2.69
67565.81	76.04	51.85	115.65	3.59	57695.01	83.51	56.94	87.17	2.71
100957.17	61.45	41.90	75.52	2.35					
47459.40	43.25	29.49	34.00	1.06					
14071.45	34.08	23.24	21.12	0.66					
7253.20	27.13	18.50	13.39	0.42					
4285.38	22.01	15.00	8.80	0.27					
3077.49	19.15	13.06	6.67	0.21					
1879.68	21.53	14.68	8.43	0.26					
4297.44	22.76	15.52	9.42	0.29					
6007.65	26.44	18.03	12.71	0.39					
9483.07	31.98	21.80	18.59	0.58					
16798.23	39.47	26.91	28.32	0.88					
55520.30	53.39	36.40	51.83	1.61					
86859.19	65.39	44.59	61.09	1.90					
62790.24	70.61	48.14	71.23	2.21					
57309.89	73.93	50.41	78.09	2.43					
54153.19	76.07	51.87	82.68	2.57					
52330.63	77.39	52.76	85.55	2.66					
51294.28	78.07	53.23	87.06	2.70					

Appendix K: Hill Series Model



Appendix L: Banked Curve #2 Calculations

Normal Force on Wheel	Rolling Friction Force	Rolling Friction Work	Coefficient of Bearing Friction	Bearing Load	Bearing Friction Force
lb ft/sec ²	lb ft/sec ²	lb ft ² /sec ²		lb ft/sec ²	lb ft/sec ²
196420	392.84	0	0.0018	196420	353.556
196420	392.84	15713.6	0.0018	196420	353.556
196420	392.84	10284.52715	0.0018	196420	353.556
196420	392.84	10284.52715	0.0018	196420	353.556
196420	392.84	10284.52715	0.0018	196420	353.556
196420	392.84	10284.52715	0.0018	196420	353.556
196420	392.84	10284.52715	0.0018	196420	353.556
196420	392.84	10284.52715	0.0018	196420	353.556
196420	392.84	23570.4	0.0018	196420	353.556

Bearing Friction Work	Denisty of Air	Area of Cross Section	Drag Coefficient	Drag Force	Drag Work	Radius of Curvature
lb ft ² /sec ²	lb/ft ³	ft ²		lb ft/sec ²	lb ft ² /sec ²	ft
0	0.0765	12	1.8	5761.59431	0	0
14142.24	0.0765	12	1.8	5761.59431	230463.7723	50
9256.074435	0.0765	12	1.8	5691.07757	148992.0623	50
9256.074435	0.0765	12	1.8	5645.42455	147796.8692	50
9256.074435	0.0765	12	1.8	5600.0953	146610.1522	50
9256.074435	0.0765	12	1.8	5555.08751	145431.851	50
9256.074435	0.0765	12	1.8	5510.39891	144261.9061	50
9256.074435	0.0765	12	1.8	5466.02723	143100.2582	50
21213.36	0.0765	12	1.8	5421.97022	325318.2131	0

Theta	G Force Before Bank
(degrees)	

0
76.84436 4.278420221
76.74172 4.244099344
76.63824 4.210021863
76.53391 4.176186052
76.42872 4.142590195
76.32268 4.109232593
76.21576 4.076111554

Appendix M: Braking Calculations

Location	Cart Mass	Gravity	Cart Weight	Height	Track Distance	Velocity	Velocity	Potential Energy
	lb	ft/sec ²	lb ft/sec ²	Feet	Feet	ft/sec	mph	lb ft ² /sec ²
Start Braking	6100	32.2	196420	10	0	80.25705	54.72072	1964200
	6100	32.2	196420	10	10	77.85013	53.07964	1964200
	6100	32.2	196420	10	10	75.37323	51.39084	1964200
	6100	32.2	196420	10	10	72.81917	49.64943	1964200
	6100	32.2	196420	10	10	70.17951	47.84967	1964200
	6100	32.2	196420	10	10	67.4442	45.98468	1964200
	6100	32.2	196420	10	10	64.60104	44.04617	1964200
	6100	32.2	196420	10	10	61.63511	42.02394	1964200
	6100	32.2	196420	10	10	58.52771	39.90526	1964200
	6100	32.2	196420	10	10	55.25497	37.67384	1964200
	6100	32.2	196420	10	10	51.7855	35.30829	1964200
	6100	32.2	196420	10	10	48.07672	32.77958	1964200
	6100	32.2	196420	10	10	44.0682	30.0465	1964200
	6100	32.2	196420	10	10	39.66917	27.04716	1964200
	6100	32.2	196420	10	10	34.7315	23.68057	1964200
	6100	32.2	196420	10	10	28.98114	19.75987	1964200
Station Start	6100	32.2	196420	10	10	21.78368	14.85251	1964200

Kinetic Energy	Angle of Track	Radius of Wheel	Coefficient of Rolling Friction	Normal Force on Wheel	Rolling Friction Force	Rolling Friction Work
lb ft ² /sec ²	degrees	in	in	lb ft/sec ²	lb ft/sec ²	lb ft ² /sec ²
19645643.81	0	5	0.01	196420	392.84	0
18484962.7	0	5	0.01	196420	392.84	3928.4
17327425.71	0	5	0.01	196420	392.84	3928.4
16173024.31	0	5	0.01	196420	392.84	3928.4
15021750.01	0	5	0.01	196420	392.84	3928.4
13873594.34	0	5	0.01	196420	392.84	3928.4
12728548.86	0	5	0.01	196420	392.84	3928.4
11586605.14	0	5	0.01	196420	392.84	3928.4
10447754.78	0	5	0.01	196420	392.84	3928.4
9311989.394	0	5	0.01	196420	392.84	3928.4
8179300.628	0	5	0.01	196420	392.84	3928.4
7049680.15	0	5	0.01	196420	392.84	3928.4
5923119.646	0	5	0.01	196420	392.84	3928.4
4799610.829	0	5	0.01	196420	392.84	3928.4
3679145.431	0	5	0.01	196420	392.84	3928.4
2561715.209	0	5	0.01	196420	392.84	3928.4
1447311.941	0	5	0.01	196420	392.84	3928.4

Coefficient of Bearing Friction	Bearing Load	Bearing Friction Force	Bearing Friction Work	Denisty of Air	Area of Cross Section	Drag Coefficient	Drag Force
	lb ft/sec^2	lb ft/sec^2	lb ft^2/sec^2	lb/ft^3	ft^2		lb ft/sec^2
0.0018	196420	353.556	0	0.0765	12	1.8	5321.7151
0.0018	196420	353.556	3535.56	0.0765	12	1.8	5321.7151
0.0018	196420	353.556	3535.56	0.0765	12	1.8	5007.3037
0.0018	196420	353.556	3535.56	0.0765	12	1.8	4693.744
0.0018	196420	353.556	3535.56	0.0765	12	1.8	4381.0337
0.0018	196420	353.556	3535.56	0.0765	12	1.8	4069.1704
0.0018	196420	353.556	3535.56	0.0765	12	1.8	3758.152
0.0018	196420	353.556	3535.56	0.0765	12	1.8	3447.9761
0.0018	196420	353.556	3535.56	0.0765	12	1.8	3138.6404
0.0018	196420	353.556	3535.56	0.0765	12	1.8	2830.1426
0.0018	196420	353.556	3535.56	0.0765	12	1.8	2522.4805
0.0018	196420	353.556	3535.56	0.0765	12	1.8	2215.6519
0.0018	196420	353.556	3535.56	0.0765	12	1.8	1909.6543
0.0018	196420	353.556	3535.56	0.0765	12	1.8	1604.4857
0.0018	196420	353.556	3535.56	0.0765	12	1.8	1300.1438
0.0018	196420	353.556	3535.56	0.0765	12	1.8	996.62621
0.0018	196420	353.556	3535.56	0.0765	12	1.8	693.93085

Drag Work	Braking Work	Braking Force	Braking Force
lb ft^2/sec^2	lb ft^2/sec^2	lb ft/sec^2	Newtons
0			0
53217.15055	1100000	110000	15208.04
50073.03667	1100000	110000	15208.04
46937.43973	1100000	110000	15208.04
43810.33666	1100000	110000	15208.04
40691.70445	1100000	110000	15208.04
37581.52016	1100000	110000	15208.04
34479.76089	1100000	110000	15208.04
31386.40384	1100000	110000	15208.04
28301.42623	1100000	110000	15208.04
25224.80537	1100000	110000	15208.04
22156.51862	1100000	110000	15208.04
19096.54341	1100000	110000	15208.04
16044.85722	1100000	110000	15208.04
13001.4376	1100000	110000	15208.04
9966.262149	1100000	110000	15208.04
6939.308544	1100000	110000	15208.04

Appendix N: Calculations for Axial Loads and Bending Moments in Supports

Support Locations

Location	Distance on Course	Height	Track Angle	Radius of Curvature	Tributary Track Distance
	feet	feet	degrees	feet	feet
Start	0.000	10.000	45.000	0.000	20.035
	40.069	38.333	45.000	0.000	40.069
	80.139	66.667	45.000	0.000	40.069
	120.208	95.000	45.000	0.000	40.069
	160.278	123.333	45.000	0.000	40.069
	200.347	151.667	45.000	0.000	40.069
Lift Peak	240.416	180.000	0.000	0.000	37.206
	274.758	148.876	65.000	0.000	34.342
	309.100	117.751	65.000	0.000	34.342
	343.442	86.627	65.000	0.000	34.342
Curve Starts	377.784	69.260	65.000	102.634	36.539
	416.520	31.696	42.000	102.634	38.736
	455.256	15.594	22.000	102.634	38.736
Bottom of Hill #1	493.991	10.053	0.000	102.634	36.035
	527.325	10.000	0.000	0.000	33.333
	560.658	10.000	0.000	0.000	33.333
End of Straight Away	593.991	10.000	0.000	0.000	34.006
	628.670	21.861	20.000	-323.055	34.679
	663.349	39.200	30.000	-323.055	34.679
	698.027	65.765	50.000	-323.055	34.679
Loop Right Side	732.706	98.446	76.000	-323.055	88.962
Loop Left Side	875.951	98.446	76.000	-323.055	88.962
	910.630	65.765	50.000	-323.055	34.679
	945.309	39.200	30.000	-323.055	34.679
	979.987	21.861	20.000	-323.055	34.679
End of Loop	1014.666	10.000	0.000	-323.055	34.006
	1047.999	10.000	0.000	0.000	33.333
	1081.333	10.000	26.765	0.000	33.333
End of Straight Away	1114.666	10.000	53.454	50.000	36.302
	1153.936	10.000	80.294	50.000	39.270
Middle of Curve	1193.206	10.000	80.069	50.000	39.270
	1232.476	10.000	79.838	50.000	39.270
End of Curve	1271.746	10.000	53.225	50.000	39.635
	1311.746	10.000	26.613	0.000	40.000
End of Straight Away	1351.746	10.000	0.000	0.000	35.721
	1383.187	26.816	22.667	60.000	31.442
	1414.629	43.632	45.333	60.000	31.442
Curve Change	1446.071	60.448	68.000	60.000	28.765
	1472.160	75.224	39.000	40.000	26.089
Hill#2 Peak	1498.248	90.000	0.000	40.000	26.089
	1524.337	75.224	39.000	40.000	26.089
Curve Change	1550.426	60.448	68.000	60.000	27.099

	1578.534	43.632	45.333	60.000	28.108
	1606.642	26.816	22.667	60.000	28.108
Bottom Hill #2	1634.751	10.000	0.000	60.000	34.054
End of Straight Away	1674.751	10.000	0.000	0.000	37.205
	1709.161	13.554	15.000	60.000	34.410
	1743.572	25.483	36.000	60.000	34.410
Curve Change	1777.982	69.695	60.000	60.000	36.860
	1817.292	94.848	30.000	50.000	39.310
Hill #3 Peak	1856.601	120.000	0.000	50.000	39.310
	1895.911	94.848	36.000	50.000	39.310
Curve Change	1935.221	69.695	72.000	50.000	38.152
	1972.214	53.130	45.000	50.000	36.993
	2009.208	36.565	20.000	50.000	36.993
Valley #1	2046.201	20.000	0.000	50.000	33.276
	2075.759	36.565	20.000	50.000	29.558
	2105.318	53.130	38.000	50.000	29.558
Curve Change	2134.876	69.695	72.000	50.000	28.625
	2162.567	109.461	47.000	55.000	27.692
	2190.259	119.794	21.000	55.000	27.692
Hill #4 Peak	2217.951	120.000	0.000	55.000	30.918
	2252.096	101.283	29.500	55.000	34.145
Curve Change	2286.241	82.566	59.000	55.000	32.472
	2317.040	65.044	39.333	70.000	30.798
	2347.838	47.522	19.667	70.000	30.798
Valley #2	2378.636	30.000	0.000	70.000	30.269
	2408.375	46.5123	22.000	70.000	29.739
	2438.115	63.0245	44.000	70.000	29.739
Curve Change	2467.854	79.537	66.000	70.000	29.296
	2496.707	94.768	33.000	50.000	28.853
Hill #5 Peak	2525.560	110.000	0.000	50.000	31.143
	2558.992	90.626	32.500	50.000	33.432
Curve Change	2592.424	71.251	65.000	50.000	34.786
	2628.564	50.8341	43.333	80.000	36.140
	2664.704	30.4171	21.667	80.000	36.140
Bottom of Hill #5	2700.844	10.000	0.000	80.000	38.070
End of Straight Away	2740.844	10.000	38.422	0.000	39.635
	2780.114	10.000	76.844	50.000	39.270
Middle of Curve	2819.384	10.000	76.534	50.000	39.270
	2858.653	10.000	76.216	50.000	39.270
End of Curve	2897.923	10.000	38.108	0.000	34.635
	2927.923	10.000	0.000	0.000	30.000
End of Straight Away	2957.923	10.000	0.000	0.000	35.000
	2997.923	10.000	0.000	0.000	40.000
	3037.923	10.000	0.000	0.000	40.000
	3077.923	10.000	0.000	0.000	40.000
End of Braking	3117.923	10.000	0.000	0.000	20.000

Track Mass	Track Mass	Track Weight	Train Mass	Train Weight	Velocity	Velocity	Normal Force
lb/ft	lb	lb ft/sec^2	lbs	lb ft/sec^2	ft/sec	mph	lb ft/sec^2
244.000	4888.465	157408.569	6100.000	196420.000	11.733	8.000	277779.828
244.000	9776.930	314817.138	6100.000	196420.000	12.711	8.667	277779.828
244.000	9776.930	314817.138	6100.000	196420.000	13.689	9.333	277779.828
244.000	9776.930	314817.138	6100.000	196420.000	14.667	10.000	277779.828
244.000	9776.930	314817.138	6100.000	196420.000	15.644	10.667	277779.828
244.000	9776.930	314817.138	6100.000	196420.000	16.622	11.333	277779.828
244.000	9078.178	292317.332	6100.000	196420.000	17.600	12.000	196420.000
244.000	8379.426	269817.525	6100.000	196420.000	34.587	23.582	464769.315
244.000	8379.426	269817.525	6100.000	196420.000	51.575	35.165	464769.315
244.000	8379.426	269817.525	6100.000	196420.000	68.562	46.747	464769.315
244.000	8915.485	287078.612	6100.000	196420.000	85.550	58.329	464769.315
244.000	9451.543	304339.699	6100.000	196420.000	97.863	66.725	264309.181
244.000	9451.543	304339.699	6100.000	196420.000	102.381	69.805	211845.794
244.000	8792.438	283116.516	6100.000	196420.000	103.524	70.584	196420.000
244.000	8133.333	261893.333	6100.000	196420.000	103.013	70.236	196420.000
244.000	8133.333	261893.333	6100.000	196420.000	102.503	69.888	196420.000
244.000	8297.458	267178.145	6100.000	196420.000	101.992	69.540	196420.000
244.000	8461.583	272462.957	6100.000	196420.000	93.187	63.537	209025.798
244.000	8461.583	272462.957	6100.000	196420.000	84.382	57.533	226806.280
244.000	8461.583	272462.957	6100.000	196420.000	75.577	51.529	305575.274
244.000	21706.743	698957.128	6100.000	196420.000	66.771	45.526	811914.934
244.000	21706.743	698957.128	6100.000	196420.000	65.276	44.507	811914.934
244.000	8461.583	272462.957	6100.000	196420.000	73.580	50.168	305575.274
244.000	8461.583	272462.957	6100.000	196420.000	81.884	55.830	226806.280
244.000	8461.583	272462.957	6100.000	196420.000	90.187	61.491	209025.798
244.000	8297.458	267178.145	6100.000	196420.000	98.491	67.153	196420.000
244.000	8133.333	261893.333	6100.000	196420.000	98.001	66.819	196420.000
244.000	8133.333	261893.333	6100.000	196420.000	97.512	66.485	219988.977
244.000	8857.595	285214.574	6100.000	196420.000	97.022	66.151	329861.033
244.000	9581.858	308535.815	6100.000	196420.000	96.457	65.766	1165092.440
244.000	9581.858	308535.815	6100.000	196420.000	95.892	65.381	1138893.536
244.000	9581.858	308535.815	6100.000	196420.000	95.333	65.000	1113265.960
244.000	9670.929	311403.907	6100.000	196420.000	94.773	64.618	328093.067
244.000	9760.000	314272.000	6100.000	196420.000	94.205	64.231	219695.456
244.000	8715.895	280651.810	6100.000	196420.000	93.636	63.843	196420.000
244.000	7671.789	247031.620	6100.000	196420.000	86.821	59.196	212860.852
244.000	7671.789	247031.620	6100.000	196420.000	80.006	54.550	279410.089
244.000	7018.717	226002.697	6100.000	196420.000	73.192	49.903	524336.740
244.000	6365.645	204973.774	6100.000	196420.000	65.584	44.716	252745.314
244.000	6365.645	204973.774	6100.000	196420.000	57.977	39.530	196420.000
244.000	6365.645	204973.774	6100.000	196420.000	60.584	41.308	252745.314
244.000	6612.051	212908.031	6100.000	196420.000	72.186	49.218	524336.740

244.000	6858.456	220842.287	6100.000	196420.000	78.432	53.476	279410.089
244.000	6858.456	220842.287	6100.000	196420.000	84.678	57.735	212860.852
244.000	8309.228	267557.144	6100.000	196420.000	90.924	61.993	196420.000
244.000	9078.060	292313.535	6100.000	196420.000	90.375	61.620	196420.000
244.000	8396.120	270355.071	6100.000	196420.000	88.825	60.562	203348.947
244.000	8396.120	270355.071	6100.000	196420.000	84.095	57.338	242788.472
244.000	8993.851	289602.008	6100.000	196420.000	64.576	44.029	392840.000
244.000	9591.582	308848.945	6100.000	196420.000	46.858	31.949	226806.280
244.000	9591.582	308848.945	6100.000	196420.000	29.140	19.868	196420.000
244.000	9591.582	308848.945	6100.000	196420.000	46.414	31.646	242788.472
244.000	9308.986	299749.353	6100.000	196420.000	63.689	43.424	635628.472
244.000	9026.390	290649.760	6100.000	196420.000	70.525	48.085	277779.828
244.000	9026.390	290649.760	6100.000	196420.000	77.360	52.746	209025.798
244.000	8119.296	261441.324	6100.000	196420.000	84.196	57.407	196420.000
244.000	7212.202	232232.888	6100.000	196420.000	76.614	52.237	209025.798
244.000	7212.202	232232.888	6100.000	196420.000	69.0316	47.067	249260.558
244.000	6984.475	224900.081	6100.000	196420.000	61.45	41.897	635628.472
244.000	6756.748	217567.273	6100.000	196420.000	34.08	23.237	288006.558
244.000	6756.748	217567.273	6100.000	196420.000	22.01	15.004	210394.300
244.000	7544.113	242920.454	6100.000	196420.000	21.53	14.681	196420.000
244.000	8331.479	268273.635	6100.000	196420.000	37.462	25.543	225677.847
244.000	7923.113	255124.249	6100.000	196420.000	53.39	36.404	381369.863
244.000	7514.747	241974.862	6100.000	196420.000	61.5879	41.992	253945.978
244.000	7514.747	241974.862	6100.000	196420.000	69.783	47.579	208587.648
244.000	7385.576	237815.535	6100.000	196420.000	77.978	53.167	196420.000
244.000	7256.404	233656.208	6100.000	196420.000	69.506	47.390	211845.794
244.000	7256.404	233656.208	6100.000	196420.000	61.034	41.614	273055.933
244.000	7148.271	230174.312	6100.000	196420.000	52.561	35.837	482916.903
244.000	7040.137	226692.416	6100.000	196420.000	40.047	27.305	234203.998
244.000	7598.804	244681.495	6100.000	196420.000	27.533	18.772	196420.000
244.000	8157.471	262670.573	6100.000	196420.000	42.155	28.742	232893.043
244.000	8487.787	273306.757	6100.000	196420.000	56.778	38.712	464769.315
244.000	8818.104	283942.940	6100.000	196420.000	65.688	44.787	270040.030
244.000	8818.104	283942.940	6100.000	196420.000	74.598	50.862	211352.583
244.000	9289.052	299107.470	6100.000	196420.000	83.508	56.937	196420.000
244.000	9670.929	311403.907	6100.000	196420.000	83.51	56.937	250710.662
244.000	9581.858	308535.815	6100.000	196420.000	82.9955	56.588	863016.810
244.000	9581.858	308535.815	6100.000	196420.000	81.9979	55.908	843475.370
244.000	9581.858	308535.815	6100.000	196420.000	81.0095	55.234	824371.848
244.000	8450.929	272119.907	6100.000	196420.000	80.6333	54.977	249628.222
244.000	7320.000	235704.000	6100.000	196420.000	80.4452	54.849	196420.000
244.000	8540.000	274988.000	6100.000	196420.000	80.2571	54.721	196420.000
244.000	9760.000	314272.000	6100.000	196420.000	65.6387	44.754	196420.000
244.000	9760.000	314272.000	6100.000	196420.000	51.0204	34.787	196420.000
244.000	9760.000	314272.000	6100.000	196420.000	36.402	24.820	196420.000
244.000	4880.000	157136.000	6100.000	196420.000	21.7837	14.853	196420.000

G Forces	Gravity	Normal Force (with G's)	Vertical Force from Train	Moving Axial Load	Stalled Axial Load
(vertical)	ft/sec^2	lbs	lbs	kips	kips
1.000	32.200	8626.703	6100.000	10.988	10.988
1.000	32.200	8626.703	6060.048	15.837	15.877
1.000	32.200	8626.703	6056.852	15.834	15.877
1.000	32.200	8626.703	6053.656	15.831	15.877
1.000	32.200	8626.703	6050.460	15.827	15.877
1.000	32.200	8626.703	6047.264	15.824	15.877
1.000	32.200	6100.000	6100.000	15.178	15.178
1.304	32.200	18816.588	10168.336	18.548	14.479
1.607	32.200	23199.346	13463.290	21.843	14.479
1.911	32.200	27582.104	16758.243	25.138	14.479
2.215	32.200	31964.862	20053.197	28.969	15.015
2.898	32.200	23787.335	21372.645	30.824	15.552
3.172	32.200	20866.896	20176.237	29.628	15.552
3.243	32.200	19781.644	19781.644	28.574	14.892
1.000	32.200	6100.000	6100.000	14.233	14.233
1.000	32.200	6100.000	6100.000	14.233	14.233
1.000	32.200	6100.000	6100.000	14.397	14.397
0.643	32.200	4173.056	5526.864	13.988	14.562
0.286	32.200	2012.388	3878.060	12.340	14.562
-0.071	32.200	-678.033	2511.165	10.973	14.562
-0.429	32.200	-10806.965	707.365	22.414	27.807
-0.410	32.200	-10328.433	-2372.009	19.335	27.807
-0.520	32.200	-4939.126	-762.282	7.699	14.562
-0.645	32.200	-4540.064	-2168.814	6.293	14.562
-0.782	32.200	-5075.786	-3434.891	5.027	14.562
-0.933	32.200	-5688.412	-5688.412	2.609	14.397
1.000	32.200	6100.000	6100.000	14.233	14.233
1.000	32.200	6831.956	6222.525	14.356	14.233
1.000	32.200	10244.131	6317.489	15.175	14.958
1.000	32.200	36182.995	6359.832	15.942	15.682
1.000	32.200	35369.364	6358.139	15.940	15.682
1.000	32.200	34573.477	6353.990	15.936	15.682
1.000	32.200	10189.226	6305.478	15.976	15.771
1.000	32.200	6822.840	6213.964	15.974	15.860
1.000	32.200	6100.000	6100.000	14.816	14.816
4.503	32.200	29768.543	28897.035	36.569	13.772
3.638	32.200	31567.869	24627.532	32.299	13.772
2.773	32.200	45151.192	19830.126	26.849	13.119
2.890	32.200	22681.170	20038.779	26.404	12.466
2.610	32.200	15919.212	15919.212	22.285	12.466
2.850	32.200	22368.279	18089.818	24.455	12.466
2.697	32.200	43919.332	21637.913	28.250	12.712

3.224	32.200	27979.445	21923.618	28.782	12.958
3.752	32.200	24801.148	24208.544	31.067	12.958
4.279	32.200	26102.117	26102.117	34.411	14.409
4.000	32.200	24400.000	24400.000	33.478	15.178
4.084	32.200	25789.682	25108.916	33.505	14.496
3.660	32.200	27599.858	23651.984	32.048	14.496
2.158	32.200	26333.048	20084.264	29.078	15.094
1.343	32.200	9459.173	10570.662	20.162	15.692
0.527	32.200	3217.243	3217.243	12.809	15.692
1.523	32.200	11486.550	11141.328	20.733	15.692
2.519	32.200	49733.139	19727.015	29.036	15.409
3.147	32.200	27150.904	20859.681	29.886	15.126
3.775	32.200	24506.728	23914.089	32.940	15.126
4.403	32.200	26858.994	26858.994	34.978	14.219
3.717	32.200	24130.107	24011.273	31.223	13.312
3.031	32.200	23465.127	20669.521	27.882	13.312
2.345	32.200	46297.329	17321.897	24.306	13.084
0.656	32.200	5866.310	10541.264	17.298	12.857
0.273	32.200	1786.551	2498.150	9.255	12.857
0.262	32.200	1596.933	1596.933	9.141	13.644
0.936	32.200	6558.316	6991.837	15.323	14.431
1.610	32.200	19065.001	13260.729	21.184	14.023
1.972	32.200	15555.115	13868.290	21.383	13.615
2.335	32.200	15126.032	15358.026	22.873	13.615
2.698	32.200	16455.915	16455.915	23.841	13.486
2.207	32.200	14520.134	14953.683	22.210	13.356
1.716	32.200	14554.669	12916.709	20.173	13.356
1.226	32.200	18382.095	10276.956	17.425	13.248
0.848	32.200	6169.750	7246.527	14.287	13.140
0.471	32.200	2872.103	2872.103	10.471	13.699
1.237	32.200	8943.829	9094.393	17.252	14.257
2.002	32.200	28901.246	15928.899	24.417	14.588
2.237	32.200	18762.469	15609.920	24.428	14.918
2.472	32.200	16226.930	16290.000	25.108	14.918
2.707	32.200	16513.589	16513.589	25.803	15.389
1.000	32.200	7786.045	6100.000	15.771	15.771
1.000	32.200	26801.764	6300.466	15.882	15.682
1.000	32.200	26194.887	6486.099	16.068	15.682
1.000	32.200	25601.610	6477.435	16.059	15.682
1.000	32.200	7752.429	6190.526	14.641	14.551
1.000	32.200	6100.000	6100.000	13.420	13.420
1.000	32.200	6100.000	6100.000	14.640	14.640
1.000	32.200	6100.000	6100.000	15.860	15.860
1.000	32.200	6100.000	6100.000	15.860	15.860
1.000	32.200	6100.000	6100.000	15.860	15.860
1.000	32.200	6100.000	6100.000	10.980	10.980

113.432

Horizontal Force from Train	Bending Moment	Axial Load (Pn)	Radius of Gyratation	Slenderness	F _e	F _{cr} (a)
lbs	ft kip	kips	in		ksi	ksi
6100.000	97.600	15.626	5.000	15.600	1176.112	49.118
6043.500	370.668	21.428	5.000	59.800	80.038	38.496
6038.980	644.158	21.423	5.000	104.000	26.463	22.673
6034.460	917.238	21.418	5.000	148.200	13.032	10.036
6029.939	1189.908	21.413	5.000	192.400	7.732	3.338
6025.419	1462.168	21.408	5.000	236.600	5.113	0.824
79.101	22.781	20.654	5.000	280.800	3.630	0.157
19498.818	4644.639	26.325	5.000	232.246	5.306	0.969
25062.812	4721.887	31.597	5.000	183.692	8.482	4.241
30626.805	4244.972	36.869	5.000	135.138	15.673	13.154
36190.798	4010.544	42.784	5.000	108.046	24.518	21.295
21439.238	1087.263	45.538	5.000	49.446	117.068	41.815
10029.301	250.229	43.624	5.000	24.326	483.677	47.883
575.219	9.252	42.202	5.000	15.682	1163.804	49.109
-299.646	-4.794	19.520	5.000	15.600	1176.112	49.118
-298.165	-4.771	19.520	5.000	15.600	1176.112	49.118
-296.684	-4.747	19.717	5.000	15.600	1176.112	49.118
6121.362	214.108	18.997	5.000	34.103	246.103	45.924
5276.756	330.959	16.359	5.000	61.152	76.538	38.038
3327.627	350.149	14.172	5.000	102.594	27.193	23.160
-7062.453	-1112.433	27.180	5.000	153.576	12.135	8.913
-9891.092	-1557.982	22.253	5.000	153.576	12.135	8.913
-634.259	-66.740	8.934	5.000	102.594	27.193	23.160
1255.962	78.774	6.684	5.000	61.152	76.538	38.038
2166.635	75.783	4.658	5.000	34.103	246.103	45.924
4279.318	68.469	0.855	5.000	15.600	1176.112	49.118
-273.442	-4.375	19.520	5.000	15.600	1176.112	49.118
2804.546	44.873	19.716	5.000	15.600	1176.112	49.118
8500.675	136.011	20.737	5.000	15.600	1176.112	49.118
35928.702	574.859	21.674	5.000	15.600	1176.112	49.118
35101.440	561.623	21.671	5.000	15.600	1176.112	49.118
34289.132	548.626	21.665	5.000	15.600	1176.112	49.118
8418.043	134.689	21.694	5.000	15.600	1176.112	49.118
2801.921	44.831	21.654	5.000	15.600	1176.112	49.118
-252.878	-4.046	20.219	5.000	15.600	1176.112	49.118
15176.747	651.169	55.441	5.000	41.833	163.553	43.995
25876.379	1806.466	48.610	5.000	68.066	61.778	35.633
45008.671	4353.108	40.151	5.000	94.299	32.187	26.098
18106.746	2179.302	39.701	5.000	117.350	20.784	18.268
3412.785	491.441	33.110	5.000	140.400	14.520	11.831
15199.296	1829.365	36.582	5.000	117.350	20.784	18.268
46313.975	4479.353	42.555	5.000	94.299	32.187	26.098

23069.316	1610.501	43.308	5.000	68.066	61.778	35.633
12990.608	557.371	46.964	5.000	41.833	163.553	43.995
3695.921	59.135	51.734	5.000	15.600	1176.112	49.118
-235.300	-3.765	49.934	5.000	15.600	1176.112	49.118
7439.860	161.348	50.250	5.000	21.145	640.161	48.392
18474.002	753.233	47.919	5.000	39.753	181.114	44.544
30793.007	3433.794	42.927	5.000	108.724	24.213	21.067
9487.143	1439.732	28.423	5.000	147.962	13.074	10.087
3244.645	622.972	16.657	5.000	187.200	8.167	3.856
9896.505	1501.855	29.336	5.000	147.962	13.074	10.087
51881.960	5785.469	42.734	5.000	108.724	24.213	21.067
21547.728	1831.731	44.207	5.000	82.883	41.665	30.257
10970.231	641.803	49.094	5.000	57.041	87.966	39.414
2827.734	90.487	52.718	5.000	31.200	294.028	46.565
12160.325	711.428	47.073	5.000	57.041	87.966	39.414
17985.449	1528.909	41.726	5.000	82.883	41.665	30.257
47201.783	5263.572	36.096	5.000	108.724	24.213	21.067
13233.285	2317.643	24.974	5.000	170.759	9.816	5.930
2957.026	566.773	12.105	5.000	186.878	8.196	3.890
70.465	13.529	11.608	5.000	187.200	8.167	3.856
5836.512	945.823	21.185	5.000	158.001	11.465	8.058
20356.897	2689.261	30.725	5.000	128.803	17.252	14.865
12757.327	1327.660	31.207	5.000	101.469	27.799	23.552
8401.747	638.829	33.591	5.000	74.134	52.079	33.454
3724.225	178.763	35.192	5.000	46.800	130.679	42.601
9419.109	700.967	32.634	5.000	72.559	54.364	34.024
13633.055	1374.747	29.374	5.000	98.318	29.609	24.661
19858.172	2527.129	25.021	5.000	124.077	18.591	16.222
7164.897	1086.409	20.043	5.000	147.839	13.095	10.114
2776.362	488.640	13.714	5.000	171.600	9.720	5.806
7692.628	1115.438	24.340	5.000	141.376	14.320	11.596
30292.147	3453.362	35.672	5.000	111.152	23.167	20.261
15735.506	1279.841	35.558	5.000	79.301	45.513	31.570
9267.147	451.007	36.646	5.000	47.451	127.120	42.410
3692.212	59.075	37.569	5.000	15.600	1176.112	49.118
4838.647	77.418	21.365	5.000	15.600	1176.112	49.118
26304.232	420.868	21.579	5.000	15.600	1176.112	49.118
25871.749	413.948	21.876	5.000	15.600	1176.112	49.118
25252.908	404.047	21.862	5.000	15.600	1176.112	49.118
4931.052	78.897	20.046	5.000	15.600	1176.112	49.118
-95.670	-1.531	18.544	5.000	15.600	1176.112	49.118
-95.447	-1.527	20.008	5.000	15.600	1176.112	49.118
-5050.389	-80.806	21.472	5.000	15.600	1176.112	49.118
-4038.320	-64.613	21.472	5.000	15.600	1176.112	49.118
-3026.250	-48.420	21.472	5.000	15.600	1176.112	49.118
-2014.181	-32.227	15.616	5.000	15.600	1176.112	49.118

> 113.432

F _{cr} (b)	Required Area (a)	Required Area (b)	Diameter	Area	Required Z _x	Z _x
ksi	in ²	in ²	in	in ²	in ³	in ³
1031.450	0.318	0.015	20.000	314.159	23.424	1333.333
70.193	0.557	0.305	20.000	314.159	88.960	1333.333
23.208	0.945	0.923	20.000	314.159	154.598	1333.333
11.429	2.134	1.874	20.000	314.159	220.137	1333.333
6.781	6.415	3.158	20.000	314.159	285.578	1333.333
4.484	25.657	4.774	20.000	314.159	350.920	1333.333
3.183	131.772	6.488	20.000	314.159	5.467	1333.333
4.654	27.175	5.657	20.000	314.159	1114.713	1333.333
7.439	7.450	4.247	20.000	314.159	1133.253	1333.333
13.745	2.803	2.682	20.000	314.159	1018.793	1333.333
21.502	2.009	1.990	20.000	314.159	962.530	1333.333
102.669	1.089	0.444	20.000	314.159	260.943	1333.333
424.185	0.911	0.103	20.000	314.159	60.055	1333.333
1020.656	0.859	0.041	20.000	314.159	2.220	1333.333
1031.450	0.397	0.019	20.000	314.159	-1.151	1333.333
1031.450	0.397	0.019	20.000	314.159	-1.145	1333.333
1031.450	0.401	0.019	20.000	314.159	-1.139	1333.333
215.832	0.414	0.088	20.000	314.159	51.386	1333.333
67.123	0.430	0.244	20.000	314.159	79.430	1333.333
23.848	0.612	0.594	20.000	314.159	84.036	1333.333
10.643	3.049	2.554	20.000	314.159	-266.984	1333.333
10.643	2.497	2.091	20.000	314.159	-373.916	1333.333
23.848	0.386	0.375	20.000	314.159	-16.018	1333.333
67.123	0.176	0.100	20.000	314.159	18.906	1333.333
215.832	0.101	0.022	20.000	314.159	18.188	1333.333
1031.450	0.017	0.001	20.000	314.159	16.433	1333.333
1031.450	0.397	0.019	20.000	314.159	-1.050	1333.333
1031.450	0.401	0.019	20.000	314.159	10.769	1333.333
1031.450	0.422	0.020	20.000	314.159	32.643	1333.333
1031.450	0.441	0.021	20.000	314.159	137.966	1333.333
1031.450	0.441	0.021	20.000	314.159	134.790	1333.333
1031.450	0.441	0.021	20.000	314.159	131.670	1333.333
1031.450	0.442	0.021	20.000	314.159	32.325	1333.333
1031.450	0.441	0.021	20.000	314.159	10.759	1333.333
1031.450	0.412	0.020	20.000	314.159	-0.971	1333.333
143.436	1.260	0.387	20.000	314.159	156.281	1333.333
54.180	1.364	0.897	20.000	314.159	433.552	1333.333
28.228	1.538	1.422	20.000	314.159	1044.746	1333.333
18.228	2.173	2.178	20.000	314.159	523.032	1333.333
12.734	2.799	2.600	20.000	314.159	117.946	1333.333
18.228	2.003	2.007	20.000	314.159	439.048	1333.333
28.228	1.631	1.508	20.000	314.159	1075.045	1333.333

Required Diameter (bending)
5.199210926
8.111774186
9.752551633
10.97189104
11.96626545
12.81700737
3.201190722
18.84103782
18.94491582
18.28433237
17.94135522
11.61178454
7.115955317
2.370645629
-1.904132646
-1.900989448
-1.89783582
6.75562345
7.811099947
7.959241189
-11.70070572
-13.09106444
-4.580529609
4.840779699
4.778717254
4.619755854
-1.846924778
4.012807638
5.807358436
9.389475549
9.31685068
9.244419705
5.788480066
4.011555334
-1.79941358
9.787806656
13.7529997
18.43828965
14.64063595
8.911373729
13.81086767
18.61483776

54.180	1.215	0.799	20.000	314.159	386.520	1333.333	13.23654086
143.436	1.067	0.327	20.000	314.159	133.769	1333.333	9.29327907
1031.450	1.053	0.050	20.000	314.159	14.192	1333.333	4.399483777
1031.450	1.017	0.048	20.000	314.159	-0.904	1333.333	-1.756716504
561.421	1.038	0.090	20.000	314.159	38.724	1333.333	6.147647523
158.837	1.076	0.302	20.000	314.159	180.776	1333.333	10.27457802
21.235	2.038	2.022	20.000	314.159	824.111	1333.333	17.03644288
11.466	2.818	2.479	20.000	314.159	345.536	1333.333	12.75111027
7.163	4.320	2.326	20.000	314.159	149.513	1333.333	9.644439153
11.466	2.908	2.559	20.000	314.159	360.445	1333.333	12.9319336
21.235	2.028	2.012	20.000	314.159	1388.512	1333.333	20.27217497
36.540	1.461	1.210	20.000	314.159	439.616	1333.333	13.81681962
77.147	1.246	0.636	20.000	314.159	154.033	1333.333	9.740652815
257.862	1.132	0.204	20.000	314.159	21.717	1333.333	5.069716373
77.147	1.194	0.610	20.000	314.159	170.743	1333.333	10.08086655
36.540	1.379	1.142	20.000	314.159	366.938	1333.333	13.00912318
21.235	1.713	1.700	20.000	314.159	1263.257	1333.333	19.64329577
8.609	4.211	2.901	20.000	314.159	556.234	1333.333	14.94409794
7.188	3.112	1.684	20.000	314.159	136.025	1333.333	9.345239513
7.163	3.010	1.621	20.000	314.159	3.247	1333.333	2.690783222
10.055	2.629	2.107	20.000	314.159	226.998	1333.333	11.08470532
15.130	2.067	2.031	20.000	314.159	645.423	1333.333	15.70357229
24.380	1.325	1.280	20.000	314.159	318.638	1333.333	12.41127757
45.673	1.004	0.735	20.000	314.159	153.319	1333.333	9.725582298
114.606	0.826	0.307	20.000	314.159	42.903	1333.333	6.361310032
47.677	0.959	0.684	20.000	314.159	168.232	1333.333	10.03120923
25.967	1.191	1.131	20.000	314.159	329.939	1333.333	12.55630304
16.305	1.542	1.535	20.000	314.159	606.511	1333.333	15.38142775
11.485	1.982	1.745	20.000	314.159	260.738	1333.333	11.60874656
8.524	2.362	1.609	20.000	314.159	117.274	1333.333	8.894408832
12.559	2.099	1.938	20.000	314.159	267.705	1333.333	11.71123476
20.317	1.761	1.756	20.000	314.159	828.807	1333.333	17.06874246
39.915	1.126	0.891	20.000	314.159	307.162	1333.333	12.26044285
111.484	0.864	0.329	20.000	314.159	108.242	1333.333	8.659947343
1031.450	0.765	0.036	20.000	314.159	14.178	1333.333	4.398011491
1031.450	0.435	0.021	20.000	314.159	18.580	1333.333	4.812847846
1031.450	0.439	0.021	20.000	314.159	101.008	1333.333	8.462578353
1031.450	0.445	0.021	20.000	314.159	99.348	1333.333	8.415942415
1031.450	0.445	0.021	20.000	314.159	96.971	1333.333	8.34829825
1031.450	0.408	0.019	20.000	314.159	18.935	1333.333	4.843292301
1031.450	0.378	0.018	20.000	314.159	-0.367	1333.333	-1.301427433
1031.450	0.407	0.019	20.000	314.159	-0.367	1333.333	-1.300413412
1031.450	0.437	0.021	20.000	314.159	-19.393	1333.333	-4.88205247
1031.450	0.437	0.021	20.000	314.159	-15.507	1333.333	-4.531351208
1031.450	0.437	0.021	20.000	314.159	-11.621	1333.333	-4.115877419
1031.450	0.318	0.015	20.000	314.159	-7.734	1333.333	-3.593577027

(5,10,15,20,25)

≤ 113.432 > 113.432

Possible Diameter	Zx	Radius of Gyration	Slenderness	F _e	F _{cr} (a)	F _{cr} (b)	Capacity
(bending)	(in ³)	(in)		ksi	ksi	ksi	(kips)
10	166.667	2.5	31.2	294.0279	46.56493	257.86248	3657.2012
10	166.667	2.5	119.6	20.00946	17.5691	17.548297	1378.24
15	562.5	3.75	138.6666667	14.88516	12.25693	13.054288	2306.8831
15	562.5	3.75	197.6	7.330336	2.878023	6.4287044	1136.0458
20	1333.33	5	192.4	7.731925	3.338045	6.7808978	2130.2819
25	2604.17	6.25	189.28	7.988924	3.641722	7.0062863	3439.2028
30	4500	7.5	187.2	8.167442	3.856319	7.1628466	5063.1179
25	2604.17	6.25	185.7968222	8.291272	4.006753	7.2714458	3569.3626
20	1333.33	5	183.6920555	8.482366	4.241189	7.4390348	2337.0417
20	1333.33	5	135.1380832	15.67264	13.1544	13.744908	4318.0901
20	1333.33	5	108.04625	24.51762	21.29458	21.501955	6689.8895
15	562.5	3.75	65.92777459	65.85078	36.38734	57.751132	6430.1735
10	166.667	2.5	48.65204364	120.9193	42.05393	106.04621	3302.908
5	20.8333	1.25	62.72909076	72.73773	37.49888	63.790991	736.28875
5	20.8333	1.25	62.4	73.50698	37.61195	64.465619	738.50897
5	20.8333	1.25	62.4	73.50698	37.61195	64.465619	738.50897
5	20.8333	1.25	62.4	73.50698	37.61195	64.465619	738.50897
10	166.667	2.5	68.20565076	61.52577	35.58345	53.958097	2794.7177
10	166.667	2.5	122.304293	19.13438	16.74852	16.780849	1317.9648
15	562.5	3.75	136.7921477	15.29591	12.72853	13.414516	2370.5406
25	2604.17	6.25	122.8606306	18.96148	16.58232	16.629219	8162.8489
25	2604.17	6.25	122.8606306	18.96148	16.58232	16.629219	8162.8489
15	562.5	3.75	136.7921477	15.29591	12.72853	13.414516	2370.5406
15	562.5	3.75	81.53619535	43.05235	30.75118	37.756911	5434.1819
10	166.667	2.5	68.20565076	61.52577	35.58345	53.958097	2794.7177
5	20.8333	1.25	62.4	73.50698	37.61195	64.465619	738.50897
5	20.8333	1.25	62.4	73.50698	37.61195	64.465619	738.50897
5	20.8333	1.25	62.4	73.50698	37.61195	64.465619	738.50897
10	166.667	2.5	31.2	294.0279	46.56493	257.86248	3657.2012
10	166.667	2.5	31.2	294.0279	46.56493	257.86248	3657.2012
10	166.667	2.5	31.2	294.0279	46.56493	257.86248	3657.2012
10	166.667	2.5	31.2	294.0279	46.56493	257.86248	3657.2012
10	166.667	2.5	31.2	294.0279	46.56493	257.86248	3657.2012
5	20.8333	1.25	62.4	73.50698	37.61195	64.465619	738.50897
5	20.8333	1.25	62.4	73.50698	37.61195	64.465619	738.50897
10	166.667	2.5	83.66610838	40.88826	29.97012	35.859002	2353.8476
15	562.5	3.75	90.75481118	34.75029	27.37958	30.476004	4838.3703
20	1333.33	5	94.29916257	32.18712	26.09751	28.228101	8198.775
15	562.5	3.75	156.4661084	11.69115	8.34775	10.253137	1811.8789
15	562.5	3.75	187.2	8.167442	3.856319	7.1628466	1265.7795
15	562.5	3.75	156.4661084	11.69115	8.34775	10.253137	1811.8789
20	1333.33	5	94.29916257	32.18712	26.09751	28.228101	8198.775

15	562.5	3.75	90.75481118	34.75029	27.37958	30.476004	4838.3703
10	166.667	2.5	83.66610838	40.88826	29.97012	35.859002	2353.8476
5	20.8333	1.25	62.4	73.50698	37.61195	64.465619	738.50897
5	20.8333	1.25	62.4	73.50698	37.61195	64.465619	738.50897
10	166.667	2.5	42.28966111	160.0403	43.87124	140.35534	3445.639
15	562.5	3.75	53.00439128	101.8765	40.71524	89.345696	7194.9774
20	1333.33	5	108.7243415	24.21275	21.06694	21.234584	6618.3748
15	562.5	3.75	197.2828943	7.35392	2.904494	6.4493876	1139.7009
20	1333.33	5	187.2	8.167442	3.856319	7.1628466	2250.2746
15	562.5	3.75	197.2828943	7.35392	2.904494	6.4493876	1139.7009
20	1333.33	5	108.7243415	24.21275	21.06694	21.234584	6618.3748
15	562.5	3.75	110.5105257	23.43638	20.4723	20.553702	3617.7541
10	166.667	2.5	114.0828943	21.99159	19.30586	19.286627	1514.7681
10	166.667	2.5	62.4	73.50698	37.61195	64.465619	2954.0359
15	562.5	3.75	76.05526287	49.48108	32.7559	43.39491	5788.4462
15	562.5	3.75	110.5105257	23.43638	20.4723	20.553702	3617.7541
20	1333.33	5	108.7243415	24.21275	21.06694	21.234584	6618.3748
20	1333.33	5	170.758983	9.815911	5.929996	8.6085542	2704.4571
20	1333.33	5	186.8780204	8.19561	3.89043	7.1875501	2258.0355
20	1333.33	5	187.2	8.167442	3.856319	7.1628466	2250.2746
20	1333.33	5	158.0014922	11.46503	8.05819	10.054835	3158.8197
20	1333.33	5	128.8029844	17.25226	14.86474	15.130228	4753.3015
15	562.5	3.75	135.2915416	15.63711	13.11424	13.713744	2423.4186
10	166.667	2.5	148.2686562	13.01964	10.0206	11.418226	896.78537
10	166.667	2.5	93.6	32.66977	26.3494	28.651386	2069.4771
10	166.667	2.5	145.1182892	13.59106	10.7212	11.919363	936.14456
15	562.5	3.75	131.0910523	16.65527	14.23228	14.606671	2581.2118
20	1333.33	5	124.0774338	18.5914	16.22198	16.304659	5122.2598
15	562.5	3.75	197.1182892	7.366207	2.918314	6.4601633	1141.6051
20	1333.33	5	171.6	9.719931	5.806459	8.5243794	2678.0128
15	562.5	3.75	188.501224	8.055071	3.72091	7.0642976	1248.3644
20	1333.33	5	111.151836	23.16672	20.26061	20.317209	6365.0598
15	562.5	3.75	105.7349653	25.60121	22.07797	22.452261	3901.5002
10	166.667	2.5	94.90122397	31.78002	25.88105	27.871074	2032.6931
5	20.8333	1.25	62.4	73.50698	37.61195	64.465619	738.50897
5	20.8333	1.25	62.4	73.50698	37.61195	64.465619	738.50897
10	166.667	2.5	31.2	294.0279	46.56493	257.86248	3657.2012
10	166.667	2.5	31.2	294.0279	46.56493	257.86248	3657.2012
10	166.667	2.5	31.2	294.0279	46.56493	257.86248	3657.2012
5	20.8333	1.25	62.4	73.50698	37.61195	64.465619	738.50897
5	20.8333	1.25	62.4	73.50698	37.61195	64.465619	738.50897
5	20.8333	1.25	62.4	73.50698	37.61195	64.465619	738.50897
5	20.8333	1.25	62.4	73.50698	37.61195	64.465619	738.50897
5	20.8333	1.25	62.4	73.50698	37.61195	64.465619	738.50897
5	20.8333	1.25	62.4	73.50698	37.61195	64.465619	738.50897
5	20.8333	1.25	62.4	73.50698	37.61195	64.465619	738.50897

Required Diameter (axial a)	Required Diameter (axial b)
0.636444	0.138886
0.841865	0.623451
1.096834	1.084133
1.648452	1.544706
2.857908	2.005168
5.715535	2.46552
12.9529	2.874112
5.882202	2.683712
3.079862	2.325502
1.889088	1.848042
1.59941	1.591678
1.177539	0.75149
1.077029	0.361859
1.046018	0.229446
0.711334	0.155228
0.711334	0.155228
0.714914	0.156009
0.725732	0.324763
0.73998	0.557049
0.88267	0.869843
1.970453	1.803237
1.782935	1.631632
0.700835	0.69065
0.472994	0.356065
0.359367	0.165768
0.148916	0.032497
0.711334	0.155228
0.714898	0.156006
0.733175	0.159994
0.749554	0.163569
0.749507	0.163558
0.749393	0.163533
0.749899	0.163644
0.749215	0.163495
0.72396	0.157983
1.266696	0.701525
1.317931	1.068811
1.399593	1.345738
1.663465	1.665282
1.887646	1.819491
1.5968	1.598544
1.440892	1.385448

Pn/Capacity	Pn/Capacity (new dia)	Required Zx/Zx (@ 20in)	Required Zx/Zx (@ new dia)
0.00101265	0.00427271	0.017568	0.140544
0.00177184	0.01554765	0.066720235	0.533761883
0.00300761	0.00928668	0.115948407	0.274840669
0.00596529	0.01885326	0.165102812	0.391354815
0.01005175	0.01005175	0.214183451	0.214183451
0.01519697	0.00622468	0.263190322	0.134753445
0.02065129	0.00407927	0.004100574	0.001214985
0.01800578	0.00737517	0.836035034	0.428049938
0.0135199	0.0135199	0.849939577	0.849939577
0.00853815	0.00853815	0.76409496	0.76409496
0.00639528	0.00639528	0.721897849	0.721897849
0.0034665	0.00708194	0.195707252	0.463898672
0.00289998	0.0132077	0.045041169	0.360329349
0.00273538	0.05731658	0.001665367	0.106583482
0.00126499	0.02643164	0.000862982	0.055230832
0.00126499	0.02643164	0.000858715	0.05495777
0.00127776	0.02669832	0.000854449	0.054684709
0.00131672	0.00679742	0.038539521	0.308316171
0.00136893	0.01241216	0.059572606	0.476580847
0.00194777	0.00597828	0.063026764	0.149396774
0.00812916	0.0033297	0.200237854	0.102521781
0.00665556	0.00272612	0.280436731	0.143583606
0.00122792	0.00376887	0.012013155	0.028475628
0.00055931	0.00122995	0.014179338	0.033610284
0.00032286	0.00166674	0.013640931	0.109127449
5.544E-05	0.0011584	0.012324437	0.788763963
0.00126499	0.02643164	0.000787513	0.050400821
0.0012777	0.02669709	0.008077092	0.516933897
0.00134387	0.00567021	0.024481944	0.195855556
0.00140458	0.00592638	0.103474663	0.827797301
0.0014044	0.00592564	0.101092147	0.808737173
0.00140397	0.00592382	0.0987527	0.790021597
0.00140587	0.00593183	0.024243964	0.193951716
0.00140331	0.0293217	0.008069532	0.516450079
0.0013103	0.02737824	0.000728288	0.046610415
0.0040113	0.02355352	0.117210403	0.937683223
0.00434236	0.01004681	0.325163892	0.770758855
0.00489715	0.00489715	0.783559377	0.783559377
0.00693291	0.02191141	0.392274284	0.92983534
0.00827637	0.02615741	0.088459399	0.209681539
0.00638836	0.02019036	0.329285726	0.780529129
0.00519042	0.00519042	0.806283513	0.806283513

1.243978	1.008837	0.00386871	0.00895093	0.289890195	0.687147129
1.165835	0.645666	0.00339793	0.01995194	0.100326798	0.80261438
1.158041	0.252709	0.00335265	0.07005258	0.010644253	0.68123217
1.137708	0.248272	0.00323595	0.06761417	0.000677665	0.04337056
1.149834	0.33758	0.0033053	0.01458354	0.029042693	0.232341547
1.170342	0.619771	0.00342425	0.00666	0.135581988	0.321379526
1.610727	1.604356	0.0064861	0.0064861	0.61808297	0.61808297
1.894093	1.776608	0.00789084	0.02493896	0.259151673	0.614285448
2.345165	1.720747	0.00740242	0.00740242	0.112134938	0.112134938
1.924276	1.804919	0.00814433	0.02574011	0.270333839	0.640791321
1.607093	1.600737	0.00645687	0.00645687	1.04138436	1.04138436
1.363911	1.241131	0.00465063	0.0122195	0.329711638	0.781538697
1.259347	0.900144	0.00396489	0.03241038	0.115524529	0.924196229
1.200613	0.510198	0.00360368	0.01784594	0.016287747	0.130301972
1.233146	0.881417	0.00380162	0.00813218	0.128057085	0.303542719
1.325081	1.205797	0.0043896	0.01153364	0.275203587	0.652334429
1.47702	1.471178	0.00545397	0.00545397	0.947442977	0.947442977
2.31565	1.921919	0.00923443	0.00923443	0.41717582	0.41717582
1.990403	1.464365	0.00536092	0.00536092	0.102019061	0.102019061
1.957708	1.436453	0.00515849	0.00515849	0.002435265	0.002435265
1.829564	1.637868	0.00670653	0.00670653	0.170248177	0.170248177
1.622264	1.607969	0.00646391	0.00646391	0.4840669	0.4840669
1.29887	1.276627	0.00421766	0.01287725	0.238978857	0.566468401
1.130676	0.967685	0.00319607	0.03745661	0.114989147	0.919913177
1.025576	0.625281	0.00262952	0.01700534	0.032177307	0.25741846
1.105079	0.933536	0.003053	0.03485955	0.126174002	1.009392019
1.231492	1.200122	0.00379143	0.01138009	0.247454513	0.586558846
1.40138	1.397822	0.00488477	0.00488477	0.454883268	0.454883268
1.588415	1.490636	0.00555499	0.01755652	0.195553684	0.463534659
1.734125	1.431214	0.00512094	0.00512094	0.087955151	0.087955151
1.634822	1.570877	0.00616913	0.01949751	0.200778901	0.475920358
1.497235	1.495148	0.00560428	0.00560428	0.621605129	0.621605129
1.197521	1.065007	0.00358514	0.00911383	0.230371359	0.546065444
1.048891	0.646934	0.00275043	0.01802816	0.081181256	0.649450049
0.986839	0.215349	0.00243463	0.05087088	0.01063357	0.680548477
0.744195	0.162399	0.00138456	0.02893007	0.013935303	0.891859378
0.74791	0.16321	0.00139842	0.00590041	0.075756189	0.606049515
0.75304	0.164329	0.00141767	0.00598162	0.074510637	0.596085099
0.752801	0.164277	0.00141677	0.00597783	0.072728375	0.581826997
0.720854	0.157306	0.00129908	0.02714382	0.014201429	0.908891471
0.693323	0.151298	0.00120174	0.02511005	0.000275531	0.01763396
0.720171	0.157157	0.00129662	0.02709243	0.000274887	0.017592773
0.746054	0.162805	0.00139149	0.0290748	0.014545121	0.930887749
0.746054	0.162805	0.00139149	0.0290748	0.011630361	0.744343087
0.746054	0.162805	0.00139149	0.0290748	0.0087156	0.557798424
0.636237	0.13884	0.00101199	0.02114531	0.00580084	0.371253761

Acceleration	Linear Forces on Rider	Linear G Forces	Linear Forces on Train
(ft/sec^2)	(lbs)		(lbs)
0.298248089	2.037719863	0.009262363	56.50041437
0.322107936	2.200737452	0.010003352	61.02044752
0.345967783	2.363755041	0.010744341	65.54048067
0.36982763	2.52677263	0.01148533	70.06051382
0.393687477	2.689790219	0.012226319	74.58054697
0.417547325	2.852807808	0.012967308	79.10058012
12.90744067	88.18748285	0.400852195	2445.198388
21.3104029	145.599026	0.661813755	4037.063903
29.71336513	203.0105692	0.922775314	5628.929418
38.11632735	260.4221124	1.183736874	7220.794934
29.15105284	199.168684	0.9053122	5522.40442
11.67869923	79.79235499	0.362692523	2212.424388
3.036400656	20.74559454	0.094298157	575.2187578
-1.581740224	-10.80692078	-0.049122367	-299.6464399
-1.573920095	-10.75349133	-0.048879506	-298.1649869
-1.566099966	-10.70006188	-0.048636645	-296.683534
-24.77865452	-169.2951551	-0.769523432	-4694.092937
-22.54296556	-154.0202616	-0.700092098	-4270.561799
-20.30727661	-138.7453681	-0.630660764	-3847.030662
-18.07158765	-123.4704746	-0.56122943	-3423.499524
-0.689092687	-4.708086679	-0.021400394	-130.5424034
16.62433793	113.582433	0.516283787	3149.331098
18.61262155	127.1669796	0.578031725	3525.993524
20.60090518	140.7515261	0.639779664	3902.65595
22.58918881	154.3360726	0.701527603	4279.318376
-1.443414903	-9.861840954	-0.04482655	-273.4419537
-1.436219924	-9.812682712	-0.044603103	-272.0789297
-1.429024945	-9.76352447	-0.044379657	-270.7159058
-1.391491258	-9.50708313	-0.043214014	-263.6054868
-1.383366442	-9.451571966	-0.042961691	-262.0663136
-1.362104697	-9.306305382	-0.042301388	-258.0384674
-1.354134815	-9.251852771	-0.042053876	-256.528645
-1.342942543	-9.175383834	-0.04170629	-254.4083699
-1.334862531	-9.120178785	-0.041455358	-252.8776845
-19.55683118	-133.6181013	-0.607355006	-3704.865535
-18.07971987	-123.5260364	-0.561481983	-3425.040099
-16.60260855	-113.4339715	-0.515608961	-3145.214664
-20.23333316	-138.2401644	-0.628364384	-3833.022741
-18.01503149	-123.0840661	-0.559473028	-3412.785468
5.925233482	40.48296168	0.184013462	1122.482119
29.52201264	201.7031919	0.916832691	5592.679413

16.73394364	114.331292	0.519687691	3170.094914
18.12177987	123.8134029	0.562788195	3433.007989
19.5096161	133.2955138	0.605888699	3695.921063
-1.242077248	-8.486242065	-0.038573828	-235.3003482
-4.038194824	-27.59015097	-0.125409777	-764.9996407
-11.88345201	-81.191287	-0.369051305	-2251.212958
-42.16573187	-288.0888513	-1.309494779	-7987.918149
-25.1136587	-171.5840035	-0.779927289	-4757.556462
-17.12747129	-117.0199902	-0.531909046	-3244.645183
16.60084136	113.4218975	0.515554079	3144.879885
24.1918834	165.2861599	0.751300727	4582.934434
12.40037592	84.72306528	0.385104842	2349.139537
13.66355088	93.3534532	0.424333878	2588.436657
14.92672584	101.9838411	0.463562914	2827.733776
-20.62564395	-140.9205487	-0.640547949	-3907.342488
-18.68061691	-127.6315441	-0.580143382	-3538.874633
-16.73558987	-114.3425395	-0.519738816	-3170.406777
-47.20698527	-322.5321975	-1.466055443	-8942.938204
-12.22958044	-83.55613967	-0.379800635	-2316.783873
-0.371961893	-2.541354546	-0.011551612	-70.46483059
13.7617678	94.02450052	0.427384093	2607.042969
21.19393893	144.8033095	0.658196861	4015.000854
15.2977091	104.5185094	0.475084134	2898.013215
17.47836749	119.4174176	0.542806444	3311.119307
19.65902588	134.3163259	0.610528754	3724.225399
-21.00797257	-143.5327318	-0.652421508	-3979.771201
-18.59434794	-127.0421288	-0.577464222	-3522.531753
-16.18072332	-110.5515258	-0.502506935	-3065.292305
-20.08335114	-137.2154426	-0.623706557	-3804.609998
-14.65555065	-100.1310914	-0.455141324	-2776.362079
15.2401674	104.1253673	0.473297124	2887.112457
21.63588333	147.8228053	0.671921842	4098.723239
15.09661622	103.1445829	0.468839013	2859.91798
17.29332611	118.1531598	0.537059817	3276.064884
19.490036	133.1617366	0.605280621	3692.211788
0	0	0	0
-1.08671877	-7.424786624	-0.03374903	-205.8690837
-2.095714254	-14.31854459	-0.065084294	-397.0141909
-2.051442804	-14.01606885	-0.063709404	-388.6273634
-0.774307892	-5.290302366	-0.024046829	-146.6856565
-0.505014018	-3.450406332	-0.015683665	-95.67035738
-0.503834476	-3.442347352	-0.015647033	-95.44690385
-26.65943186	-182.1451866	-0.827932667	-5050.389266
-21.31703184	-145.644317	-0.662019623	-4038.319697
-15.97463183	-109.1434473	-0.496106578	-3026.250129
-10.63223181	-72.64257759	-0.330193534	-2014.18056

Appendix O: Material Calculations for Support Structure

(5,10,15,20,25)					(Control)		
					≤ 113.432		> 113.432
Required Diameter	Possible Diameter	Zx	Radius of Gyration	Slenderness	F _e	F _{cr} (a)	F _{cr} (b)
(bending)	(bending)	(in ³)	(in)		ksi	ksi	ksi
5.199210926	10	166.667	2.5	31.2	294.0279	46.56493	257.86248
8.111774186	10	166.667	2.5	119.6	20.00946	17.5691	17.548297
9.752551633	15	562.5	3.75	138.6666667	14.88516	12.25693	13.054288
10.97189104	15	562.5	3.75	197.6	7.330336	2.878023	6.4287044
11.96626545	20	1333.33	5	192.4	7.731925	3.338045	6.7808978
12.81700737	25	2604.17	6.25	189.28	7.988924	3.641722	7.0062863
3.201190722	30	4500	7.5	187.2	8.167442	3.856319	7.1628466
18.84103782	25	2604.17	6.25	185.7968222	8.291272	4.006753	7.2714458
18.94491582	20	1333.33	5	183.6920555	8.482366	4.241139	7.4390348
18.28433237	20	1333.33	5	135.1380832	15.67264	13.1541	13.744908
17.94135522	20	1333.33	5	108.04625	24.51762	21.29458	21.501955
11.61178454	15	562.5	3.75	65.92777459	65.85078	36.38734	57.751132
7.115955317	10	166.667	2.5	48.65204364	120.9193	42.05393	106.04621
2.370645629	5	20.8333	1.25	62.72909076	72.73773	37.49888	63.790991
-1.904132646	5	20.8333	1.25	62.4	73.50698	37.61195	64.465619
-1.900989448	5	20.8333	1.25	62.4	73.50698	37.61195	64.465619
-1.89783582	5	20.8333	1.25	62.4	73.50698	37.61195	64.465619
6.75562345	10	166.667	2.5	68.20565076	61.52577	35.58345	53.958097
7.811099947	10	166.667	2.5	122.304293	19.13438	16.74852	16.780849
7.959241189	15	562.5	3.75	136.7921477	15.29591	12.72853	13.414516
-11.70070572	25	2604.17	6.25	122.8606306	18.96148	16.58232	16.629219
-13.09106444	25	2604.17	6.25	122.8606306	18.96148	16.58232	16.629219
-4.580529609	15	562.5	3.75	136.7921477	15.29591	12.72853	13.414516
4.840779699	15	562.5	3.75	81.53619535	43.05235	30.75118	37.756911
4.778717254	10	166.667	2.5	68.20565076	61.52577	35.58345	53.958097
4.619755854	5	20.8333	1.25	62.4	73.50698	37.61195	64.465619
-1.846924778	5	20.8333	1.25	62.4	73.50698	37.61195	64.465619
4.012807638	5	20.8333	1.25	62.4	73.50698	37.61195	64.465619
5.807358436	10	166.667	2.5	31.2	294.0279	46.56493	257.86248
9.389475549	10	166.667	2.5	31.2	294.0279	46.56493	257.86248
9.31685068	10	166.667	2.5	31.2	294.0279	46.56493	257.86248
9.244419705	10	166.667	2.5	31.2	294.0279	46.56493	257.86248
5.788480066	10	166.667	2.5	31.2	294.0279	46.56493	257.86248
4.011555334	5	20.8333	1.25	62.4	73.50698	37.61195	64.465619
-1.79941358	5	20.8333	1.25	62.4	73.50698	37.61195	64.465619
9.787806656	10	166.667	2.5	83.66610838	40.88826	29.97012	35.859002
13.7529997	15	562.5	3.75	90.75481118	34.75029	27.37958	30.476004
18.43828965	20	1333.33	5	94.29916257	32.18712	26.09751	28.228101
14.64063595	15	562.5	3.75	156.4661084	11.69115	8.34775	10.253137
8.911373729	15	562.5	3.75	187.2	8.167442	3.856319	7.1628466
13.81086767	15	562.5	3.75	156.4661084	11.69115	8.34775	10.253137

18.61483776	20	1333.33	5	94.29916257	32.18712	26.09751	28.228101
13.23654086	15	562.5	3.75	90.75481118	34.75029	27.37958	30.476004
9.29327907	10	166.667	2.5	83.66610838	40.88826	29.97012	35.859002
4.399483777	5	20.8333	1.25	62.4	73.50698	37.61195	64.465619
-1.756716504	5	20.8333	1.25	62.4	73.50698	37.61195	64.465619
6.147647523	10	166.667	2.5	42.28966111	160.0403	43.87124	140.35534
10.27457802	15	562.5	3.75	53.00439128	101.8765	40.71524	89.345696
17.03644288	20	1333.33	5	108.7243415	24.21275	21.06694	21.234584
12.75111027	15	562.5	3.75	197.2828943	7.35392	2.904494	6.4493876
9.644439153	20	1333.33	5	187.2	8.167442	3.856319	7.1628466
12.9319336	15	562.5	3.75	197.2828943	7.35392	2.904494	6.4493876
20.27217497	20	1333.33	5	108.7243415	24.21275	21.06694	21.234584
13.81681962	15	562.5	3.75	110.5105257	23.43638	20.4723	20.553702
9.740652815	10	166.667	2.5	114.0828943	21.99159	19.30586	19.286627
5.069716373	10	166.667	2.5	62.4	73.50698	37.61195	64.465619
10.08086655	15	562.5	3.75	76.05526287	49.48108	32.7559	43.39491
13.00912318	15	562.5	3.75	110.5105257	23.43638	20.4723	20.553702
19.64329577	20	1333.33	5	108.7243415	24.21275	21.06694	21.234584
14.94409794	20	1333.33	5	170.758983	9.815911	5.929996	8.6085542
9.345239513	20	1333.33	5	186.8780204	8.19561	3.89043	7.1875501
2.690783222	20	1333.33	5	187.2	8.167442	3.856319	7.1628466
11.08470532	20	1333.33	5	158.0014922	11.46503	8.05819	10.054835
15.70357229	20	1333.33	5	128.8029844	17.25226	14.86474	15.130228
12.41127757	15	562.5	3.75	135.2915416	15.63711	13.11424	13.713744
9.725582298	10	166.667	2.5	148.2686562	13.01964	10.0206	11.418226
6.361310032	10	166.667	2.5	93.6	32.66977	26.3494	28.651386
10.03120923	10	166.667	2.5	145.1182892	13.59106	10.7212	11.919363
12.55630304	15	562.5	3.75	131.0910523	16.65527	14.23228	14.606671
15.38142775	20	1333.33	5	124.0774338	18.5914	16.22198	16.304659
11.60874656	15	562.5	3.75	197.1182892	7.366207	2.918314	6.4601633
8.894408832	20	1333.33	5	171.6	9.719931	5.806459	8.5243794
11.71123476	15	562.5	3.75	188.501224	8.055071	3.72091	7.0642976
17.06874246	20	1333.33	5	111.151836	23.16672	20.26061	20.317209
12.26044285	15	562.5	3.75	105.7349653	25.60121	22.07797	22.452261
8.659947343	10	166.667	2.5	94.90122397	31.78002	25.88105	27.871074
4.398011491	5	20.8333	1.25	62.4	73.50698	37.61195	64.465619
4.812847846	5	20.8333	1.25	62.4	73.50698	37.61195	64.465619
8.462578353	10	166.667	2.5	31.2	294.0279	46.56493	257.86248
8.415942415	10	166.667	2.5	31.2	294.0279	46.56493	257.86248
8.34829825	10	166.667	2.5	31.2	294.0279	46.56493	257.86248
4.843292301	5	20.8333	1.25	62.4	73.50698	37.61195	64.465619
-1.301427433	5	20.8333	1.25	62.4	73.50698	37.61195	64.465619
-1.300413412	5	20.8333	1.25	62.4	73.50698	37.61195	64.465619
-4.88205247	5	20.8333	1.25	62.4	73.50698	37.61195	64.465619
-4.531351208	5	20.8333	1.25	62.4	73.50698	37.61195	64.465619
-4.115877419	5	20.8333	1.25	62.4	73.50698	37.61195	64.465619
-3.593577027	5	20.8333	1.25	62.4	73.50698	37.61195	64.465619

(Increase F_y)
 ≤ 103.549 > 103.549

Capacity (kips)	Slenderness	F _e ksi	F _{cr} (a) ksi	F _{cr} (b) ksi	Capacity (kips)	Slenderness	F _e ksi
3657.2012	31.2	294.02791	55.088128	257.86248	4326.6115	31.2	294.02791
1378.24	119.6	20.009461	17.10357	17.548297	1378.24	119.6	20.009461
2306.8831	138.6666667	14.885163	11.103129	13.054288	2306.8831	138.6666667	14.885163
1136.0458	197.6	7.3303357	1.9511936	6.4287044	1136.0458	197.6	7.3303357
2130.2819	192.4	7.7319246	2.3311915	6.7808978	2130.2819	192.4	7.7319246
3439.2028	189.28	7.988924	2.5879467	7.0062863	3439.2028	189.28	7.988924
5063.1179	187.2	8.1674419	2.7720099	7.1628466	5063.1179	187.2	8.1674419
3569.3626	185.7968222	8.2912723	2.9022738	7.2714458	3569.3626	185.7968222	8.2912723
2337.0417	183.6920555	8.4823658	3.1072229	7.4390348	2337.0417	183.6920555	8.4823658
4318.0901	135.1380832	15.672643	12.085387	13.744908	4318.0901	135.1380832	15.672643
6689.8895	108.04625	24.517622	21.543196	21.501955	6755.0383	108.04625	24.517622
6430.1735	65.92777459	65.850778	40.975815	57.751132	7241.0242	65.92777459	65.850778
3302.908	48.65204364	120.91928	48.747816	106.04621	3828.6445	48.65204364	120.91928
736.28875	62.72909076	72.737732	42.482413	63.790991	834.14023	62.72909076	72.737732
738.50897	62.4	73.506977	42.636182	64.465619	837.15948	62.4	73.506977
738.50897	62.4	73.506977	42.636182	64.465619	837.15948	62.4	73.506977
738.50897	62.4	73.506977	42.636182	64.465619	837.15948	62.4	73.506977
2794.7177	68.20565076	61.525766	39.891919	53.958097	3133.104	68.20565076	61.525766
1317.9648	122.304293	19.134378	16.149498	16.780849	1317.9648	122.304293	19.134378
2370.5406	136.7921477	15.295913	11.617727	13.414516	2370.5406	136.7921477	15.295913
8162.8489	122.8606306	18.961481	15.957383	16.629219	8162.8489	122.8606306	18.961481
8162.8489	122.8606306	18.961481	15.957383	16.629219	8162.8489	122.8606306	18.961481
2370.5406	136.7921477	15.295913	11.617727	13.414516	2370.5406	136.7921477	15.295913
5434.1819	81.53619535	43.05235	33.48277	37.756911	5916.8938	81.53619535	43.05235
2794.7177	68.20565076	61.525766	39.891919	53.958097	3133.104	68.20565076	61.525766
738.50897	62.4	73.506977	42.636182	64.465619	837.15948	62.4	73.506977
738.50897	62.4	73.506977	42.636182	64.465619	837.15948	62.4	73.506977
738.50897	62.4	73.506977	42.636182	64.465619	837.15948	62.4	73.506977
3657.2012	31.2	294.02791	55.088128	257.86248	4326.6115	31.2	294.02791
3657.2012	31.2	294.02791	55.088128	257.86248	4326.6115	31.2	294.02791
3657.2012	31.2	294.02791	55.088128	257.86248	4326.6115	31.2	294.02791
3657.2012	31.2	294.02791	55.088128	257.86248	4326.6115	31.2	294.02791
3657.2012	31.2	294.02791	55.088128	257.86248	4326.6115	31.2	294.02791
738.50897	62.4	73.506977	42.636182	64.465619	837.15948	62.4	73.506977
738.50897	62.4	73.506977	42.636182	64.465619	837.15948	62.4	73.506977
2353.8476	83.66610838	40.888258	32.464849	35.859002	2549.7833	83.66610838	40.888258
4838.3703	90.75481118	34.75029	29.127237	30.476004	5147.2077	90.75481118	34.75029
8198.775	94.29916257	32.187116	27.49832	28.228101	8638.852	94.29916257	32.187116
1811.8789	156.4661084	11.691149	7.0027818	10.253137	1811.8789	156.4661084	11.691149
1265.7795	187.2	8.1674419	2.7720099	7.1628466	1265.7795	187.2	8.1674419
1811.8789	156.4661084	11.691149	7.0027818	10.253137	1811.8789	156.4661084	11.691149

8198.775	94.29916257	32.187116	27.49832	28.228101	8638.852	94.29916257	32.187116
4838.3703	90.75481118	34.75029	29.127237	30.476004	5147.2077	90.75481118	34.75029
2353.8476	83.66610838	40.888258	32.464849	35.859002	2549.7833	83.66610838	40.888258
738.50897	62.4	73.506977	42.636182	64.465619	837.15948	62.4	73.506977
738.50897	62.4	73.506977	42.636182	64.465619	837.15948	62.4	73.506977
3445.639	42.28966111	160.04029	51.286507	140.35534	4028.0328	42.28966111	160.04029
7194.9774	53.00439128	101.87651	46.891669	89.345696	8286.4419	53.00439128	101.87651
6618.3748	108.7243415	24.212753	21.267137	21.234584	6671.0414	108.7243415	24.212753
1139.7009	197.2828943	7.3539197	1.9727493	6.4493876	1139.7009	197.2828943	7.3539197
2250.2746	187.2	8.1674419	2.7720099	7.1628466	2250.2746	187.2	8.1674419
1139.7009	197.2828943	7.3539197	1.9727493	6.4493876	1139.7009	197.2828943	7.3539197
6618.3748	108.7243415	24.212753	21.267137	21.234584	6671.0414	108.7243415	24.212753
3617.7541	110.5105257	23.436376	20.548836	20.553702	3632.1389	110.5105257	23.436376
1514.7681	114.0828943	21.991593	19.152001	19.286627	1514.7681	114.0828943	21.991593
2954.0359	62.4	73.506977	42.636182	64.465619	3348.6379	62.4	73.506977
5788.4462	76.05526287	49.481083	36.118921	43.39491	6382.7402	76.05526287	49.481083
3617.7541	110.5105257	23.436376	20.548836	20.553702	3632.1389	110.5105257	23.436376
6618.3748	108.7243415	24.212753	21.267137	21.234584	6671.0414	108.7243415	24.212753
2704.4571	170.758983	9.8159113	4.6457147	8.6085542	2704.4571	170.758983	9.8159113
2258.0355	186.8780204	8.1956102	2.8014598	7.1875501	2258.0355	186.8780204	8.1956102
2250.2746	187.2	8.1674419	2.7720099	7.1628466	2250.2746	187.2	8.1674419
3158.8197	158.0014922	11.465035	6.712314	10.054835	3158.8197	158.0014922	11.465035
4753.3015	128.8029844	17.252256	13.995105	15.130228	4753.3015	128.8029844	17.252256
2423.4186	135.2915416	15.637109	12.041461	13.713744	2423.4186	135.2915416	15.637109
896.78537	148.2686562	13.019642	8.7188563	11.418226	896.78537	148.2686562	13.019642
2069.4771	93.6	32.669768	27.817118	28.651386	2184.7513	93.6	32.669768
936.14456	145.1182892	13.591064	9.4553882	11.919363	936.14456	145.1182892	13.591064
2581.2118	131.0910523	16.655269	13.283626	14.606671	2581.2118	131.0910523	16.655269
5122.2598	124.0774338	18.591402	15.542182	16.304659	5122.2598	124.0774338	18.591402
1141.6051	197.1182892	7.3662067	1.9840185	6.4601633	1141.6051	197.1182892	7.3662067
2678.0128	171.6	9.7199309	4.5298194	8.5243794	2678.0128	171.6	9.7199309
1248.3644	188.501224	8.0550714	2.6556215	7.0642976	1248.3644	188.501224	8.0550714
6365.0598	111.151836	23.166715	20.294127	20.317209	6382.8396	111.151836	23.166715
3901.5002	105.7349653	25.60121	22.49771	22.452261	3967.642	105.7349653	25.60121
2032.6931	94.90122397	31.780016	27.224855	27.871074	2138.2351	94.90122397	31.780016
738.50897	62.4	73.506977	42.636182	64.465619	837.15948	62.4	73.506977
738.50897	62.4	73.506977	42.636182	64.465619	837.15948	62.4	73.506977
3657.2012	31.2	294.02791	55.088128	257.86248	4326.6115	31.2	294.02791
3657.2012	31.2	294.02791	55.088128	257.86248	4326.6115	31.2	294.02791
3657.2012	31.2	294.02791	55.088128	257.86248	4326.6115	31.2	294.02791
738.50897	62.4	73.506977	42.636182	64.465619	837.15948	62.4	73.506977
738.50897	62.4	73.506977	42.636182	64.465619	837.15948	62.4	73.506977
738.50897	62.4	73.506977	42.636182	64.465619	837.15948	62.4	73.506977
738.50897	62.4	73.506977	42.636182	64.465619	837.15948	62.4	73.506977
738.50897	62.4	73.506977	42.636182	64.465619	837.15948	62.4	73.506977
738.50897	62.4	73.506977	42.636182	64.465619	837.15948	62.4	73.506977
738.50897	62.4	73.506977	42.636182	64.465619	837.15948	62.4	73.506977
738.50897	62.4	73.506977	42.636182	64.465619	837.15948	62.4	73.506977

(Decrease Fy)
 ≤ 135.577 > 135.577

F _{cr} (a)	F _{cr} (b)	Capacity
ksi	ksi	(kips)

33.298933	257.86248	2615.2921
16.831149	17.548297	1321.9153
13.081462	13.054288	2306.8831
4.7441131	6.4287044	1136.0458
5.263003	6.7808978	2130.2819
5.5937591	7.0062863	3439.2028
5.8225081	7.1628466	5063.1179
5.9805877	7.2714458	3569.3626
6.2234383	7.4390348	2337.0417
13.74459	13.744908	4317.9904
19.256502	21.501955	6049.6084
28.019104	57.751132	4951.3844
31.006565	106.04621	2435.2499
28.615533	63.790991	561.86467
28.675907	64.465619	563.05012
28.675907	64.465619	563.05012
28.675907	64.465619	563.05012
27.584346	53.958097	2166.4695
16.276933	16.780849	1278.3873
13.431788	13.414516	2370.5406
16.1637	16.629219	7934.3379
16.1637	16.629219	7934.3379
13.431788	13.414516	2370.5406
24.905329	37.756911	4401.1349
27.584346	53.958097	2166.4695
28.675907	64.465619	563.05012
28.675907	64.465619	563.05012
28.675907	64.465619	563.05012
33.298933	257.86248	2615.2921
33.298933	257.86248	2615.2921
33.298933	257.86248	2615.2921
33.298933	257.86248	2615.2921
33.298933	257.86248	2615.2921
28.675907	64.465619	563.05012
28.675907	64.465619	563.05012
24.460817	35.859002	1921.1481
22.960838	30.476004	4057.515
22.202834	28.228101	6975.226
9.9974137	10.253137	1811.8789
5.8225081	7.1628466	1265.7795
9.9974137	10.253137	1811.8789

(Increase E)
 ≤ 124.258 > 124.258

Slenderness	F _e	F _{cr} (a)	F _{cr} (b)	Capacity
	ksi	ksi	ksi	(kips)

31.2	352.83349	47.1206	309.43497	3700.8433
119.6	24.011353	20.914766	21.057956	1642.6418
138.6666667	17.862195	15.493391	15.665145	2768.2597
197.6	8.7964028	4.6316979	7.7144453	1363.255
192.4	9.2783095	5.240892	8.1370774	2556.3383
189.28	9.5867088	5.6353032	8.4075436	4127.0433
187.2	9.8009303	5.9107028	8.5954159	6075.7415
185.7968222	9.9495268	6.1022338	8.725735	4283.2352
183.6920555	10.178839	6.3983506	8.9268417	2804.45
135.1380832	18.807171	16.432838	16.493889	5181.7081
108.04625	29.421147	24.55006	25.802345	7712.6289
65.92777459	79.020934	38.366623	69.301359	6779.942
48.65204364	145.10314	43.284642	127.25545	3399.5679
62.72909076	87.285279	39.340834	76.54919	772.45547
62.4	88.208373	39.439667	77.358743	774.39605
62.4	88.208373	39.439667	77.358743	774.39605
62.4	88.208373	39.439667	77.358743	774.39605
68.20565076	73.830919	37.658966	64.749716	2957.7283
122.304293	22.961253	20.097502	20.137019	1578.4541
136.7921477	18.355096	15.988592	16.097419	2844.6487
122.8606306	22.753778	19.93117	19.955063	9783.6904
122.8606306	22.753778	19.93117	19.955063	9783.6904
136.7921477	18.355096	15.988592	16.097419	2844.6487
81.53619535	51.66282	33.34621	45.308293	5892.7617
68.20565076	73.830919	37.658966	64.749716	2957.7283
62.4	88.208373	39.439667	77.358743	774.39605
62.4	88.208373	39.439667	77.358743	774.39605
62.4	88.208373	39.439667	77.358743	774.39605
31.2	352.83349	47.1206	309.43497	3700.8433
31.2	352.83349	47.1206	309.43497	3700.8433
31.2	352.83349	47.1206	309.43497	3700.8433
31.2	352.83349	47.1206	309.43497	3700.8433
31.2	352.83349	47.1206	309.43497	3700.8433
62.4	88.208373	39.439667	77.358743	774.39605
62.4	88.208373	39.439667	77.358743	774.39605
83.66610838	49.065909	32.63889	43.030802	2563.4524
90.75481118	41.700348	30.270337	36.571205	5349.2101
94.29916257	38.62454	29.084454	33.873721	9137.1507
156.4661084	14.029378	11.249578	12.303765	2174.2547
187.2	9.8009303	5.9107028	8.5954159	1518.9354
156.4661084	14.029378	11.249578	12.303765	2174.2547

22.202834	28.228101	6975.226	94.29916257	38.62454	29.084454	33.873721	9137.1507
22.960838	30.476004	4057.515	90.75481118	41.700348	30.270337	36.571205	5349.2101
24.460817	35.859002	1921.1481	83.66610838	49.065909	32.63889	43.030802	2563.4524
28.675907	64.465619	563.05012		62.4	88.208373	39.439667	77.358743 774.39605
28.675907	64.465619	563.05012		62.4	88.208373	39.439667	77.358743 774.39605
31.938533	140.35534	2508.4465	42.28966111	192.04835	44.837864	168.4264	3521.5576
30.312305	89.345696	5356.6265	53.00439128	122.25181	42.133338	107.21483	7445.5754
19.112173	21.234584	6004.2664	108.7243415	29.055304	24.331165	25.481501	7643.8609
4.7746157	6.4493876	1139.7009	197.2828943	8.8247036	4.6671718	7.7392651	1367.641
5.8225081	7.1628466	2250.2746		187.2	9.8009303	5.9107028	8.5954159 2700.3295
4.7746157	6.4493876	1139.7009	197.2828943	8.8247036	4.6671718	7.7392651	1367.641
19.112173	21.234584	6004.2664	108.7243415	29.055304	24.331165	25.481501	7643.8609
18.732929	20.553702	3310.3818	110.5105257	28.123651	23.757489	24.664442	4198.2948
17.979243	19.286627	1412.0865	114.0828943	26.389911	22.623993	23.143952	1776.8842
28.675907	64.465619	2252.2005		62.4	88.208373	39.439667	77.358743 3097.5842
26.031055	43.39491	4600.0671	76.05526287	59.3773	35.148193	52.073892	6211.1984
18.732929	20.553702	3310.3818	110.5105257	28.123651	23.757489	24.664442	4198.2948
19.112173	21.234584	6004.2664	108.7243415	29.055304	24.331165	25.481501	7643.8609
7.8691374	8.6085542	2704.4571	170.758983	11.779094	8.4600645	10.330265	3245.3485
5.8585127	7.1875501	2258.0355	186.8780204	9.8347322	5.9542403	8.6250602	2709.6426
5.8225081	7.1628466	2250.2746		187.2	9.8009303	5.9107028	8.5954159 2700.3295
9.7533836	10.054835	3158.8197	158.0014922	13.758041	10.923444	12.065802	3790.5836
	14.97267	15.130228	128.8029844	20.702707	18.195313	18.156274	5703.9617
13.715427	13.713744	2423.7161	135.2915416	18.76453	16.391338	16.456493	2908.1024
11.360947	11.418226	896.78537	148.2686562	15.62357	13.099045	13.701871	1076.1424
22.352626	28.651386	1755.5712		93.6	39.203721	29.318199	34.381663 2302.6459
11.911308	11.919363	936.14456	145.1182892	16.309276	13.857914	14.303235	1123.3735
14.523831	14.606671	2566.5728	131.0910523	19.986322	17.547843	17.528005	3097.4541
15.917022	16.304659	5000.4798	124.0774338	22.309682	19.569585	19.565591	6147.9665
4.790507	6.4601633	1141.6051	197.1182892	8.839448	4.6856702	7.7521959	1369.9261
7.7540214	8.5243794	2678.0128		171.6	11.663917	8.3129367	10.229255 3213.6153
5.678628	7.0642976	1248.3644	188.501224	9.6660857	5.7372344	8.4771571	1498.0373
18.597128	20.317209	5842.4599		111.151836	27.800058	23.552599	24.380651 7399.2673
	19.7497	22.452261	105.7349653	30.721452	25.300418	26.942713	4470.9529
22.073764	27.871074	1733.6694	94.90122397	38.13602	28.883287	33.445289	2268.4881
28.675907	64.465619	563.05012		62.4	88.208373	39.439667	77.358743 774.39605
28.675907	64.465619	563.05012		62.4	88.208373	39.439667	77.358743 774.39605
33.298933	257.86248	2615.2921		31.2	352.83349	47.1206	309.43497 3700.8433
33.298933	257.86248	2615.2921		31.2	352.83349	47.1206	309.43497 3700.8433
33.298933	257.86248	2615.2921		31.2	352.83349	47.1206	309.43497 3700.8433
28.675907	64.465619	563.05012		62.4	88.208373	39.439667	77.358743 774.39605
28.675907	64.465619	563.05012		62.4	88.208373	39.439667	77.358743 774.39605
28.675907	64.465619	563.05012		62.4	88.208373	39.439667	77.358743 774.39605
28.675907	64.465619	563.05012		62.4	88.208373	39.439667	77.358743 774.39605
28.675907	64.465619	563.05012		62.4	88.208373	39.439667	77.358743 774.39605
28.675907	64.465619	563.05012		62.4	88.208373	39.439667	77.358743 774.39605
28.675907	64.465619	563.05012		62.4	88.208373	39.439667	77.358743 774.39605
28.675907	64.465619	563.05012		62.4	88.208373	39.439667	77.358743 774.39605

(Decrease E)
 ≤ 94.904 > 94.904

Slenderness	F _e	F _{cr} (a)	F _{cr} (b)	Capacity
	ksi	ksi	ksi	(kips)
31.2	205.81954	45.165975	180.50373	3547.3274
119.6	14.006623	11.222348	12.283808	964.76802
138.666667	10.419614	6.709669	9.1380015	1614.8182
197.6	5.131235	0.8466793	4.5000931	795.23209
192.4	5.4123472	1.0464442	4.7466285	1491.1973
189.28	5.5922468	1.1850503	4.9044004	2407.4419
187.2	5.7172093	1.2860561	5.0139926	3544.1825
185.7968222	5.8038906	1.3583206	5.0900121	2498.5538
183.6920555	5.937656	1.4732651	5.2073243	1635.9292
135.1380832	10.97085	7.4221323	9.6214354	3022.6631
108.04625	17.162335	14.77057	15.051368	4728.5268
65.92777459	46.095545	31.75404	40.425793	5611.4021
48.65204364	84.643499	39.047543	74.232349	3066.7868
62.72909076	50.916413	33.148779	44.653694	650.87475
62.4	51.454884	33.291668	45.125933	653.68037
62.4	51.454884	33.291668	45.125933	653.68037
62.4	51.454884	33.291668	45.125933	653.68037
68.20565076	43.068036	30.756624	37.770668	2415.6196
122.304293	13.394064	10.481123	11.746594	922.57537
136.7921477	10.707139	7.0814901	9.390161	1659.3784
122.8606306	13.273037	10.332859	11.640453	5713.9942
122.8606306	13.273037	10.332859	11.640453	5713.9942
136.7921477	10.707139	7.0814901	9.390161	1659.3784
81.53619535	30.136645	24.968176	26.429837	4412.2409
68.20565076	43.068036	30.756624	37.770668	2415.6196
62.4	51.454884	33.291668	45.125933	653.68037
62.4	51.454884	33.291668	45.125933	653.68037
62.4	51.454884	33.291668	45.125933	653.68037
31.2	205.81954	45.165975	180.50373	3547.3274
31.2	205.81954	45.165975	180.50373	3547.3274
31.2	205.81954	45.165975	180.50373	3547.3274
31.2	205.81954	45.165975	180.50373	3547.3274
31.2	205.81954	45.165975	180.50373	3547.3274
62.4	51.454884	33.291668	45.125933	653.68037
62.4	51.454884	33.291668	45.125933	653.68037
83.66610838	28.62178	24.067165	25.101301	1890.2307
90.75481118	24.325203	21.151283	21.333203	3737.7403
94.29916257	22.530982	19.750723	19.759671	6204.8725
156.4661084	8.183804	3.8761252	7.1771961	1268.3152
187.2	5.7172093	1.2860561	5.0139926	886.04563
156.4661084	8.183804	3.8761252	7.1771961	1268.3152

Required Diameter	Required Diameter
(axial a)	(axial b)
0.636444	0.138886
0.841865	0.623451
1.096834	1.084133
1.648452	1.544706
2.857908	2.005168
5.715535	2.46552
12.9529	2.874112
5.882202	2.683712
3.079862	2.325502
1.889088	1.848042
1.59941	1.591678
1.177539	0.75149
1.077029	0.361859
1.046018	0.229446
0.711334	0.155228
0.711334	0.155228
0.714914	0.156009
0.725732	0.334763
0.73998	0.557049
0.88267	0.869843
1.970453	1.803237
1.782935	1.631632
0.700835	0.69065
0.472994	0.356065
0.359367	0.165768
0.148916	0.032497
0.711334	0.155228
0.714898	0.156006
0.733175	0.159994
0.749554	0.163569
0.749507	0.163558
0.749393	0.163533
0.749899	0.163644
0.749215	0.163495
0.72396	0.157983
1.266696	0.701525
1.317931	1.068811
1.399593	1.345738
1.663465	1.665282
1.887646	1.819491
1.5968	1.598544

94.29916257	22.530982	19.750723	19.759671	6204.8725	1.440892	1.385448
90.75481118	24.325203	21.151283	21.333203	3737.7403	1.243978	1.008837
83.66610838	28.62178	24.067165	25.101301	1890.2307	1.165835	0.645666
62.4	51.454884	33.291668	45.125933	653.68037	1.158041	0.252709
62.4	51.454884	33.291668	45.125933	653.68037	1.137708	0.248272
42.28966111	112.0282	41.480242	98.248735	3257.8506	1.149834	0.33758
53.00439128	71.313554	37.284035	62.541987	6588.6329	1.170342	0.619771
108.7243415	16.948927	14.54552	14.864209	4669.729	1.610727	1.604356
197.2828943	5.1477438	0.8578263	4.5145713	797.7906	1.894093	1.776608
187.2	5.7172093	1.2860561	5.0139926	1575.1922	2.345165	1.720747
197.2828943	5.1477438	0.8578263	4.5145713	797.7906	1.924276	1.804919
108.7243415	16.948927	14.54552	14.864209	4669.729	1.607093	1.600737
110.5105257	16.405463	13.962565	14.387591	2542.4972	1.363911	1.241131
114.0828943	15.394115	12.840109	13.500639	1060.3377	1.259347	0.900144
62.4	51.454884	33.291668	45.125933	2614.7215	1.200613	0.510198
76.05526287	34.636758	27.325583	30.376437	4828.829	1.233146	0.881417
110.5105257	16.405463	13.962565	14.387591	2542.4972	1.325081	1.205797
108.7243415	16.948927	14.54552	14.864209	4669.729	1.47702	1.471178
170.758983	6.8711379	2.3781182	6.0259879	1893.1199	2.31565	1.921919
186.8780204	5.7369271	1.3023381	5.0312851	1580.6248	1.990403	1.464365
187.2	5.7172093	1.2860561	5.0139926	1575.1922	1.957708	1.436453
158.0014922	8.0255242	3.6854882	7.0383847	2211.1738	1.829564	1.637868
128.8029844	12.076579	8.8385417	10.59116	3327.311	1.622264	1.607969
135.2915416	10.945976	7.3900286	9.599621	1696.3931	1.29887	1.276627
148.2686562	9.1137493	5.0317371	7.9927582	627.74976	1.130676	0.967685
93.6	22.868837	20.023615	20.05597	1572.651	1.025576	0.625281
145.1182892	9.5137445	5.5417424	8.3435539	655.30119	1.105079	0.933536
131.0910523	11.658688	8.3062499	10.224669	1806.8482	1.231492	1.200122
124.0774338	13.013981	10.013593	11.413262	3585.5819	1.40138	1.397822
197.1182892	5.1563447	0.8636631	4.5221143	799.12356	1.588415	1.490636
171.6	6.8039516	2.3076607	5.9670656	1874.6089	1.734125	1.431214
188.501224	5.63855	1.2220332	4.9450083	873.8551	1.634822	1.570877
111.151836	16.216701	13.756774	14.222047	4467.9877	1.497235	1.495148
105.7349653	17.920847	15.552913	15.716583	2777.3494	1.197521	1.065007
94.90122397	22.246011	19.517115	19.509752	1532.8707	1.048891	0.646934
62.4	51.454884	33.291668	45.125933	653.68037	0.986839	0.215349
62.4	51.454884	33.291668	45.125933	653.68037	0.744195	0.162399
31.2	205.81954	45.165975	180.50373	3547.3274	0.74791	0.16321
31.2	205.81954	45.165975	180.50373	3547.3274	0.75304	0.164329
31.2	205.81954	45.165975	180.50373	3547.3274	0.752801	0.164277
62.4	51.454884	33.291668	45.125933	653.68037	0.720854	0.157306
62.4	51.454884	33.291668	45.125933	653.68037	0.693323	0.151298
62.4	51.454884	33.291668	45.125933	653.68037	0.720171	0.157157
62.4	51.454884	33.291668	45.125933	653.68037	0.746054	0.162805
62.4	51.454884	33.291668	45.125933	653.68037	0.746054	0.162805
62.4	51.454884	33.291668	45.125933	653.68037	0.746054	0.162805
62.4	51.454884	33.291668	45.125933	653.68037	0.636237	0.13884

Pn/Capacity	Pn/Capacity (new dia)	Pn/Capacity (new dia)	Comparison	Pn/Capacity (new dia)	Comparison
		(Increase Fy)		(Decrease Fy)	
0.00101265	0.00427271	0.003611639	-15%	0.005974919	40%
0.00177184	0.01554765	0.015547649	0%	0.01621011	4%
0.00300761	0.00928668	0.009286677	0%	0.009286677	0%
0.00596529	0.01885326	0.018853258	0%	0.018853258	0%
0.01005175	0.01005175	0.010051745	0%	0.010051745	0%
0.01519697	0.00622468	0.00622468	0%	0.00622468	0%
0.02065129	0.00407927	0.004079268	0%	0.004079268	0%
0.01800578	0.00737517	0.007375168	0%	0.007375168	0%
0.0135199	0.0135199	0.013519902	0%	0.013519902	0%
0.00853815	0.00853815	0.00853815	0%	0.008538347	0%
0.00639528	0.00639528	0.006333598	-1%	0.007072143	11%
0.0034665	0.00708194	0.006288901	-11%	0.009197041	30%
0.00289998	0.0132077	0.011394067	-14%	0.017913493	36%
0.00273538	0.05731658	0.050592879	-12%	0.075109823	31%
0.00126499	0.02643164	0.023316943	-12%	0.034668317	31%
0.00126499	0.02643164	0.023316943	-12%	0.034668317	31%
0.00127776	0.02669832	0.023552202	-12%	0.035018108	31%
0.00131672	0.00679742	0.006063278	-11%	0.00876859	29%
0.00136893	0.01241216	0.012412164	0%	0.012796431	3%
0.00194777	0.00597828	0.005978283	0%	0.005978283	0%
0.00812916	0.0033297	0.003329705	0%	0.003425601	3%
0.00665556	0.00272612	0.002726116	0%	0.002804629	3%
0.00122792	0.00376887	0.003768865	0%	0.003768865	0%
0.00055931	0.00122995	0.001129612	-8%	0.001518653	23%
0.00032286	0.00166674	0.001486728	-11%	0.002150076	29%
5.544E-05	0.0011584	0.001021896	-12%	0.001519386	31%
0.00126499	0.02643164	0.023316943	-12%	0.034668317	31%
0.0012777	0.02669709	0.023551116	-12%	0.035016492	31%
0.00134387	0.00567021	0.004792919	-15%	0.00792917	40%
0.00140458	0.00592638	0.005009454	-15%	0.008287396	40%
0.0014044	0.00592564	0.005008828	-15%	0.00828636	40%
0.00140397	0.00592382	0.005007294	-15%	0.008283822	40%
0.00140587	0.00593183	0.005014058	-15%	0.008295012	40%
0.00140331	0.0293217	0.025866448	-12%	0.038458995	31%
0.0013103	0.02737824	0.024151998	-12%	0.035909901	31%
0.0040113	0.02355352	0.021743574	-8%	0.028858475	23%
0.00434236	0.01004681	0.009443994	-6%	0.011980288	19%
0.00489715	0.00489715	0.004647685	-5%	0.005756181	18%
0.00693291	0.02191141	0.02191141	0%	0.02191141	0%
0.00827637	0.02615741	0.026157411	0%	0.026157411	0%
0.00638836	0.02019036	0.020190358	0%	0.020190358	0%

0.00519042	0.00519042	0.004926016	-5%	0.006100895	18%
0.00386871	0.00895093	0.00841387	-6%	0.010673512	19%
0.00339793	0.01995194	0.018418749	-8%	0.024445704	23%
0.00335265	0.07005258	0.061797616	-12%	0.091882514	31%
0.00323595	0.06761417	0.059646547	-12%	0.088684241	31%
0.0033053	0.01458354	0.012474975	-14%	0.020032163	37%
0.00342425	0.00666	0.005782762	-13%	0.008945652	34%
0.0064861	0.0064861	0.006434894	-1%	0.00714949	10%
0.00789084	0.02493896	0.024938963	0%	0.024938963	0%
0.00740242	0.00740242	0.007402424	0%	0.007402424	0%
0.00814433	0.02574011	0.025740108	0%	0.025740108	0%
0.00645687	0.00645687	0.006405897	-1%	0.007117274	10%
0.00465063	0.0122195	0.012171109	0%	0.013354096	9%
0.00396489	0.03241038	0.03241038	0%	0.034767141	7%
0.00360368	0.01784594	0.015742982	-12%	0.023407129	31%
0.00380162	0.00813218	0.007374995	-9%	0.010233042	26%
0.0043896	0.01153364	0.011487963	0%	0.012604551	9%
0.00545397	0.00545397	0.00541091	-1%	0.006011793	10%
0.00923443	0.00923443	0.00923443	0%	0.00923443	0%
0.00536092	0.00536092	0.005360915	0%	0.005360915	0%
0.00515849	0.00515849	0.005158495	0%	0.005158495	0%
0.00670653	0.00670653	0.006706529	0%	0.006706529	0%
0.00646391	0.00646391	0.006463908	0%	0.006531928	1%
0.00421766	0.01287725	0.012877247	0%	0.012875667	0%
0.00319607	0.03745661	0.037456609	0%	0.037456609	0%
0.00262952	0.01700534	0.016108083	-5%	0.020045986	18%
0.003053	0.03485955	0.034859549	0%	0.034859549	0%
0.00379143	0.01138009	0.011380089	0%	0.011444998	1%
0.00488477	0.00488477	0.004884769	0%	0.005003731	2%
0.00555499	0.01755652	0.017556516	0%	0.017556516	0%
0.00512094	0.00512094	0.005120935	0%	0.005120935	0%
0.00616913	0.01949751	0.019497507	0%	0.019497507	0%
0.00560428	0.00560428	0.00558867	0%	0.006105576	9%
0.00358514	0.00911383	0.008961897	-2%	0.010188248	12%
0.00275043	0.01802816	0.017138305	-5%	0.021137666	17%
0.00243463	0.05087088	0.044876281	-12%	0.066723375	31%
0.00138456	0.02893007	0.025520961	-12%	0.037945316	31%
0.00139842	0.00590041	0.0049875	-15%	0.008251076	40%
0.00141767	0.00598162	0.005056148	-15%	0.008364644	40%
0.00141677	0.00597783	0.005052944	-15%	0.008359343	40%
0.00129908	0.02714382	0.023945206	-12%	0.035602437	31%
0.00120174	0.02511005	0.022151096	-12%	0.032934901	31%
0.00129662	0.02709243	0.023899867	-12%	0.035535025	31%
0.00139149	0.0290748	0.025648637	-12%	0.038135149	31%
0.00139149	0.0290748	0.025648637	-12%	0.038135149	31%
0.00139149	0.0290748	0.025648637	-12%	0.038135149	31%
0.00101199	0.02114531	0.018653555	-12%	0.027734654	31%

Pn/Capacity (new dia)	Comparison	Pn/Capacity (new dia)	Comparison	Required Zx/Zx (@ 20in)	Required Zx/Zx (@ new dia)	Required Zx/Zx (@ new dia)
(Increase E)		(Decrease E)				(higher Fy)
0.00422232	-1%	0.00440505	3%	0.017568	0.140544	0.11712
0.01304508	-16%	0.02221093	43%	0.066720235	0.533761883	0.44480157
0.0077389	-17%	0.01326668	43%	0.115948407	0.274840669	0.229033891
0.01571105	-17%	0.02693323	43%	0.165102812	0.391354815	0.326129012
0.00837645	-17%	0.01435964	43%	0.214183451	0.214183451	0.178486209
0.00518723	-17%	0.0088924	43%	0.263190322	0.134753445	0.112294537
0.00339939	-17%	0.00582753	43%	0.004100574	0.001214985	0.001012487
0.00614597	-17%	0.01053595	43%	0.836035034	0.428049938	0.356708281
0.01126659	-17%	0.01931415	43%	0.849939577	0.849939577	0.708282981
0.00711512	-17%	0.01219736	43%	0.76409496	0.76409496	0.6367458
0.00554723	-13%	0.009048	41%	0.721897849	0.721897849	0.601581541
0.00671659	-5%	0.00811528	15%	0.195707252	0.463898672	0.386582226
0.01283217	-3%	0.01422461	8%	0.045041169	0.360329349	0.300274458
0.05463299	-5%	0.06483821	13%	0.001665367	0.106583482	0.088819568
0.02520674	-5%	0.02986169	13%	0.000862982	0.055230832	0.046025693
0.02520674	-5%	0.02986169	13%	0.000858715	0.05495777	0.045798142
0.02546107	-5%	0.03016298	13%	0.000854449	0.054684709	0.045570591
0.00642279	-6%	0.00786419	16%	0.038539521	0.308316171	0.256930142
0.01036381	-17%	0.01773166	43%	0.059572606	0.476580847	0.397150706
0.0049819	-17%	0.0085404	43%	0.063026764	0.149396774	0.124497311
0.00277808	-17%	0.00475672	43%	0.200237854	0.102521781	0.085434818
0.00227449	-17%	0.00389445	43%	0.280436731	0.143583606	0.119653005
0.00314072	-17%	0.00538409	43%	0.012013155	0.028475628	0.02372969
0.00113424	-8%	0.00151483	23%	0.014179338	0.033610284	0.02800857
0.00157488	-6%	0.00192831	16%	0.013640931	0.109127449	0.090939541
0.00110472	-5%	0.00130873	13%	0.012324437	0.788763963	0.657303303
0.02520674	-5%	0.02986169	13%	0.000787513	0.050400821	0.042000684
0.02545989	-5%	0.03016159	13%	0.008077092	0.516933897	0.430778248
0.00560334	-1%	0.00584584	3%	0.024481944	0.195855556	0.163212963
0.00585649	-1%	0.00610994	3%	0.103474663	0.827797301	0.689831084
0.00585576	-1%	0.00610918	3%	0.101092147	0.808737173	0.673947644
0.00585397	-1%	0.00610731	3%	0.0987527	0.790021597	0.658351331
0.00586187	-1%	0.00611556	3%	0.024243964	0.193951716	0.16162643
0.02796288	-5%	0.0331268	13%	0.008069532	0.516450079	0.430375066
0.02610947	-5%	0.03093113	13%	0.000728288	0.046610415	0.038842012
0.02162763	-8%	0.0293305	25%	0.117210403	0.937683223	0.781402686
0.00908736	-10%	0.01300524	29%	0.325163892	0.770758855	0.642299046
0.00439422	-10%	0.00647083	32%	0.783559377	0.783559377	0.652966147
0.01825951	-17%	0.03130201	43%	0.392274284	0.92983534	0.774862783
0.02179784	-17%	0.03736773	43%	0.088459399	0.209681539	0.174734616
0.0168253	-17%	0.02884337	43%	0.329285726	0.780529129	0.650440941

0.00465737	-10%	0.00685834	32%	0.806283513	0.806283513	0.671902928
0.00809614	-10%	0.01158666	29%	0.289890195	0.687147129	0.572622607
0.01832053	-8%	0.02484555	25%	0.100326798	0.80261438	0.668845317
0.0668062	-5%	0.07914336	13%	0.010644253	0.68123217	0.567693475
0.06448079	-5%	0.07638851	13%	0.000677665	0.04337056	0.036142133
0.01426914	-2%	0.01542416	6%	0.029042693	0.232341547	0.193617956
0.00643584	-3%	0.00727291	9%	0.135581988	0.321379526	0.267816272
0.00561594	-13%	0.00919271	42%	0.61808297	0.61808297	0.515069141
0.02078247	-17%	0.03562709	43%	0.259151673	0.614285448	0.51190454
0.00616869	-17%	0.01057489	43%	0.112134938	0.112134938	0.093445781
0.02145009	-17%	0.03677158	43%	0.270333839	0.640791321	0.533992768
0.00559063	-13%	0.00915128	42%	1.04138436	1.04138436	0.8678203
0.01052979	-14%	0.0173873	42%	0.329711638	0.781538697	0.651282247
0.02762938	-15%	0.04630054	43%	0.115524529	0.924196229	0.770163525
0.01701892	-5%	0.02016182	13%	0.016287747	0.130301972	0.108584977
0.00757868	-7%	0.00974826	20%	0.128057085	0.303542719	0.252952266
0.00993877	-14%	0.01641138	42%	0.275203587	0.652334429	0.543612024
0.00472227	-13%	0.00772987	42%	0.947442977	0.947442977	0.789535814
0.00769536	-17%	0.01319204	43%	0.41717582	0.41717582	0.347646517
0.00446743	-17%	0.00765845	43%	0.102019061	0.102019061	0.085015884
0.00429875	-17%	0.00736928	43%	0.002435265	0.002435265	0.002029387
0.00558877	-17%	0.00958076	43%	0.170248177	0.170248177	0.141873481
0.00538659	-17%	0.00923415	43%	0.4840669	0.4840669	0.403389084
0.01073104	-17%	0.01839607	43%	0.238978857	0.566468401	0.472057001
0.03121384	-17%	0.05350944	43%	0.114989147	0.919913177	0.766594314
0.01528335	-10%	0.0223776	32%	0.032177307	0.25741846	0.214515383
0.02904962	-17%	0.04979936	43%	0.126174002	1.009392019	0.841160016
0.00948341	-17%	0.01625727	43%	0.247454513	0.586558846	0.488799039
0.00406981	-17%	0.00697824	43%	0.454883268	0.454883268	0.37906939
0.01463043	-17%	0.02508074	43%	0.195553684	0.463534659	0.386278882
0.00426745	-17%	0.00731562	43%	0.087955151	0.087955151	0.073295959
0.01624792	-17%	0.02785358	43%	0.200778901	0.475920358	0.396600299
0.00482096	-14%	0.00798381	42%	0.621605129	0.621605129	0.518004275
0.00795302	-13%	0.01280271	40%	0.230371359	0.546065444	0.455054536
0.01615425	-10%	0.0239066	33%	0.081181256	0.649450049	0.541208374
0.04851342	-5%	0.05747244	13%	0.01063357	0.680548477	0.567123731
0.02758939	-5%	0.03268434	13%	0.013935303	0.891859378	0.743216148
0.00583083	-1%	0.00608316	3%	0.075756189	0.606049515	0.505041263
0.00591108	-1%	0.00616689	3%	0.074510637	0.596085099	0.496737583
0.00590734	-1%	0.00616298	3%	0.072728375	0.581826997	0.484855831
0.02588592	-5%	0.0306663	13%	0.014201429	0.908891471	0.757409559
0.0239464	-5%	0.0283686	13%	0.000275531	0.01763396	0.014694967
0.02583691	-5%	0.03060823	13%	0.000274887	0.017592773	0.014660644
0.02772741	-5%	0.03284786	13%	0.014545121	0.930887749	0.775739791
0.02772741	-5%	0.03284786	13%	0.011630361	0.744343087	0.620285906
0.02772741	-5%	0.03284786	13%	0.0087156	0.557798424	0.46483202
0.02016539	-5%	0.02388935	13%	0.00580084	0.371253761	0.309378134

Required Zx/Zx (@ new dia)
(lower Fy)

0.1952
 0.741335949
 0.381723152
 0.543548354
 0.297477015
 0.187157562
 0.001687479
 0.594513802
 1.180471634
 1.061242999
 1.002635902
 0.64430371
 0.500457429
 0.148032614
 0.076709489
 0.076330237
 0.075950985
 0.428216904
 0.661917843
 0.207495519
 0.142391363
 0.199421675
 0.039549483
 0.04668095
 0.151565902
 1.095505504
 0.07000114
 0.717963746
 0.272021605
 1.149718473
 1.123246073
 1.097252218
 0.269377383
 0.717291777
 0.064736687
 1.30233781
 1.07049841
 1.088276912
 1.291437972
 0.29122436
 1.084068235

1.119838213
 0.954371012
 1.114742195
 0.946155792
 0.060236889
 0.322696594
 0.446360453
 0.858448569
 0.853174233
 0.155742969
 0.889987946
 1.446367167
 1.085470412
 1.283605874
 0.180974962
 0.42158711
 0.90602004
 1.315893023
 0.579410861
 0.141693141
 0.003382312
 0.236455801
 0.672315139
 0.786761668
 1.27765719
 0.357525638
 1.40193336
 0.814665064
 0.631782316
 0.643798137
 0.122159931
 0.661000498
 0.863340458
 0.758424227
 0.902013957
 0.945206218
 1.23869358
 0.841735438
 0.827895971
 0.808093051
 1.262349265
 0.024491611
 0.024434407
 1.292899652
 1.033809843
 0.774720033
 0.515630223